

**FUNDAÇÃO OSWALDO CRUZ
INSTITUTO GONÇALO MONIZ**

Programa de Pós-Graduação em Biotecnologia em Saúde e Medicina Investigativa

TESE DE DOUTORADO

**MODULAÇÃO DE VIAS DE SINALIZAÇÃO E INDUÇÃO DE MORTE CELULAR:
UM ESTUDO SOBRE O EFEITO ANTILEUCÊMICO DE DOIS TRITERPENOS E
UM ALCALOIDE EM LEUCEMIA MIELOIDE AGUDA COM ENFOQUE NO
ESTRESSE OXIDATIVO**

ANA CAROLINA BORGES DA CRUZ RODRIGUES

Salvador – BA

2023

**FUNDAÇÃO OSWALDO CRUZ
INSTITUTO GONÇALO MONIZ**

Programa de Pós-Graduação em Biotecnologia em Saúde e Medicina Investigativa

**MODULAÇÃO DE VIAS DE SINALIZAÇÃO E INDUÇÃO DE MORTE CELULAR:
UM ESTUDO SOBRE O EFEITO ANTILEUCÊMICO DE DOIS TRITERPENOS E
UM ALCALOIDE EM LEUCEMIA MIELOIDE AGUDA COM ENFOQUE NO
ESTRESSE OXIDATIVO**

ANA CAROLINA BORGES DA CRUZ RODRIGUES

Tese apresentada ao Programa de Pós-graduação em Biotecnologia em Saúde e Medicina Investigativa do Instituto Gonçalo Moniz, como requisito obrigatório para obtenção do grau de Doutora.

Orientador: Prof. Dr. Daniel Pereira Bezerra

Salvador – BA

2023

Ficha Catalográfica elaborada pela Biblioteca do
Instituto Gonçalo Moniz/ FIOCRUZ – Bahia - Salvador

R696m Rodrigues, Ana Carolina Borges da Cruz

Modulação de vias de sinalização e indução de morte celular: um estudo sobre o efeito antileucêmico de dois triterpenos e um alcaloide em leucemia mieloide aguda com enfoque no estresse oxidativo. / Ana Carolina Borges da Cruz Rodrigues. _ Salvador, 2023.

182 f.: il.: 30 cm

Orientador: Prof. Dr. Daniel Pereira Bezerra

Tese (Doutorado em Biotecnologia em Saúde e Medicina Investigativa) – Instituto Gonçalo Moniz, Fundação Oswaldo Cruz, Salvador, 2023.

1. Leucemia mieloide aguda. 2. Triterpenos quinonametídeos. 3. Piplartina. 4. Citotoxicidade. I. Título.

CDU 616.155.392


“MODULAÇÃO DE VIAS DE SINALIZAÇÃO E INDUÇÃO DE MORTE CELULAR: UM ESTUDO SOBRE O EFEITO ANTILEUCÊMICO DE DOIS TRITERPENOS E UM ALCALOIDE EM LEUCEMIA MIELOIDE AGUDA COM ENFOQUE NO ESTRESSE OXIDATIVO”.

ANA CAROLINA BORGES DA CRUZ RODRIGUES


FOLHA DE APROVAÇÃO

Salvador, **07 de junho 2023.**


COMISSÃO EXAMINADORA

Documento assinado digitalmente
 **RAQUEL CARVALHO MONTENEGRO**
Data: 19/09/2023 21:39:02-0300
Verifique em <https://validar.it.gov.br>

Dra. Raquel Carvalho Montenegro
Professora Associado III
UFC

Documento assinado digitalmente
 **LETICIA VERAS COSTA LOTUFO**
Data: 14/09/2023 17:41:00-0300
Verifique em <https://validar.it.gov.br>

Dra. Leticia Veras Costa Lotufo
Professora titular
USP

Documento assinado digitalmente
 **JULIANA PERRONE BEZERRA DE MENEZES**
Data: 09/08/2023 16:19:57-0300
Verifique em <https://validar.it.gov.br>

Dra. Juliana Perrone Bezerra de Menezes
Pesquisadora em Saúde Pública
IGM/FIOCRUZ

FONTES DE FINANCIAMENTO

O presente trabalho foi realizado com apoio da Coordenação de Aperfeiçoamento de Pessoal de Nível Superior - Brasil (CAPES) - Código de Financiamento 001.
Conselho Nacional de Desenvolvimento Científico e Tecnológico (CNPq).
Fundação de Amparo à Pesquisa do Estado da Bahia (FAPESB).

AGRADECIMENTOS

Primeiramente à Deus, que esteve me orientando e confortando ao longo dessa jornada. Por ter me concedido saúde e resiliência para enfrentar todos os obstáculos, sempre me mostrando que os planos DELE são maiores do que tudo e ele sempre age no momento certo.

À minha mãe, minha referência, exemplo de mulher guerreira, mãe loba que defende e protege a mim e ao meu irmão acima de tudo. Essa etapa é mais uma conquista nossa, mãe!

Ao meu pai e ao meu irmão, por todo incentivo e por sempre demonstrar orgulho e confiança nos meus objetivos.

As minhas avós, Dinária e Maria (*in memoriam*), que hoje não estão mais presentes neste plano, mas as levo para onde for dentro do meu coração.

A Gonçalo Abrantes, meu noivo e melhor amigo, por todo amor, paciência, dedicação, apoio e todas as ajudas possíveis e impossíveis que me deste para que eu conseguisse terminar essa tese. E principalmente, por ser abrigo nos momentos mais difíceis, obrigada.

À minha melhor amiga da vida inteira, Jéssica Castelo Branco, por ser luz na minha vida. Você faz a vida ser leve. E como dizia minha avó: essa é amiga de verdade!

A todos os meus familiares por estarem presentes em todas minhas batalhas, sempre me enviando energias positivas.

Ao meu orientador, Dr. Daniel Pereira Bezerra, pela oportunidade, suporte, paciência, compreensão e ensinamentos ao longo dessa jornada de mais 9 anos em seu grupo de pesquisa, que foi fundamental para que eu realizasse este e todos os trabalhos que desenvolvi ao longo desses anos. Meu muito obrigada!

A minha segunda orientadora, Cristina Pina, que me recebeu em seu laboratório na Brunel University London e me deu a oportunidade de realizar o sonho de fazer o doutorado sanduíche na Inglaterra. Sou muito grata pela confiança, pelo respeito, paciência, por compartilhar tanto conhecimento e ensinamentos durante o ano de 2022. You are a role model, thank you!

Ao melhor grupo de pesquisa, do Câncer (Rafaela, Sara, Larissa, Rosane, Valdenizia, Luciano, Ingrid, Suellen, Sheila, Mateus, Maiara e Felipe) e aos colegas do LETI, que ajudaram tornar os dias de trabalho mais agradáveis. E um destaque para a turminha do buraco, as amigas (especialmente Sara e Larissa) que ultrapassaram os limites do laboratório e vieram para vida.

Meus agradecimentos ao curso de Pós-Graduação em Biotecnologia em Saúde e Medicina Investigativa – IGM e aos membros do corpo docente e funcionários.

Meus agradecimentos aos colegas de laboratório e aos funcionários da Brunel University London.

As plataformas de citometria, microscopia e histologia do IGM, pelo auxílio.

A Biblioteca do IGM, pela contribuição e cuidados na revisão das normas desta tese.

Meus agradecimentos a CAPES, CNPq e FAPESB, órgãos financiadores deste projeto.

A todos que direta ou indiretamente fizeram parte da minha caminhada durante esses dois anos de mestrado, meus sinceros agradecimentos.

RODRIGUES, Ana Carolina Borges da Cruz. **Modulação de vias de sinalização e indução de morte celular: um estudo sobre o efeito antileucêmicos de dois triterpenos e um alcaloide em leucemia mieloide aguda com enfoque no estresse oxidativo.** 2023.182 f. il. Tese (Doutorado em Biotecnologia em Saúde e Medicina Investigativa) – Instituto Gonçalo Moniz, Fundação Oswaldo Cruz, Salvador, 2023.

RESUMO

INTRODUÇÃO: A leucemia mieloide aguda (LMA) é um tipo heterogêneo comum de câncer hematológico e a forma mais letal de leucemia. É uma doença caracterizada pela expansão clonal de precursores mielóides com capacidade diminuída de diferenciação, sendo diagnosticada com mais frequência em pessoas com mais de 60 anos. Houve um limitado avanço no tratamento anti-LMA padrão nas últimas quatro décadas e o prognóstico da doença permanece ruim, com menos de 30% de sobrevivência em 5 anos para pacientes diagnosticados com a doença. Nesse contexto, o desenvolvimento de novos medicamentos é urgentemente necessário, a fim de melhorar a recidiva e diminuir a toxicidade, principalmente para pacientes idosos, que representam uma população vulnerável ao padrão terapêutico intensivo. **OBJETIVO:** Diante disto, o objetivo do presente trabalho é investigar o potencial antileucêmico dos triterpenos quinonametídeos, tingenona (TG) e 22-hidroxitingenona (22-HTG) e o alcaloide/amida, piplartina (PL) em diferentes modelos de LMA. **MATERIAL E MÉTODOS:** O potencial citotóxico dos três compostos foi avaliado num painel de 28 linhagens de células cancerosas, representando 11 tipos de tumores, incluindo cânceres sólidos e hematológicos, a fim de determinar a CI_{50} . A avaliação do padrão de morte e mecanismo de ação dos compostos foi determinado através da análise do ciclo celular, detecção de morte celular por apoptose, potencial transmembrânico mitocondrial e produção de espécies reativas de oxigênio (ERO) por citometria de fluxo. Além disso, a modulação da expressão gênica e de vias de sinalização importantes para o desenvolvimento e progressão da leucemia foi investigado através de qPCR após tratamento com TG, 22-HTG e PL. A capacidade de inibir células-tronco e progenitores leucêmicas (CTPLs), o potencial clonogênico e a interação de PL com fármacos usados na terapia convencional de LMA também foi avaliada. Por último, o efeito antileucêmico de PL *in vivo* foi estudado através de um modelo xenográfico de leucemia humana. **RESULTADOS:** Os compostos apresentaram-se citotóxicos contra as linhagens cancerosas testadas, e as linhagens leucêmicas foram particularmente mais sensíveis aos tratamentos. A apoptose induzida por TG e 22-HTG se deu pela supressão do sistema tioredoxina, consequentemente induzindo estresse oxidativo que levou ao dano do DNA e ativação da via de sinalização MAPK. Estudos mecanísticos mostraram que PL tem como alvo a via de sinalização canônica do NF- κ B e induz a apoptose através do acúmulo de espécies reativas de oxigênio mitocondrial. Interessantemente, PL não demonstrou toxicidade a atividade progenitora hematopoiética saudável quando testada em células de medula óssea de camundongos. Além disso, ao combinar PL com citarabina ou daunorribicina, demonstramos que PL possui um efeito sinérgico com esses medicamentos nos modelos de LMA testados. **CONCLUSÃO:** Nossos achados demonstram o efeito antileucêmico de TG, 22-HTG e PL, através da indução do estresse oxidativo culminando na inibição de vias de sinalizações importantes na leucemia, evidenciado assim que estes compostos são candidatos promissores para o desenvolvimento de novos fármacos para o tratamento de LMA.

Palavras-chave: Leucemia mieloide aguda. Triterpenos quinonametídeos. Piplartina. Citotoxicidade.

RODRIGUES, Ana Carolina Borges da Cruz. **Modulation of signaling pathways and induction of cell death: a study on the anti-leukemic effects of two triterpenes and one alkaloid in acute myeloid leukemia with a focus on oxidative stress.** 2023.182 f. il. Tese (Doutorado em Biotecnologia em Saúde e Medicina Investigativa) – Instituto Gonçalo Moniz, Fundação Oswaldo Cruz, Salvador, 2023.

ABSTRACT

INTRODUCTION: Acute myeloid leukaemia (AML) is a common and heterogeneous type of hematological cancer and the most lethal form of leukaemia. It is characterized by clonal expansion of myeloid precursors with impaired ability to differentiate, and it is diagnosed more frequently in adults over 60 years old. Despite over four decades of research, there have been limited advances in standard anti-AML treatment, and the prognosis for the disease remains poor, with less than 30% of survival rate of patients five years following diagnosis. In this context, the development of new drugs is urgently needed in order to improve relapse rates and decrease toxicity, especially for elderly patients, who represent a vulnerable population for standard intensive treatments. **OBJECTIVE:** Thus, the aim of this study is to investigate the antileukemic potential of the quinonamethide triterpenes tingenone (TG) and 22-hydroxytingenone (22-HTG) as well as the alkaloid/amide piplartine (PL), using different AML models. **MATERIAL AND METHODS:** The cytotoxic potential of the three compounds was evaluated in a panel of 28 cancer cell lines, representing 11 types of tumours, including solid and haematological cancers, in order to determine the IC₅₀ values. The mechanism of cell death induced by the compounds was assessed through cell cycle analysis, detection of apoptosis, measurement of mitochondrial transmembrane potential, and assessment of reactive oxygen species (ROS) production using flow cytometry. In addition, the study investigated the modulation of gene expression and important signalling pathways involved in the development and progression of leukaemia by treating cells with TG, 22-HTG, and PL, and using RT-qPCR. The study also evaluated the ability of the compounds to inhibit leukemic stem cells and progenitor cells (LSPCs), their clonogenic potential, and their interactions with drugs commonly used in conventional AML therapy. Finally, the antileukemic effect of PL was investigated in vivo using a human leukaemia xenograft mouse model. **RESULTS:** The compounds demonstrated cytotoxicity against all cancer cell lines tested, with leukaemia cells being particularly sensitive to treatment. TG and 22-HTG induced apoptosis by suppressing the thioredoxin system, leading to oxidative stress, DNA damage, and activation of the MAPK signalling pathway. Mechanistic studies showed that PL targets the canonical NF-κB signalling pathway and induces apoptosis by accumulating mitochondrial reactive oxygen species. Interestingly, when tested in mouse bone marrow cells, PL did not demonstrate toxicity to healthy hematopoietic progenitor activity. Moreover, by combining PL with cytarabine or daunorubicin, we showed that PL has a synergistic effect with these drugs in the AML models tested. **CONCLUSION:** Our findings demonstrate the antileukemic effect of TG, 22-HTG and PL, through the induction of oxidative stress culminating in the inhibition of important signaling pathways in leukaemia. These results support the observation that these compounds are promising candidates for the development of anti-AML drugs.

Keywords: Acute myeloid leukaemia. Quinomethide triterpenes. Piplartine. Cytotoxicity.

LISTA DE FIGURAS

Figura 1	Esquema da hematopoiese e possível desenvolvimento de leucemia.	19
Figura 2	O sistema de estadiamento da OMS (Organização Mundial de Saúde) divide a LMA em duas principais famílias.	21
Figura 3	Comparação entre as classificações de LMA da 5ª edição da OMS <i>versus</i> CCI	22
Figura 4	A quimioterapia convencional é ineficaz para eliminar as CTLs, levando à recidiva da LMA	32
Figura 5	Organização das vias MAPK	34
Figura 6	Via de sinalização canônica e não canônica de NF- κ B	37
Figura 7	Estrutura química da TG e 22-HTG	40

LISTA DE TABELAS

Tabela 1	Classificação de risco da ELN 2022	25
Tabela 2	Visão geral de medicamentos mais recentes aprovados para LMA	28

LISTA DE ABREVIATURAS E SIGLAS

22-HTG	22- hidroxitingenona
Ara-C	Citarabina
ATO	Trióxido de arsênio
ATRA	Ácido trans-retinóico
Akt	Proteína kinase B
AZA	Azacitidina
BAD	Antagonista de morte celular Bcl-2
Bcl-2	Linfoma de células B 2
BRAF	Homólogo B1 do oncogene viral de sarcoma de murino v-raf
CCI	Classificação de Consenso Internacional
CEBPA	Proteína alfa CCAAT/enhancer-binding
CI₅₀	Concentração inibitória média
CTC	Células-tronco cancerosas
CTHNS	Células-tronco hematopoiéticas normais
CTLs	Células-tronco leucêmicas
CTPLs	Células-tronco e progenitoras leucêmicas
DNMT3A	DNA (citosina-5) - metiltransferase 3A
DRM	Doença residual mensurável
ELN	European Leukemia Network
ERK	Quinase regulada por sinal extracelular
ERO	Espécies reativas de oxigênio
EZH₂	Potenciador do homólogo 2 de zeste
FDA	Food and Drug Administration
FLT3-ITD	Tirosina quinase 3 Semelhante a fms/ duplicação em tandem interna
GO	Gemtuzumab ozogamicina
HC	Health Canada
IDH	Isocitrato desidrogenase 1
IκB	Inibidor do fator nuclear kappa B
IKK	Complexo IKK
IL-1	Interleucina 1
INCA	Instituto Nacional do Câncer

IP	Iodeto de Propídio
JAK	Janus quinase
JNK	c-Jun N-terminal quinase
KMT2A	Lisina (k)-metiltransferase específica 2A
KRAS	Gene homólogo do oncogene viral do sarcoma de rato Kirsten
LLA	Leucemia linfoide aguda
LLC	Leucemia linfoide crônica
LMA	Leucemia mieloide aguda
LMC	Leucemia mieloide crônica
LPA	Leucemia promielocítica aguda
MAPK	Proteína-quinases ativadas por mitógenos
MLL	Mixed-lineage leukemia
mTOR	Proteína alvo da rapamicina em mamíferos
MMP	Metaloproteinases da matriz
NF-κB	Fator nuclear kappa B
NIK	Quinase indutora de NF-κB
NMD	Neoplasias mielodisplásicas
NRAS	Homólogo do oncogene de neuroblastoma viral RAS
NPM1	Fosfoproteína nucleolar B23, numatrina
OMS	Organização mundial de saúde
PARP1	Poli [ADP-ribose] polimerase 1
PI3K	Fosfoinositídeo 3-quinase
PL	Piplartina/Piperlongumina
RAS	Vírus do sarcoma de rato
RT-qPCR	Reação em cadeia da polimerase via transcriptase reversa quantitativa
RUNX1	Fator de transcrição 1 relacionado ao runt
SMD	Síndrome Mielodisplásica
STAT	Transdutor de sinal e ativador de transcrição
TCTH	Transplante de células-tronco hematopoiéticas
TET2	Metilcitosinadioxigenase 2
TIM-3	Domínios de mucina e imunoglobulina de célula T
TG	Tingenona
t-LMA	LMA relacionada à terapia

TLR	do inglês <i>Toll like receptor</i>
TNF	Fator de necrose tumoral
TP53	Proteína de tumor 53
TrxR1	Tiorredoxina redutase 1
VAF	Frequência do alelo variante

SUMÁRIO

1	INTRODUÇÃO	16
2	REVISÃO DE LITERATURA	18
2.1	Leucemia	18
2.1.1	Leucemia Mieloide Aguda (LMA)	19
2.1.2	Panorama genético da LMA e prognóstico	23
2.1.3	Intervenções terapêuticas da LMA	26
2.2	Alvos terapêuticos para o tratamento da LMA	30
2.2.1	Células-tronco leucêmicas (CTLs)	30
2.2.2	Vias de sinalização	33
2.3	Produtos naturais	39
2.3.1	Tingenona e 22-hidroxitingenona	39
2.3.2	Piplartina	41
3	OBJETIVOS	42
3.1	Objetivo geral	42
3.2	Objetivos específicos	42
4	RESULTADOS	43
4.1	Capítulo I	43
4.2	Capítulo II	68
5	DISCUSSÃO	144
6	CONCLUSÃO	151
	REFERÊNCIAS	152
	ANEXOS	163

1 INTRODUÇÃO

A leucemia mieloide aguda (LMA) é uma neoplasia hematológica geneticamente heterogênea, caracterizada pela proliferação descoordenada de células precursoras mieloides e pela substituição da hematopoiese normal na medula óssea (YANG et al., 2019; NEWELL; COOK, 2021). De acordo com a Sociedade Americana de Câncer, a LMA é um dos tipos de leucemia mais comum em adultos, geralmente é uma doença da idade adulta tardia, mas pode ocorrer em todas as idades (AMERICAN CANCER SOCIETY, 2023).

Segundo a projeção do Globocan, em 2020, houve uma estimativa de 474.519 novos casos e 311.594 mortes por leucemia em todo o mundo (SUNG et al., 2021). Entre as formas de leucemia, a LMA é a mais letal, e cerca de 20.380 novos casos e 11.310 mortes foram estimados nos Estados Unidos para o ano de 2023. A LMA continua sendo uma doença com mau prognóstico e a taxa de sobrevivência relativa em 5 anos (2008-2014) é de 25% em adultos (20 anos ou mais) e 67% em pacientes de 0 a 19 anos (AMERICAN CANCER SOCIETY, 2023). Para o Brasil, o número estimado de casos novos de leucemia, para cada ano do triênio de 2023 a 2025, é de 11.540 casos, o que corresponde a um risco estimado de 5,33 por 100 mil habitantes, sendo 6.250 em homens e 5.290 em mulheres (INCA, 2022).

A quimioterapia intensiva anti-LMA padrão permanece quase inalterada por décadas, que inclui o uso de citarabina (Ara-C) e antraciclínicas (daunorrubicina ou idarrubicina) (NEWELL; COOK, 2021). Embora as reduções nos blastos leucêmicos possam ser alcançadas inicialmente com a quimioterapia convencional e transplante de células-tronco, os resultados a longo prazo não são satisfatórios, devido as altas taxas de recidiva (GREEN; KONIG, 2020).

A recidiva ainda é um cenário muito comum no tratamento de LMA e ocorre em 40 a 50% dos pacientes mais jovens e na grande maioria dos pacientes idosos (THOL; GANSER, 2020). Ainda que os avanços no tratamento tenham levado a melhorias significativas nos resultados para pacientes mais jovens, a sobrevivência em pacientes idosos permanece baixa, com apenas pequenas melhorias (de 8 para 17%) (DE LEEUW et al., 2022). Além disso, até 80% dos pacientes que desenvolvem LMA, com 65 anos ou mais morrerá dentro de um ano após o diagnóstico (SHALLIS et al., 2019). Portanto, o desenvolvimento de novas terapias anti-LMA são urgentemente necessárias, especialmente com intuito de melhorar os resultados para pacientes mais velhos ou que não são elegíveis a terapia padrão e aqueles que desenvolvem doença refratária.

Os produtos naturais representam uma fonte importante e útil de agentes antineoplásicos ao longo dos anos. No que diz respeito a terapia do câncer, até 60% dos candidatos

antineoplásicos em uso clínico que apresentaram eficácia significativa são derivados de produtos naturais (ALI ABDALLA et al., 2022; NAEEM et al., 2022). Nesse contexto, no presente trabalho investigamos o efeito antileucêmico dos produtos naturais, tingenona (TG) e a 22-hidroxitingenona (22-HTG) e a piplartina (PL, também conhecida como piperlongumina). A TG e 22-HTG são triterpenos quinonametídeos encontrados na planta amazônica *Salacia impressifolia* (Celastraceae). Esses compostos foram relatados como agentes citotóxicos em diferentes tipos de câncer, como por exemplo, câncer de mama, colón, fígado, melanoma e leucemias (BAVOVADA et al., 1990; CEVATEMRE et al., 2016; RODRIGUES et al., 2019; ARANHA et al., 2020; ARANHA et al., 2021). No nosso estudo, investigamos pela primeira vez o mecanismo de ação anti-LMA desses compostos.

PL é um alcalóide amida que pode ser isolado dos frutos e raízes de plantas da espécie *Piper*. Este produto natural tem sido estudado amplamente, pois apresenta uma gama de propriedades biológicas, incluindo um potencial significativo na prevenção e tratamento do câncer (PARAMA et al., 2021). A PL já vem sendo estudada pelo nosso grupo e por outros grupos de pesquisa, devido as numerosas evidências que demonstram a capacidade deste alcaloide e seus análogos e nanoformulações em modular várias vias moleculares complexas, e inibir diferentes características do câncer, como sobrevivência celular, proliferação, invasão, angiogênese, transição epitelial-mesenquimal, metástases etc. (BEZERRA, 2021; PARAMA et al., 2021). Diante do exposto, decidimos estudar o efeito antileucêmico de PL com enfoque nas células-tronco e progenitoras leucêmicas (CTPLs), uma vez que a recidiva é um cenário comum na LMA e acredita-se que seja devida à resistência dessa subpopulação de células às terapias padrão atuais.

2 REVISÃO DE LITERATURA

2.1 Leucemia

A leucemia é uma neoplasia maligna dos glóbulos brancos (leucócitos), geralmente, de origem desconhecida. Trata-se de uma doença complexa caracterizada pela expansão clonal de células progenitoras defeituosas na medula óssea e consequente falha na hematopoiese, levando a supressão de células sanguíneas normais (CI et al., 2022). No Brasil, é a décima neoplasia mais prevalente (sem considerar os tumores de pele não melanoma) e estimam-se 11.540 casos novos de leucemia para cada ano do triênio 2023-2025. Esses valores correspondem a um risco estimado de 5,90 casos novos a cada 100 mil homens e 4,78 a cada 100 mil mulheres. Em relação à mortalidade, em 2020, ocorreram 6.738 óbitos por leucemia no Brasil (3,18 por 100 mil) (INCA, 2022).

A hematopoiese é o processo de formação dos diferentes tipos de células sanguíneas da medula óssea. Esse processo se inicia com as células-tronco hematopoiéticas multipotentes, as quais possuem a capacidade de se dividir em uma célula progenitora multipotente ou de se autorrenovar. As células progenitoras multipotentes possuem a capacidade de se dividir em duas principais linhagens celulares: o progenitor mielóide comum ou o progenitor linfóide comum. Os progenitores mielóides comuns darão origem aos granulócitos, eritrócitos, megacariócitos e monócitos; e os progenitores linfóides produzirão as células *natural killer* (NK), bem como os linfócitos B e T. As células mielóides proliferam nas células terminais maduras dentro da própria medula óssea, enquanto os precursores linfóides migram para os órgãos linfóides (linfonodos, baço e timo) para completar a maturação (ZHANG et al., 2018).

As leucemias são classificadas com base na taxa proliferativa, sendo divididas em agudas ou crônicas, e com base na célula de origem, sendo classificadas como mielóides ou linfóides. Desta forma, a classificação combinada geram quatro subtipos: a leucemia linfóide crônica (LLC), como o nome sugere afeta a célula linfóide, originada de células mais diferenciadas, desenvolve-se de maneira lenta e acomete pessoas com idade superior a 55 anos; a leucemia linfóide aguda (LLA) tem um processo de agravamento mais acelerado, originário de células progenitoras, e é o tipo mais comum em crianças, mas pode haver casos deste tipo em adultos; a leucemia mielóide crônica (LMC) afeta a célula mielóide, originada de células diferenciadas e se manifesta lentamente principalmente em adultos e, a leucemia mielóide aguda (LMA) que tem uma rápida evolução e ocorre em qualquer uma das faixas etárias, sendo o tipo mais agressivo com prognóstico variável dependendo dos subtipos moleculares, e é

originada de células progenitoras (**Figura 1**). Esta multiplicação preferencial de células leucêmicas leva à diminuição da produção de células normais. Tanto a leucemia mieloide, quanto a linfóide, surgem de múltiplas mutações genéticas que permitem a proliferação não controlada e a maturação anormal. Geralmente as leucemias agudas requerem um diagnóstico precoce, para que se inicie o tratamento de forma imediata devido ao prognóstico desfavorável (INCA, 2022; AMERICAN CANCER SOCIETY, 2023).

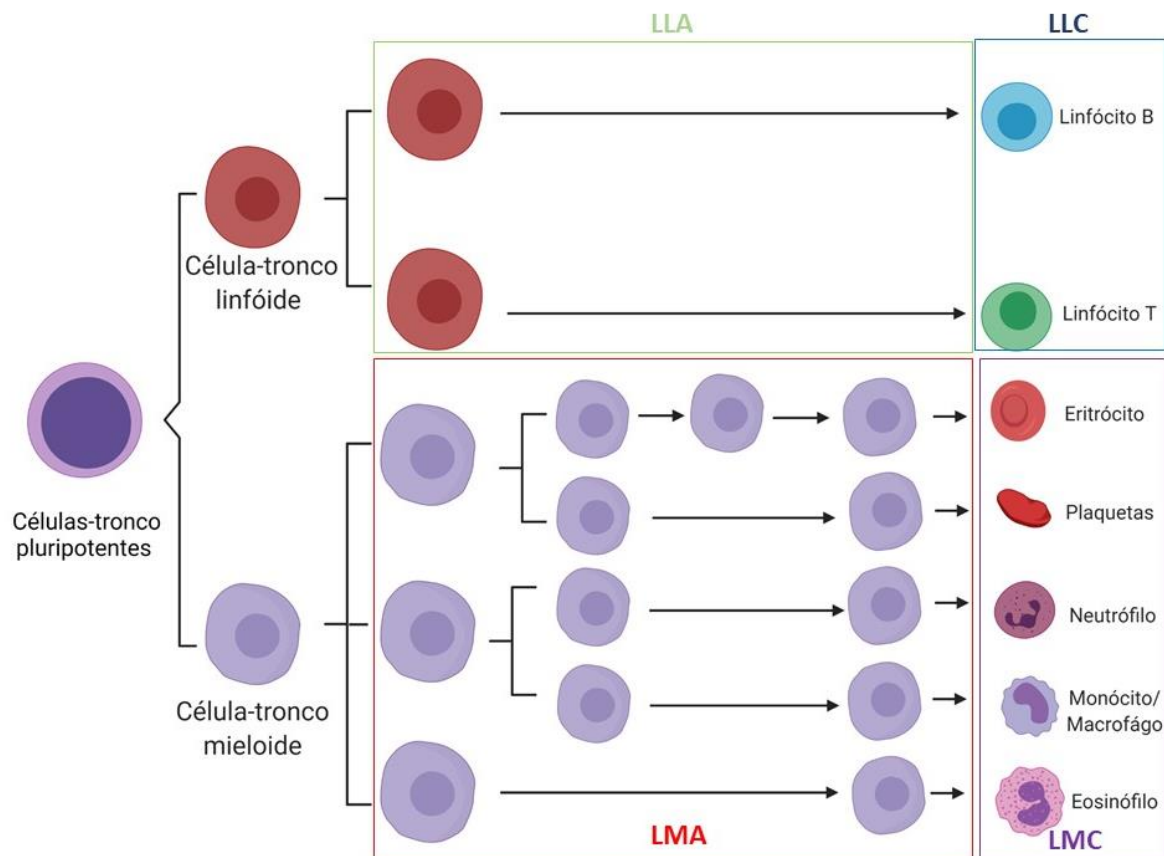


Figura 1 - Esquema da hematopoiese e possível desenvolvimento de leucemia. Após a ativação, as células-tronco são capazes de se diferenciar em progenitores clonais que podem se expandir exponencialmente, bem como continuar o processo de diferenciação. As células hematopoiéticas são amplamente divididas em células "linfóides" e "mielóides". As células linfóides se diferenciam em células T, células B, células NK e células dendríticas. As células mielóides incluem glóbulos vermelhos, plaquetas, monócitos/macrófagos e granulócitos. Diferentes tipos de leucemia podem ocorrer durante a hematopoiese: leucemia mieloide aguda (LMA), leucemia linfóide aguda (LLA), leucemia mieloide crônica (LMC) e leucemia linfóide crônica (LLC).

Fonte: Elaborado pela autora. Criado com BioRender.com.

2.1.1 Leucemia Mieloide Aguda (LMA)

A leucemia mieloide aguda é uma neoplasia maligna dos precursores de células-tronco da linhagem mieloide (hemácias, plaquetas e glóbulos brancos, exceto B e T). Assim como outras doenças malignas, a LMA ocorre devido a variações genéticas que resultam em

alterações neoplásicas e proliferação clonal. Ainda é considerada uma doença maligna rara, sendo mais comum em adultos, com uma incidência de mais de 20.000 casos por ano apenas nos Estados Unidos (PELCOVITS; NIROULA, 2020).

Como citado anteriormente, a LMA é uma neoplasia comum em adultos e a segunda leucemia mais comum em crianças. A incidência aumenta com a idade, e esse fator também está associado a uma maior frequência de anormalidades citogenéticas e moleculares. A idade mediana no diagnóstico de LMA é de 67 anos, com aproximadamente um terço dos pacientes diagnosticado acima dos 75 anos (DAVER et al., 2020). A sobrevida de cinco anos para pacientes com LMA é de 28,3%, e assim como a incidência, a porcentagem de mortes também aumenta com a idade, sendo maior em pacientes com 75 anos ou mais (43,7%). Sendo assim, a LMA ainda se apresenta num cenário preocupante, devido ao seu baixo prognóstico (NEWELL; COOK, 2021).

A LMA possui vários subtipos e neoplasias precursoras que se distinguem umas das outras pela morfologia, imunofenótipo, citoquímica e anormalidades genéticas, na qual todas têm implicações importantes no que diz respeito ao prognóstico e o tratamento da doença (HWANG, 2020). Um sistema de classificação de LMA atualizado e um novo foram publicados no ano de 2022, ambos utilizando novas descobertas na fisiopatologia da LMA e enfatizando a integração da análise molecular na prática diária da doença (SHIMONY et al., 2023). Na 5ª edição revisada da classificação da OMS publicada em 2022, a LMA é classificada em duas principais famílias: LMA com anormalidades genéticas definidas (**Figura 2**) e LMA definida por diferenciação.

Classificação OMS - 5ª edição

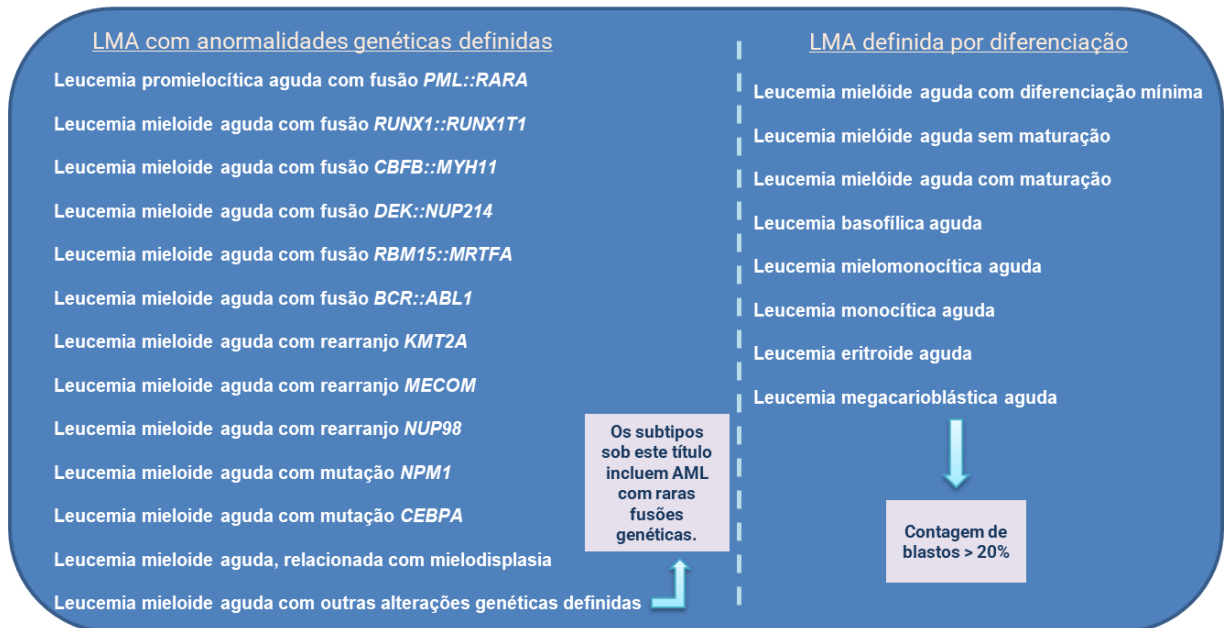


Figura 2 - O sistema de estadiamento da OMS (Organização Mundial de Saúde) divide a LMA em duas principais famílias (KHOURY et al., 2022).

Fonte: Elaborada pela autora.

Já a Classificação de Consenso Internacional (CCI) da European Leukemia Network (ELN 2022), baseia sua estrutura de acordo com uma ordem hierárquica, sendo dividida em: LMA com anormalidades genéticas recorrentes, LMA com mutação em *TP53* (VAF > 10%), LMA com mutações genéticas relacionadas à mielodisplasia, LMA com anormalidades citogenéticas relacionadas à mielodisplasia, LMA não especificada e sarcoma mieloide (ARBER et al., 2022). Ambos os sistemas de classificação incorporaram consideração especial para exposição citotóxica prévia e predisposição genética. Na classificação da OMS, foram reclassificadas em uma nova categoria diagnóstica denominada neoplasias mieloides secundárias, que engloba as neoplasias mieloides surgidas após terapia citotóxica ou que possuem uma predisposição germinativa definida. Na classificação CCI, estes não foram definidos como um grupo separado, mas como qualificadores adicionados ao diagnóstico da LMA (SHIMONY et al., 2023). A **figura 3** exemplifica as principais diferenças e similaridades entre as duas classificações.

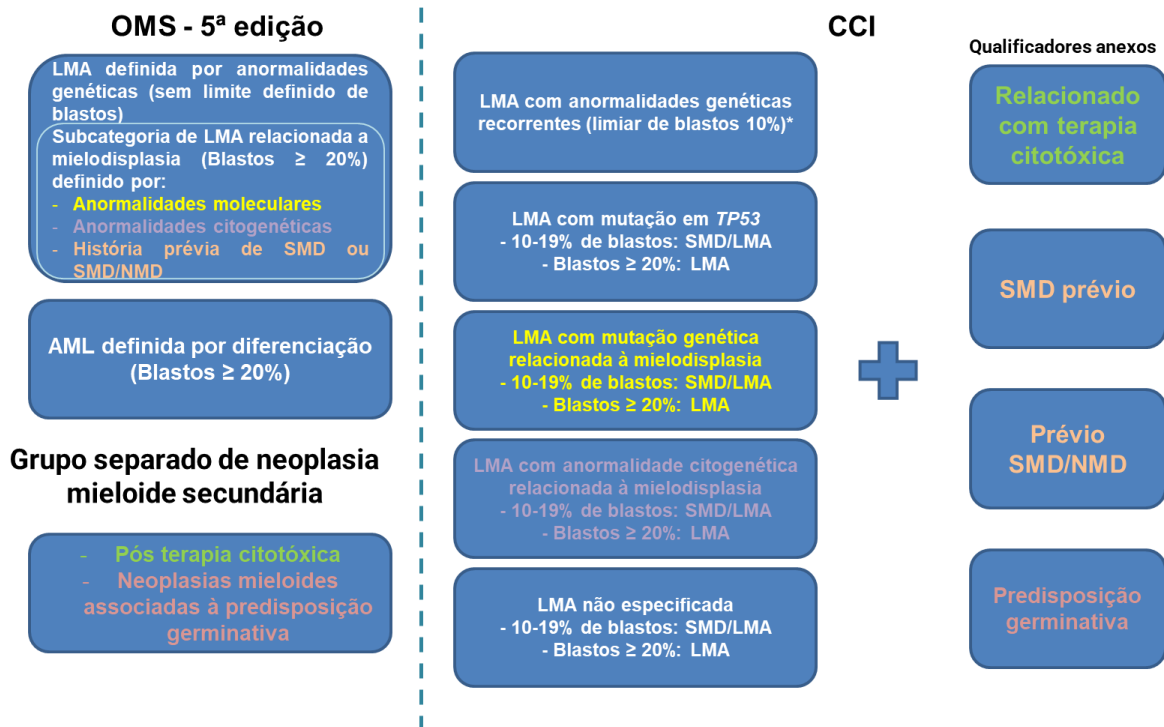


Figura 3 - Comparação entre as classificações de LMA da 5ª edição da OMS versus CCI. *com exceção $\geq 20\%$ exigido para LMA com *BCR:: ABL1* e LMA com *CEBPA* de acordo com a OMS e $\geq 20\%$ pra LMA com *BCR:: ABL1*. As cores sinalizam subgrupos semelhantes entre as duas classificações. LMA: mieloide leucemia aguda; SMD: síndrome mielodisplásica; CCI: classificação de consenso internacional; NMD: neoplasia mielodisplásica; OMS: Organização Mundial da Saúde.

Fonte: Adaptado de (SHIMONY et al., 2023).

O desenvolvimento de LMA tem sido associado a alguns fatores de risco. Geralmente, os fatores de risco conhecidos representam apenas um pequeno número de casos observados. Estes incluem idade, doença hematológica antecedente e distúrbios genéticos; bem como exposições a vírus, radiação, produtos químicos ou outros riscos ocupacionais e quimioterapia prévia (AMERICAN CANCER SOCIETY, 2018). Sem dúvida, a predisposição genética também tem um papel importante no desenvolvimento da LMA, além disso, várias desordens genéticas, como por exemplo, síndrome de Down, anemia de Fanconi, síndrome de Bloom, ataxia-telangiectásica, síndrome de Schwachman-Diamond, neurofibromatose tipo 1, são associadas com um aumento do risco da doença (TEBBI, 2021). Adicionalmente, um estudo realizado por pesquisadores chineses demonstrou que o tabagismo, o alto índice de massa corporal, exposição ocupacional ao benzeno e formaldeído foram os principais fatores de risco para mortalidade relacionada à LMA (YI et al., 2020).

A leucemia promielocítica aguda (LPA) é uma forma rara, porém agressiva, de LMA e possui características biológicas e clínicas particulares. A LPA representa aproximadamente 10-15% dos casos de LMA recém-diagnosticados, e é resultado de uma translocação balanceada, $t(15;17)(q22;q12-21)$, que leva à fusão do gene da leucemia promielocítica (PML)

com o gene do receptor alfa do ácido retinóico (RAR α). A oncoproteína de fusão PML-RAR α induz leucemia resultando em proliferação descontrolada e inibição da diferenciação mielóide normal (KAMATH et al., 2019; YILMAZ et al., 2021).

A LPA geralmente se desenvolve em pacientes mais jovens comparado com a LMA não LPA; a idade média no momento do diagnóstico é de 40 anos. É uma doença conhecida por ocorrer com mais frequência em pacientes de origem hispânica ou latina em comparação com brancos; e a obesidade também já foi relatada como característica prevalente nesta doença (JIMENEZ et al., 2020; YILMAZ et al., 2021). Ao contrário de outras formas de LMA, a LPA é única, pois pode causar coagulopatia e morte se não for prontamente diagnosticada. E, embora a LPA tenha um prognóstico historicamente ruim, os regimes de tratamento contendo ácido trans-retinóico (ATRA), antraciclinas e trióxido de arsênico (ATO) alcançam taxas de remissão próximas a 90% e taxas de cura de 80%. Apesar da melhora na sobrevida global, a LPA é considerada uma emergência médica. A morte precoce, dentro de 1 mês após o diagnóstico, ocorre em cerca de 17,3% dos casos, mais frequentemente atribuída a hemorragia intracraniana ou pulmonar grave (JIMENEZ et al., 2020). Além disso, de 5 a 10% dos pacientes com LPA desenvolvem doença recidivante e/ou refratária (R/R). A maioria das recaídas ocorre nos primeiros três anos, e recaídas tardias acima de três a quatro anos são muito raras (YILMAZ et al., 2021).

2.1.2 Panorama genético da LMA e prognóstico

Como mencionado anteriormente, a LMA é uma doença complexa e heterogênea em termos de características clínicas, patogênese e resposta ao tratamento. É marcada por uma variedade de anormalidades citogenéticas recorrentes e mutações que influenciam o fenótipo da doença, a resposta às terapias convencionais, o risco de recorrência e a sobrevida do paciente (SHORT et al., 2020). Os avanços recentes nas técnicas genômicas desvendaram a complexidade molecular da leucemogênese da LMA, o que, por sua vez, levou ao refinamento da estratificação de risco e estratégias terapêuticas personalizadas para pacientes que desenvolvem a doença (HOU; TIEN, 2020). Embora os casos possam ser estratificados em grupos favoráveis, intermediários e de risco adverso com base em seu perfil citogenético, o prognóstico nessas categorias varia amplamente (PELCOVITS; NIROULA, 2020). Dessa forma, discutir os marcadores genéticos mais relevantes na LMA tem um papel fundamental no prognóstico e implicações terapêuticas da doença (HOU; TIEN, 2020).

O prognóstico na LMA depende de vários fatores, embora um dos mais fortes seja a genética subjacente da LMA. Já é descrito na literatura que mais de 95% dos pacientes com LMA têm mutações condutoras e concomitantes, independentemente da presença de anormalidades citogenéticas (HOU; TIEN, 2020). Ademais, pacientes diagnosticados com LMA cujas células leucêmicas possuem certas mutações genéticas podem ter um melhor ou pior prognóstico. Como citado anteriormente, de acordo com a ELN 2022, a LMA divide-se em categorias de risco favorável, intermediário e adverso (ARBER et al., 2022).

Esta classificação é baseada em alterações citogenéticas detectadas por cariótipo ou por hibridização fluorescente *in situ* (FISH), bem como mutações em um único gene. De acordo com esse sistema, pacientes com LMA que possuem mutação, por exemplo, em *NPM1* (sem outras alterações), ou algumas mutações do *CEPBA* estão associadas a um melhor prognóstico. Já mutações em *RUNX1*, *ASXL1* e *TP53* estão relacionadas a um prognóstico desfavorável.

Além disso, a categorização da ELN 2022, incorpora interações gene-gene específicas para estimar o prognóstico (por exemplo, pacientes com *FLT3-ITD* têm um prognóstico relativamente melhor com uma mutação *NPM1* concomitante) (**Tabela 1**). Vale ressaltar, que embora essa estratificação de risco seja útil para orientar a terapia adaptada ao risco para pacientes com LMA, eles não irão prever adequadamente os resultados em pacientes idosos e naqueles que recebem tratamento não intensivo (STUBBINS et al., 2022).

Tabela 1 - Classificação de risco da ELN 2022.

Categoria de risco	Anormalidade Genética
Favorável	t (8;21) (q22;q22.1); <i>RUNX1-RUNX1T1</i> inv (16) (p13.1q22) ou t (16;16) (p13.1;q22); <i>CBFB-MYH11</i> <i>NPM1</i> mutante sem <i>FLT3-ITD</i> bZIP mutante in-frame <i>CEBPA</i>
Intermediário	<i>NPM1</i> mutante com <i>FLT3-ITD</i> <i>NPM1</i> de tipo selvagem com <i>FLT3-ITD</i> t (9;11) (p21.3;q23.3); <i>MLLT3-KMT2A</i> Anormalidades citogenéticas não classificadas como favoráveis ou adversas
Adverso	t (6;9) (p23;q34.1); <i>DEK-NUP214</i> t (v;11q23.3); rearranjo <i>KMT2A</i> t (9;22) (q34.1;q11.2); <i>BCR-ABL1</i> inv(3) (q21.3q26.2) ou t (3;3) (q21.3;q26.2); <i>GATA2</i> , <i>MECOM(EV11)</i> t (3q26.2;v); rearranjo <i>MECOM (EV11)</i> -5 ou del (5q); -7; -17/abn (17p) Cariótipo complexo, cariótipo monossômico <i>ASXL1</i> , <i>BCOR</i> , <i>EZH2</i> , <i>RUNX1</i> , <i>SF3B1</i> , <i>SRSF2</i> , <i>STAG2</i> , <i>U2AF1</i> ou <i>ZRSR2</i> mutante <i>TP53</i> mutante

Fonte: (STUBBINS et al., 2022)

A desregulação de modificadores epigenéticos, incluindo alterações na metilação do DNA, hidroximetilação do DNA e modificações nas histonas, como metilação, acetilação, fosforilação, sumoilação e ubiquitinação, desempenham um papel crítico na patogênese da LMA. Mutações somáticas em genes que regulam modificações epigenéticas, como *IDH*, *TET2*, *DNMT3A*, *ASXL1*, *EZH2* e *KMT2A* são frequentemente detectadas em pacientes com LMA, especialmente aqueles com citogenética de risco intermediário (HOU; TIEN, 2020).

Vários estudos demonstram que 70% das mutações recorrentes em pacientes com LMA ocorrem em reguladores de expressão gênica, como proteínas epigenéticas, fatores de transcrição e componentes da maquinaria de *splicing* (TYNER et al., 2018). Adicionalmente, as alterações epigenéticas geralmente se apresentam como eventos pré-leucêmicos precoces, que cooperam com outras alterações genéticas no desenvolvimento da LMA. Mutações em *ASXL1*, *TET2* e *DNMT3A*, bem como rearranjos *KMT2A* conferem um mau prognóstico,

enquanto mutações *IDH* e *EZH2* podem significar um prognóstico mais favorável (HOU E TIEN, 2020; KANTARJIAN et al., 2021).

Além dos fatores genéticos e moleculares, vários outros fatores relacionados ao paciente são importantes a serem considerados ao estimar o prognóstico. Subgrupos, como LMA relacionada à terapia (t-LMA) ou LMA decorrente de uma neoplasia mieloide prévia (ou seja, LMA secundária), têm um prognóstico pior do que a LMA de novo. Além disso, o resultado dos pacientes neste grupo ainda é afetado pela genética da doença. A resposta ao tratamento inicial é outro fator prognóstico importante e os pacientes que não entram em remissão após 1 a 2 ciclos de quimioterapia intensiva têm um resultado desfavorável. Mesmo em pacientes que entram em remissão morfológica, a presença de doença residual mensurável (DRM) tem sido consistentemente associada a um pior resultado e é um fator prognóstico independente para recívida e sobrevida global de 5 anos, em estudos prévios realizados (STUBBINS et al., 2022).

2.1.3 Intervenções terapêuticas da LMA

O tratamento da LMA irá depender da condição médica geral do paciente. Pacientes clinicamente aptos tendem a ser mais jovens e apresentam anormalidades citogenéticas de menor risco, melhor estado funcional e menos comorbidades do que pacientes clinicamente frágeis. Além disso, uma incidência aumentada de citogenética desfavorável contribui para um resultado ruim em pacientes com idade maior do que 56 anos. Fatores relacionados à idade, incluindo comorbidades, provavelmente interagem com fatores de risco biológicos, resultando em uma grande diferença nos resultados. A identificação de anormalidades citogenéticas recorrentes avança nossa compreensão da biologia da LMA e irá orientar a tomada de decisões na prática clínica (ROLOFF et al., 2022).

Em geral, a quimioterapia continua sendo uma importante modalidade de terapia para os pacientes que desenvolvem LMA (MIRANDA et al., 2018). Até recentemente, a genética ou o subtipo de LMA não tinham um impacto significativo na escolha de indução de primeira linha. Historicamente, a primeira linha de tratamento para LMA para todos os pacientes elegíveis e aptos seria com uma combinação padrão de antraciclina (geralmente daunorrubicina ou idarrubicina) administrado por 3 dias e citarabina administrada por 7 dias consecutivos, que passou a ser conhecido como regime quimioterápico “7 + 3” (NEWELL; COOK, 2021). Os tratamentos de menor intensidade também pode ser empregados, com um agente hipometilante, como azacitidina (AZA) ou decitabina, ou baixa dose de citarabina (STANCHINA et al., 2020).

Embora o regime de quimioterapia “7 + 3” possa induzir remissão em até 60% dos pacientes, a quimioterapia intensiva muitas vezes não é uma opção viável para alguns pacientes devido à idade avançada, estado funcional ruim, comorbidades significativas ou disfunção orgânica.

Apesar da idade por si só não ser um motivo específico para evitar a quimioterapia intensiva, os pacientes mais velhos em geral apresentam características de alto risco, como LMA com alterações relacionadas à mielodisplasia, LMA relacionada à terapia, cariótipo complexo ou mutação em *TP53*, e são menos propensos a responder à quimioterapia. Apesar de novas terapias serem necessárias para melhorar os regimes de quimioterapia intensiva padrão, regimes de menor intensidade mais eficazes têm recebido uma maior atenção nos últimos anos, pois são extremamente necessários para pacientes idosos (KANTARJIAN et al., 2021; STANCHINA et al., 2020).

A quimioterapia intensiva padrão para LMA está em uso há mais de 40 anos. Há pouco tempo, grandes avanços na biologia molecular e celular melhoraram a compreensão da fisiopatologia da doença, expandiram as opções de tratamento e forneceram uma compreensão mais profunda de como e por que pacientes individuais podem estar sob risco aumentado de desenvolvimento de leucemia. Esses avanços fornecem opções de tratamento personalizadas para muitos pacientes e podem fornecer oportunidades futuras para prevenir o desenvolvimento de LMA (HOU; TIEN, 2020).

Nos últimos 5 anos, esse cenário vem sendo mudado, devido a aprovação de novos agentes no tratamento de linha de frente, incluindo midostaurina para pacientes com mutações *FLT3*, gemtuzumab-ozogamicina (GO) para pacientes com cariótipo de risco intermediário ou favorável e CPX-351 para pacientes com LMA secundária (STUBBINS et al., 2022). A **tabela 2** sumariza as terapias incorporadas para o tratamento de LMA nos últimos anos.

Tabela 2 - Visão geral de medicamentos mais recentes aprovados para LMA.

Tratamento	Indicação	Status de aprovação
Midostaurina	FLT3 + linha de frente com quimioterapia intensiva	Aprovado HC/FDA (linha de frente)
Gilteritinibe	FLT3 + R/R	Aprovado HC/FDA (R/R)
Gemtuzumabe- ozogomicina	Favorável/Intermediária/Citogenética desconhecida Linha de frente com quimioterapia intensiva	Aprovado HC/FDA (linha de frente)
CPX-351	Linha de frente LMA secundária	Aprovado HC/FDA (linha de frente)
Azacitidina oral (CC-486)	Manutenção após quimioterapia intensiva, pacientes não elegíveis para TCTH	Aprovado HC/FDA (manutenção pós terapia indutora)
Venetoclax	Idosos/inaptos linha de frente com azacitidina	Aprovado HC/FDA (linha de frente e terapia de indução para pacientes inaptos)

HC, Health Canada; FDA, Food and Drug Administration.

Fonte: (STUBBINS et al., 2022).

Embora a maioria dos pacientes aptos atinja inicialmente a remissão completa após a quimioterapia de indução, um número significativo de pacientes eventualmente apresenta recidiva ou doença refratária, o que ressalta a necessidade não atendida de novas terapias que foquem nessas dificuldades. Além disso, a sobrevida a longo prazo dos pacientes não é otimista devido à alta taxa de recidiva após a remissão completa (MEDEIROS et al., 2019). A remissão é um importante alvo de tratamento, pois geralmente é um requisito para a administração de terapia pós-remissão com intenção curativa, como quimioterapia de consolidação baseada em citarabina ou transplante de células-tronco hematopoiéticas (TCTH). A LMA recidivante após TCTH apresenta um desafio clínico particularmente complicado porque as toxicidades relacionadas ao transplante, como enxerto contra hospedeiro e infecções, aumentam o risco de morbidade e mortalidade relacionadas ao tratamento. Em geral, o prognóstico da recidiva de LMA após TCTH é ruim, com a maioria dos pacientes falhando em alcançar uma remissão subsequente e sobrevida de 2 anos < 15% (WEBSTER et al., 2021).

Dessa forma, por ser uma doença altamente heterogênea, a LMA exige aconselhamento e abordagens terapêuticas específicas para cada paciente, apresentando muitos desafios e questões não resolvidas. A necessidade de medicamentos mais eficazes e direcionados a alvos importantes, faz-se necessário no intuito de diminuir a recorrência e aumentar a sobrevida dos pacientes (KANTARJIAN et al., 2021). Para isso, é fundamental o desenvolvimento de novas terapias tanto na linha de frente quanto no cenário de recidiva ou refratariedade (R/R) (BEWERSDORF; ABDEL-WAHAB, 2022).

Em relação ao tratamento da LPA, a utilização de ATRA e ATO revolucionou o tratamento da doença (STAHL; TALLMAN, 2019). O ATRA causa uma alteração conformacional dos transcritos de fusão PML-RAR α , levando à liberação dos co-repressores, recrutamento de histonas acetiltransferases e alívio da repressão transcricional, o que faz com que as células de LPA tratadas sofram diferenciação mieloide terminal e, finalmente, apoptose. Espera-se que mais de 80-90% dos pacientes com LPA sejam curados com uma combinação de ATRA, ATO e/ou quimioterapia (YILMAZ et al., 2021).

Embora a utilização de ATRA e ATO tenha melhorado a sobrevida a longo prazo para 80-90% ou mais dos pacientes, alguns desafios permanecem no tratamento de LPA. Os principais obstáculos remanescentes para a cura dos pacientes são o risco de morte precoce, relativamente alto devido a coagulopatia e hemorragia, bem como o cuidado de pacientes de alto risco e pacientes com doença recidivante (STAHL; TALLMAN, 2019). A probabilidade de recidiva é significativamente maior no subconjunto de pacientes de alto risco em tratamento para LPA; em geral, aproximadamente 10-20% dos pacientes com LPA recidiva,

independentemente de sua estratificação de risco. Ademais, o desenvolvimento de resistência ao ATO também é um problema associado ao tratamento deste subtipo de leucemia, e os pacientes que se tornam resistentes a este medicamento têm um risco aumentado de mortalidade (JIMENEZ et al., 2020). Tratamentos alternativos e abordagens considerando esses resultados clínicos são necessários para abordar a resistência ATO, bem como a taxa de recaída em LPA de alto risco e atender às necessidades terapêuticas de pacientes que não respondem ao tratamento convencional.

2.2 Alvos terapêuticos para o tratamento da LMA

2.2.1 Células-tronco leucêmicas (CTLs)

O conceito de células-tronco cancerosas (CTCs) foi introduzido há mais de um século e refere-se a uma subpopulação de células relativamente inativas em um tumor que possuem a capacidade de se autorrenovar e se diferenciar em células filhas não-tronco. Essas células são responsáveis pela iniciação do câncer e são resistentes às abordagens terapêuticas anticâncer (ATASHZAR et al., 2020).

As células-tronco leucêmicas (CTLs) foram identificadas como tendo um papel importante na patogênese, no desenvolvimento e na manutenção da leucemia (PASSEGUE et al., 2008; KIZAKI, 2018). Embora o número de CTLs seja pequeno, estas têm o mesmo potencial de autorrenovação, diferenciação multidirecional, proliferação ilimitada, resistência à morte celular, resistência a múltiplos fármacos, metástase e recorrência, pois podem escapar da inibição pela maioria dos quimioterápicos e podem ficar em um estado relativamente inativo por um longo tempo (YANG et al., 2019).

As CTLs e as células-tronco hematopoiéticas normais (CTHNs) compartilham algumas características importantes, como autorrenovação, multipotência, quiescência e heterogeneidade. Em comparação com as CTHNs, as CTLs exibem mutações específicas, modificações epigenéticas e um perfil metabólico específico (MARCHAND; PINHO, 2021). A aplicação de metodologias genômicas levou à identificação de CTHNs pré-leucêmicas em pacientes com LMA que não geram leucemia *in vivo*, mas carregam mutações motoras competitivas precoces, normalmente em genes reguladores epigenéticos (THOMAS; MAJETTI, 2017). As CTHNs pré-leucêmicas têm melhor vantagem de clonagem do que CTHNs normais e não perdem sua capacidade de diferenciação em diferentes linhagens. Com

o acúmulo de mutações, as CTNHs pré-leucêmicas são eventualmente transformadas em CTLs, que iniciam a LMA (VETRIE et al., 2020).

Quando as CTHNs se transformam em CTLs, estas células adquirem algumas propriedades biológicas exclusivas, devido às mutações genéticas e epigenéticas, como por exemplo, aquisição de vias de sinalização de sobrevivência favoráveis para manter a autorrenovação, proliferação e resistência aos medicamentos e mudança do estado celular ou molecular, refletindo na plasticidade dessas células. Além disso, as CTLs estão localizadas em nichos na medula óssea e são capazes de manter níveis baixos de ERO e possuem uma dependência maior da função mitocondrial em comparação com as CTHNs (TAN et al., 2020).

A maioria das amostras de LMA (75%) são positivas para a expressão de CD34, estando presente em 0,1% dos blastos, e quase todos os estudos de CTLs de LMA focalizaram neste subgrupo. Em estudos pioneiros, as CTLs mostraram ser positivas para a expressão de CD34 e negativas para a expressão de CD38. Elas possuem a capacidade de se autorrenovar e diferenciar quando transplantadas em camundongos imunodeficientes, identificando-as então como uma pequena população de células CD34⁺/CD38⁻ na medula óssea (BONNET; DICK, 1997; LAPIDOT et al., 1994; THOMAS; MAJETTI, 2017).

No entanto, outros trabalhos mostraram que dependendo do tipo e estágio da doença, algumas CTLs também podem ser encontradas em subpopulações de células CD34⁺ CD38⁺ ou em subfração de células CD34⁻ (TAUSSIG et al., 2010; SARRY et al., 2011; HERRMANN et al., 2020). Em muitos estudos, as CTLs ainda são consideradas residindo na fração CD34⁺ CD38⁻, porque é possível estabelecer com sucesso um modelo de leucemia em animais com menos defeitos imunológicos, e o CD34⁺ CD38⁻ tem uma frequência de CTLs mais alta do que a população CD34⁺ CD38⁺ (EPPERT et al., 2011; SARRY et al., 2011). Além disso, alguns outros marcadores de superfície celular foram avaliados como alvos de CTLs, incluindo CD123 (JORDAN ET AL., 2000), CD96 (HOSEN et al., 2007), CLL-1 (VAN RHENEN et al., 2007), TIM-3 (KIKUSHIGE et al., 2010; KIKUSHIGE; MIYAMOTO, 2013), CD93 (IWASAKI et al., 2015) e CD99 (CHUNG et al., 2014, 2017).

Como discutido anteriormente, a recidiva é um problema significativo na LMA e acredita-se que seja devida à resistência das CTLs subjacentes às terapias atuais, apesar dos avanços consideráveis nas terapias anticâncer (**Figura 4**) (KHALDOYANIDI et al., 2022). As CTLs são um reservatório importante de DRM, pois possuem propriedades biológicas únicas e possuem uma sensibilidade mais baixa ao tratamento em comparação ao “bulk” de células na LMA (MITCHELL; STEIDL, 2020). Essas características aumentam sua resistência e são consideradas a causa de uma eventual recaída. Portanto, existe um grande interesse no

desenvolvimento de estratégias que reduzam ou eliminem a DRM de forma específica e eficaz e que também melhorem os resultados na LMA, visando a subpopulação de CTLs (BERNASCONI; BORSANI, 2021; VAN GILS et al., 2021). De fato, muitos estudos têm demonstrado que o desenvolvimento de agentes direcionados a vias específicas de CTLs é uma abordagem promissora para a pesquisa de LMA (RODRIGUES et al., 2021; KHALDOYANIDI et al., 2022).

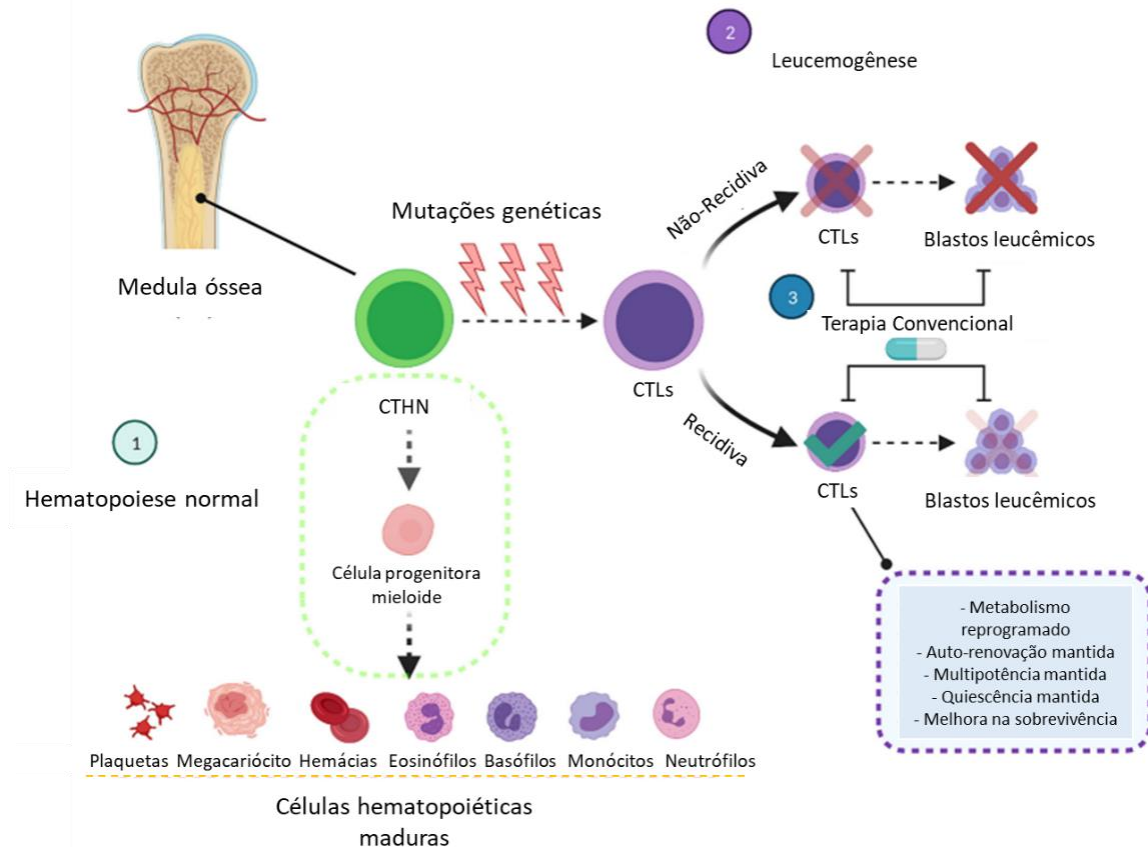


Figura 4 - A quimioterapia convencional é ineficaz para eliminar as CTLs, levando à recidiva da LMA. No sistema hematopoiético normal, as CTHNs se diferenciam em células progenitoras mielóides e eventualmente produzem células hematopoiéticas maduras. Na LMA, essas CTHNs adquirem mutações genéticas que prejudicam o processo de diferenciação e as transformam em CTLs. Embora as estratégias de tratamento atuais eliminem os blastos leucêmicos, elas são incapazes de destruir completamente as CTLs, o que causará a recidiva da LMA. CTHNs, células-tronco hematopoéticas; CTLs, células-tronco leucêmicas.

Fonte: Adaptado de (MESBAHI et al., 2022).

A quimioterapia de maneira geral, visa eliminar as células leucêmicas com metabolismo e proliferação superativados, podendo ter efeitos limitados sobre as CTLs, que geralmente se encontram quiescentes (SAITO et al., 2010). Os tratamentos direcionados às CTLs, especialmente em combinação com regimes de quimioterapia existentes ou TCTH, podem ajudar a atingir uma taxa de remissão completa mais alta e melhorar a sobrevida geral. Além disso, as CTLs mantêm sua quiescência e são concentradas e sequestradas para áreas da medula óssea, em um microambiente especializado denominado “nicho”, no qual a ação de fármacos

anticâncer é menor, e conferem a elas uma proteção maior contra espécies reativas de oxigênio e do metabolismo anaeróbico (MARCHAND; PINHO, 2021; SUMBLY et al., 2022).

Diferentes estratégias terapêuticas que visam modular a autorrenovação, proliferação, apoptose e diferenciação de CTLs, como também ter como alvo os nichos de CTLs representa uma opção promissora para tratar a LMA e estão sob investigação (TAN et al., 2020).

Interessantemente, Hanekamp e colaboradores (2018) demonstraram que a carga de CTLs no momento do diagnóstico é um preditor significativo de recaída em pacientes jovens com LMA e pode ajudar a personalizar o tratamento (HANEKAMP et al., 2018). Sendo assim, a relevância clínica das CTLs é enfatizada por estudos que mostram uma chance aumentada de recaída e pior sobrevida global em pacientes com LMA com alta frequência de CD34⁺/CD38⁻ no diagnóstico e após a terapia de indução em comparação com pacientes com baixa frequência de CTLs (HANSEN et al., 2022). Desta forma, o modelo de CTLs implica que, para erradicar a doença e obter remissões duradouras, os esquemas terapêuticos devem eliminar a população de CTLs. Embora esse objetivo final ainda não tenha sido alcançado, a caracterização detalhada das CTLs em LMA tem demonstrado suas propriedades de autorrenovação, quiescência relativa, resistência à apoptose e aumento do efluxo de fármacos, o que provavelmente as tornam menos suscetíveis a terapias convencionais voltadas para a doença (THOMAS; MAJETI, 2017).

Portanto, pesquisas e análises relevantes sobre as características biológicas das CTLs podem fornecer novas ideias para regimes terapêuticos. A descoberta de CTLs ampliou o tratamento da leucemia, e a terapia direcionada de vias de sinalização relacionadas pode se tornar um novo ponto de acesso à pesquisa, para desenvolver terapias específicas contra essa subpopulação de células.

2.2.2 Vias de sinalização

A via da proteína quinase ativada por mitogênio (MAPK) é um elo importante na mudança de sinais extracelulares para respostas intracelulares. Alterações nas cascatas de sinalização desta via são encontradas em várias doenças, incluindo o câncer, como resultado de alterações genéticas e epigenéticas. Mutações causadas pelo câncer levam à desregulação dessa via com consequente aumento da malignidade tumoral. É, portanto, uma via crítica para a sobrevivência, disseminação e resistência de células cancerosas. Tendo em vista, que a sinalização de MAPK está alterada em muitas doenças, seus componentes têm sido alvo de

estudos para o desenvolvimento de fármacos nas últimas duas décadas (BRAICU et al., 2019; LEE et al., 2020).

Existem 4 vias MAPK principais em mamíferos: a quinase regulada por sinal extracelular (ERK), quinase regulada por sinal extracelular 5 (ERK 5), quinase de junção N-terminal (JNK) e a via p38. Cada cascata consiste em 3 quinases (MAP3K, MAPKK e MAPK), onde o sinal é propagado por fosforilação e ativação sequencial de quinases que levam a fosforilação de proteínas alvo regulatórias. Geralmente a via ERK responde a sinais dos fatores de crescimento, enquanto JNK e p38 respondem a sinais de estresse extracelulares, sendo que a resposta depende da intensidade do sinal e do contexto ou tecido em que o sinal é ativado de forma aberrante (ROUX et al., 2004; KRISHNA; NARANG, 2008).

Como citado anteriormente, as vias MAPK são cascatas de três quinases, a MAPKKK pode responder a vários sinais extra e intracelulares levando a fosforilação da quinase MAPKK em seu resíduo serina e treonina. E então, as MAPKKs fosforilam e ativam exclusivamente uma MAPK, que normalmente tem muitos substratos que executam decisões de destino celular específicas adequadas ao sinal inicial (**Figura 5**) (LEE et al., 2020).

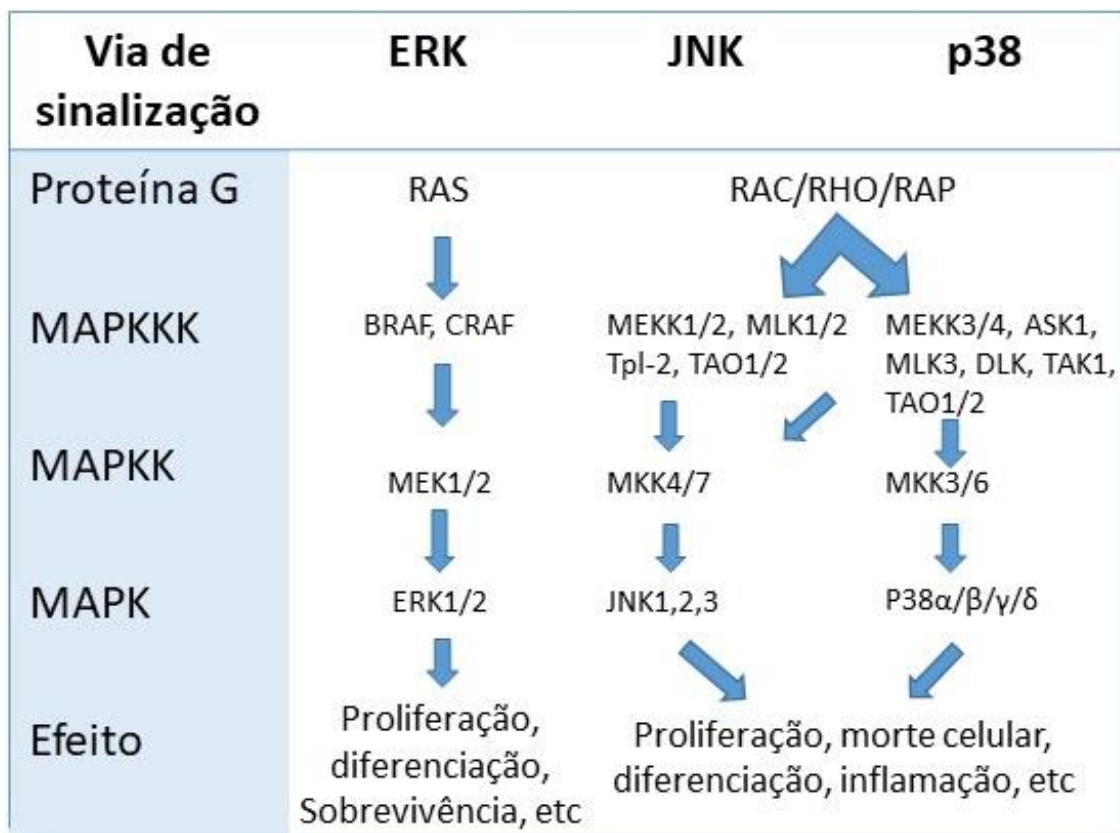


Figura 5 - Organização das vias MAPK. O núcleo de MAPK consiste em três quinases (MAPKKK, MAPKK e MAPK), que formam uma cascata de transdução de sinal que recebe entrada de proteínas G e produz diferentes efeitos biológicas.

Fonte: Adaptado de (LEE et al., 2020).

A via de sinalização ERK é responsável por processos celulares básicos, incluindo proliferação e diferenciação celular. A via RAS-RAF-MEK-ERK é alterada em ~ 40% de todos os cânceres humanos, principalmente devido a mutações em BRAF (~ 10%) e seu ativador RAS (~ 30%) (SANTARPIA et al., 2012). A disfunção na via Ras - ERK é o principal estímulo para o desenvolvimento da maioria dos tipos de câncer (GUO et al., 2020). Vários estímulos podem culminar na ativação de ERK como fatores de crescimento, citocinas, vírus, ligantes do receptor acoplado à proteína G e oncogenes. As moléculas-chave nesta via de sinalização incluem principalmente as pequenas proteínas G Ras e a quinase Raf, MEK1/2 e ERK1/2 (LEE et al., 2020).

A família JNK é codificada por três genes: JNK1, JNK2 e JNK3, que produzem pelo menos 10 subtipos de proteínas. JNK1/2 são expressos de forma ubíqua, enquanto a expressão de JNK3 é específica para alguns tecidos, como cérebro, coração e testículo (PELUSO et al., 2019). Como as outras MAPKs, a atividade aumentada de JNK requer sua fosforilação dupla nos resíduos tirosina e treonina por uma MAPK quinase (MKK4 e MKK7). Por exemplo, enquanto MKK4 também pode ativar p38 MAPK, MKK7 funciona como um ativador específico de JNK. Além disso, MKK4 e MKK7 são seletivamente regulados por estímulos extracelulares e têm uma afinidade distinta para JNK, com MKK4 e MKK7 preferencialmente fosforilando JNK em resíduos de tirosina e treonina, respectivamente (TOURNIER et al., 2013). Diversas evidências indicam que esta sinalização promove a sobrevivência das células cancerosas. Além disso, JNK atua sinergicamente com NF- κ B, JAK/STAT e outras moléculas de sinalização para exercer uma função de sobrevivência. JNK também regula positivamente a autofagia para neutralizar a apoptose, e seu efeito na autofagia está relacionado ao desenvolvimento de resistência quimioterápica (WU et al., 2019).

As vias de sinalização JNK e p38 apresentam certo grau de redundância em suas ações; entretanto, a extensão da interferência entre elas e suas implicações na regulação da fisiologia celular depende do tipo celular, tecido e organismo. Diversos relatos demonstram que essas quinases promovem o desenvolvimento do câncer aumentando a sobrevivência, migração ou resistência ao estresse e agentes quimioterápicos em células tumorais (MARTÍNEZ-LIMÓN et al., 2020). A via p38 responde principalmente a sinais de estresse ambiental e estímulos inflamatórios e desempenha papéis importantes na manutenção da homeostase celular em diferentes tecidos, incluindo os sistemas neuronal e cardiovascular, mas também no câncer.

Esta apresenta uma regulação complexa, pois além da ativação usual por duas MAPKs - MKK3 e MKK6 - as p38 MAPKs também podem ser ativadas pela ligação de TAB1 (proteína

1 de ligação de TAK1) ou pela fosforilação de tirosina quinases ZAP70 e LCK. Além disso, p38 possui 4 isoformas (p38 $\alpha/\beta/\gamma/\delta$), codificados por quatro genes diferentes (LEE et al., 2020). Sendo assim, essas vias são consideradas potenciais alvos terapêuticos para o tratamento do câncer. O estudo de medicamentos direcionados as mesmas têm sido conduzidos no intuito de desenvolver abordagens terapêuticas promissoras.

O fator nuclear kappa B (NF- κ B) é um fator de transcrição dimérico que desempenha um papel importante na sobrevivência, proliferação e diferenciação celular. Cinco tipos de NF- κ B foram identificados e estudados em mamíferos: NF- κ B1 (p50/p105); NF- κ B2 (p52/p100); RelA (p65); RelB; e c-Rel. No estado inativo, o NF- κ B é translocado para o citoplasma por seu inibidor (I κ B), resultando na não ativação dos genes-alvo; entretanto, após ativação por meio de proteínas que fosforilam I κ B e o direcionam para a degradação, o complexo é translocado para o núcleo, levando a ativação destes genes. A sinalização de NF- κ B ocorre através da via canônica (clássica), iniciada por NF- κ B1 (p50/p105), ou pela via não canônica (alternativa), iniciada por NF- κ B2 (p52/p100) (ZHOU et al., 2015; RODRIGUES et al., 2021). A ativação do NF- κ B pode ser iniciada por meio de vários estímulos extracelulares, mas a cascata de transdução de sinal resulta basicamente na transferência de fosfato. A **figura 6** exemplifica as vias de sinalização, canônica e não-canônica.

Na via canônica, a sinalização depende da proteína inibidora I κ B, particularmente a I κ B α , que interage com outras proteínas, impedindo a translocação dos dímeros p65/p50 e c-Rel/p50 para o núcleo celular. Para a ativação do complexo NF- κ B, os receptores de citocinas pró-inflamatórias são ativados, incluindo: membros do receptor do fator de necrose tumoral (TNF) (TNFR); receptor de interleucina (IL) -1 (IL-1R); membros da família de receptores do tipo toll-like (TLR) (TLR3, TLR4, TLR7); receptores de antígenos, tais como receptor de células T (TCR) e receptor de células B (BCR); e fatores de crescimento, como membros da família EGFR. A ativação desses receptores culminará na ativação do complexo trimérico I κ B quinase (IKK), que é composto por duas subunidades catalíticas IKK α e IKK β , e uma subunidade reguladora IKK γ (também de modulador NEMO). Este complexo então, irá fosforilar e facilitar a ubiquitinação do I κ B e sua posterior degradação, liberando as proteínas envolvidas para serem translocadas para o núcleo da célula, culminando na ativação de genes-alvo (GUPTA et al., 2010; SUN, 2011; PIRES et al., 2018; RODRIGUES et al., 2021).

Na via não canônica, a sinalização ocorre sem a participação de I κ B. Essa via depende do processamento induzível de p100, uma molécula que funciona como um precursor de p52 e como um inibidor específico de RelB. Ao contrário da via de sinalização canônica, que responde a sinais gerados por diferentes receptores, a via não canônica é ativada por um

conjunto específico de receptores. Assim, a ativação desta via ocorre por um subconjunto de membros da superfamília TNFR, incluindo fator de ativação de células B pertencente ao receptor da família TNF (BAFFR) CD40, receptor de linfotóxina β (LT β R), ativador de receptor para fator nuclear κ B (RANK), TNFR2, Fn14 etc. Esses sinais resultarão na ativação da quinase indutora de NF- κ B (NIK), levando a fosforilação IKK α e IKK β e, conseqüentemente, induzindo o processamento de p100, que será ubiquitinado e processado no proteossoma em p52. Por fim, RelB/p52 é translocado para o núcleo da célula, levando à ativação dos genes alvo (SUN, 2011; PIRES et al., 2018; RODRIGUES et al., 2021).

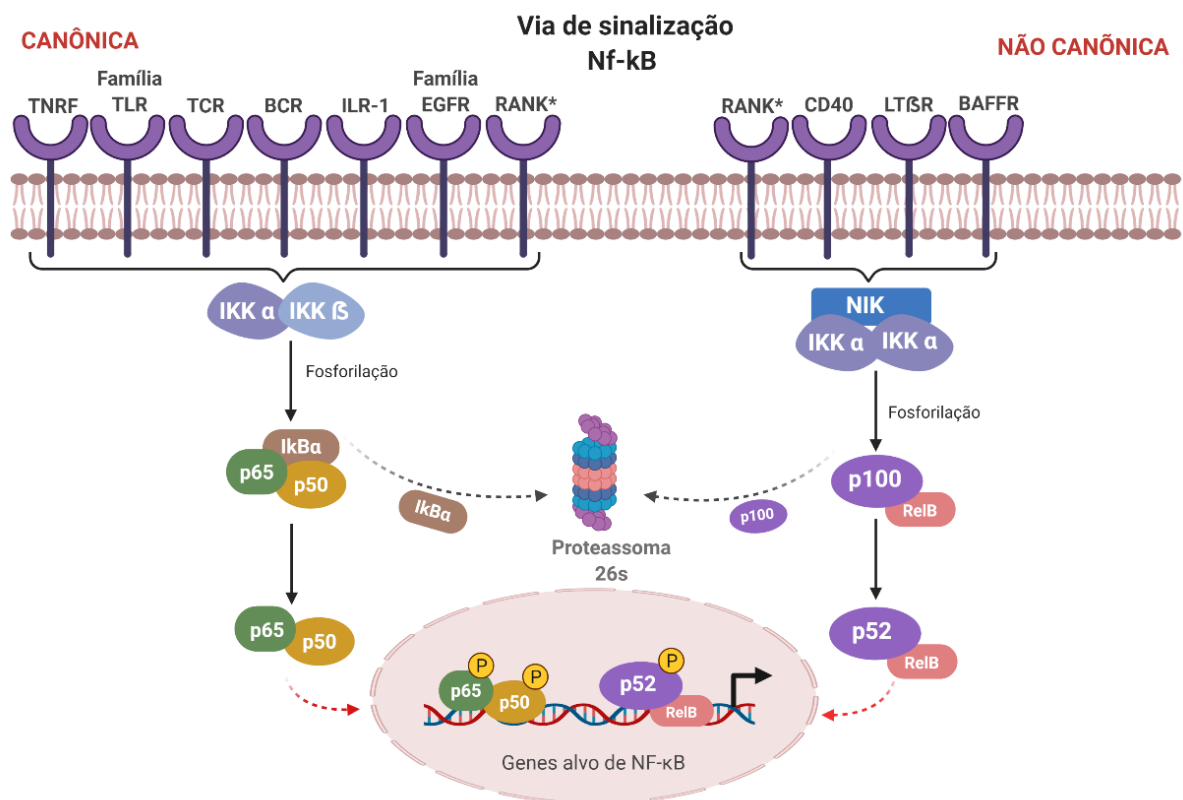


Figura 6 - Via de sinalização canônica e não canônica de NF- κ B.

Fonte: Adaptado de (RODRIGUES et al., 2021). Criado com BioRender.com.

O NF- κ B é considerado o principal regulador da resposta inflamatória e está associado ao desenvolvimento e à patogênese do câncer. A ativação desse fator de transcrição tem sido descrita como responsável pela resistência à apoptose, proliferação celular e invasão tumoral. Em muitos tipos de câncer, genes alvo de NF- κ B são encontrados superexpressos (DOLCET et al., 2005; GHOSH et al., 2006; BAI et al., 2009; PIRES et al., 2018). Evidências crescentes indicam que o NF- κ B atua como um elo entre a inflamação e a progressão do câncer, tornando-o essencial e um alvo potencial para fármacos em neoplasias hematológicas e tumores sólidos (BOURS et al., 2000; KARIN, 2006). A ativação constitutiva de NF- κ B no núcleo é observada

em alguns distúrbios hematológicos, como síndromes mielodisplásicas (GROSJEAN-RAILLARD et al., 2009; BRAUN et al., 2006) e mieloma múltiplo (NI et al., 2001) e na LMA (PIRES et al., 2018; RODRIGUES et al., 2021).

Diversos relatos demonstraram que expressão de NF- κ B nas CTHNs é baixa, enquanto é significativamente alta nas CTLs (JI et al., 2016). Portanto, NF- κ B poderia distinguir CTLs e CTHNs, servindo como um alvo terapêutico potencial para a eliminação seletiva de CTLs, sem toxicidade significativa para as CTHNs (GUZMAN et al., 2005, 2007; RODRIGUES et al., 2021). Curiosamente, os agentes quimioterápicos de LMA comumente utilizados (por exemplo, citarabina) não inibem o NF- κ B, ao contrário, levam a uma maior regulação positiva da atividade do NF- κ B (TERGAONKAR et al., 2002).

Tendo em vista que a expressão constitutiva de NF- κ B está fortemente associada as CTLs de LMA, diversos estudos têm sido direcionados a investigação de terapias que atuem nesta via de sinalização (POLLYEA; JORDAN, 2017; RODRIGUES et al., 2021). A primeira observação de que células de LMA primitivas CD34⁺/CD38⁻/CD123⁺ expressam de forma aberrante NF- κ B, também demonstrou que o tratamento celular *in vitro* com um inibidor de proteassoma, MG-132 (inibidor bem conhecido de NF- κ B), causou uma inibição rápida de NF- κ B levando a apoptose dessas células, enquanto as CTHNs mostraram pouco ou nenhum efeito (GUZMAN et al., 2001). Além do MG-132, outros medicamentos que atuam em alguma etapa dessa via ou em vias relacionadas que culminam na inibição de NF- κ B, como BAY11-7802 (LI et al., 2017), GO-203 (TAGDE et al., 2016), Silmitasertibe (TUBI et al., 2017), Niclosamida (JIN et al., 2010), Parthenolide/DMAPT (GUZMAN et al., 2007; 2014), Micheliolide (JI et al., 2016), Disulfiram em combinação com cobre (XU et al., 2017), Verteporfina (XIU et al., 2018) demonstraram capacidade promissora em inibir as CTLs (RODRIGUES et al., 2021).

Tomados em conjunto, esses dados indicam que as CTLs de LMA expressam constitutivamente NF- κ B e a presença desse fator pode fornecer oportunidades únicas para a eliminação preferencial desta população de células, poupando as suas contrapartes normais. Assim, os regimes de quimioterapia incluindo fármacos que inibem o NF- κ B poderiam adicionar benefícios na redução da toxicidade dos quimioterápicos padrões e na sensibilização das células leucêmicas a esses agentes e, conseqüentemente, diminuir a taxa de recidiva da LMA.

2.3 Produtos naturais

2.3.1 Tingenona e 22-hidroxitingenona

Uma ampla variedade de produtos naturais derivados de plantas terrestres, microrganismos, organismos marinhos e fungos tem sido uma fonte vital de medicamentos por milênios e tem sido utilizada nos campos da medicina, farmácia e biologia geral (ATANASOV et al., 2021). Nos dias de hoje, as plantas e fontes naturais formam a base da medicina moderna e contribuem amplamente para as preparações de fármacos comerciais fabricadas atualmente (ZHU et al., 2022).

Os produtos naturais são enriquecidos com muitos compostos que possuem um amplo espectro de indicações terapêuticas, os metabólitos secundários de plantas, como flavonoides, taninos, alcaloides e terpenoides, são conhecidos por possuir capacidades anticancerosas substanciais. Eles desencadeiam, promovem ou modulam as vias metabólicas que podem alterar a proliferação, migração e apoptose em células cancerosas por meio de uma infinidade de mecanismos biológicos (ALI ABDALLA et al., 2022). Os terpenos, também chamados de terpenóides ou isoprenóides, constituem a maior classe de produtos naturais com mais 55.000 compostos conhecidos estruturalmente diversificados. Esses produtos químicos fazem parte do metabolismo secundário de espécies vegetais e animais, são formados pela fusão de unidades isoprênicas de cinco carbonos (C5) e são classificados de acordo com o número de unidades C5 que apresentam (GUIMARÃES et al., 2014; KAMRAN et al., 2022)

Os triterpenos, devido ao seu valor medicinal versátil, possui propriedades biológicas relacionadas a atividade anticâncer, antiinflamatória, antioxidante, antiviral, antibacteriana e antifúngica (YIN et al., 2012; KAMRAN et al., 2022). Nas redes de sinalização, os triterpenos visam principalmente os receptores de membrana que controlam e modulam o nível de expressão das respostas biológicas. Os diferentes alvos dos triterpenos inclui o NF- κ B, fator de necrose tumoral (TNF), transdutores de sinal e ativadores da transcrição 3 (STAT3), receptores Toll-like (TLR) e a via de sinalização PI3K/Akt/mTOR. Alguns estudos demonstraram que triterpenos em diferentes plantas e fungos visam principalmente a via de sinalização PI3K/Akt/mTOR e NF- κ B no câncer (GILL; KUMAR, 2015; GILL et al., 2016). Os triterpenos isolados de plantas e fungos atuam principalmente no processo de apoptose, enquanto outras áreas de sinalização do câncer ainda estão encobertas. Alguns triterpenos já foram aprovados em ensaios clínicos, enquanto muitos outros mostraram produzir resultados eficazes (GILL et al., 2016; KAMRAN et al., 2022).

Os triterpenos mais estudados são os quinonametídeos (85% dos estudos com triterpenos). Estes são constituintes comuns de sistemas biológicos e alguns possuem atividades biológicas importantes, incluindo alquilação e reticulação do DNA (WANG et al., 2005; HERNANDES et al., 2017). Eles também se apresentam na literatura com um potencial interessante na medicina, por possuir diferentes atividades biológicas já identificadas, e são considerados promissores agentes anticâncer, entre os quais podemos citar o celastrol e a pristimerina, como os representantes mais importantes e mais estudados dessa classe química (SALMIEN et al., 2008; HERNANDES et al., 2017; HERNANDES et al., 2019; LI et al., 2019).

A tingenona e 22-hidroxitingenona (**Figura 7**) pertencem à classe dos triterpenos quinonametídeos e foi isolada a partir da casca do caule da espécie amazônica *Salacia impressifolia* (Miers) A. C. Smith. (DA SILVA et al., 2016; RODRIGUES et al., 2019). Estudos prévios realizados por nosso laboratório, demonstraram o efeito citotóxico e antitumoral de extratos e frações da casca do caule de *S. impressifolia* contra LMA e esse efeito foi atribuído a presença dos triterpenos quinonametídeos (RODRIGUES et al., 2019). Ainda nesse estudo, TG e 22-HTG demonstraram serem citotóxicos em várias linhagens celulares de câncer, dentre elas carcinoma de mama, colón, hepatocelular, boca, leucemias e melanoma murino (RODRIGUES et al., 2019).

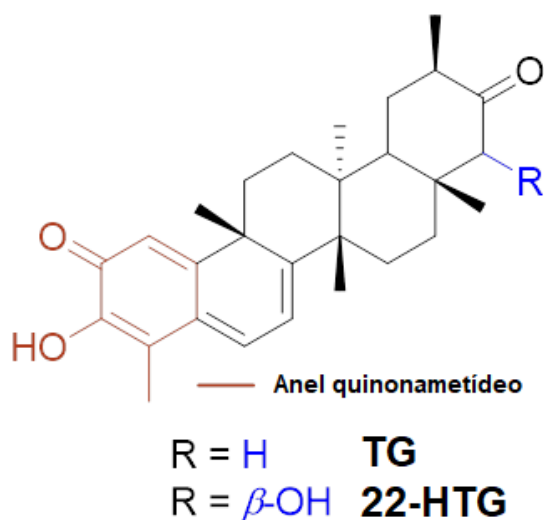


Figura 7 - Estrutura química da TG e 22-HTG.
Fonte: Elaborado pela autora.

2.3.2 Piplartina

A PL é um alcaloide amida biologicamente ativo da *Piper longum L.* (pimenta longa), uma planta medicinal conhecida da medicina ayurvédica. As propriedades farmacológicas desse alcaloide já vêm sendo descrita desde a última década, incluindo atividade anticancerígena por indução de estresse oxidativo, além de demonstrar baixa toxicidade e boa biodisponibilidade (BEZERRA et al., 2013; BEZERRA, 2021).

Essa molécula derivada de plantas, tem sido objeto de estudo do nosso grupo, principalmente no que diz respeito ao seu efeito anticâncer (BEZERRA et al., 2007; COSTA et al., 2017; BALIZA et al., 2019). PL exibiu citotoxicidade contra um amplo espectro de linhagens celulares de câncer humano, incluindo, leucemia, câncer colorretal, hepatocelular, de bexiga, dentre outros (BEZERRA et al., 2007; LI et al., 2015; LIU et al., 2017; ZHANG et al., 2019). Além disso, PL é um agente pró-apoptótico (LI et al., 2015; ZHANG et al., 2019), anti-invasivo (CHEN et al., 2015), antiangiogênico (LIU et al., 2014), e é capaz de sinergizar com agentes quimioterápicos utilizados na clínica (GONG et al., 2014; CHEN et al., 2019; RAWAT et al., 2020). Em virtude do efeito citotóxico deste composto, diversos estudos relataram a capacidade da pipartina de induzir apoptose e/ou autofagia por meio da modulação das vias de sinalização, como PI3K/Akt/mTOR,(SEOK et al., 2018) NF-κB (GINZBURG et al., 2014), JAK1,2/STAT3 (YAO et al., 2016) e/ou JNK (LI et al., 2015; XIONG et al., 2015) em células cancerosas (PARAMA et al., 2021). Ademais, PL é um inibidor direto do sistema antioxidante TrxR1 (ZHANG et al., 2019).

Considerando as atividades descritas anteriormente e os vários relatos sobre o efeito desta molécula contra diversos alvos moleculares importantes em diferentes estágios do desenvolvimento e progressão do câncer, além de sua baixa toxicidade e propriedades farmacocinéticas favoráveis, neste trabalho propomos investigar seu potencial antileucêmico com o objetivo de desenvolver estratégias terapêuticas promissoras contra a LMA.

3 OBJETIVOS

3.1 Objetivo geral

Investigar o potencial antileucêmico de TG, 22-HTG e PL utilizando diferentes modelos celulares de LMA.

3.2 Objetivos específicos

- Avaliar o efeito citotóxico de TG, 22-HTG e PL num painel de linhagens celulares cancerosas e não cancerosas;
- Investigar a indução de morte celular apoptótica provocada por TG, 22-HTG e PL;
- Analisar o efeito de TG, 22-HTG e PL na expressão gênica de genes envolvidos em vias de sinalização, proliferação celular e morte celular;
- Investigar o efeito de TG, 22-HTG e PL na ativação de proteínas relacionadas a vias de sinalização de morte celular;
- Avaliar o efeito de TG, 22-HTG e PL na indução do estresse oxidativo;
- Avaliar o efeito de PL sobre a proliferação de células-tronco e progenitoras leucêmicas utilizando modelos *in vitro* e *in vivo*;
- Investigar o efeito sinérgico de PL em combinação com fármacos antileucêmicos utilizados na terapia convencional.

4 RESULTADOS

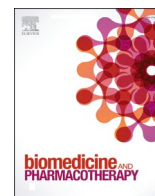
4.1 Capítulo I

Neste capítulo, descrevemos o efeito antileucêmico de TG e 22-HTG e elucidamos o mecanismo de ação dos compostos na indução de apoptose em células de leucemia mieloide aguda HL-60.

Artigo publicado na revista *Biomedicine & Pharmacotherapy*, v. 142, p.112034, 2021. Doi: 10.1016/j.biopha.2021.112034.

Tingenone and 22-hydroxytingenone target oxidative stress through downregulation of thioredoxin, leading to DNA double-strand break and JNK/p38-mediated apoptosis in acute myeloid leukemia HL-60 cells.

Ana Carolina B. da C. Rodrigues^a, Larissa M. Bomfim^a, Sara P. Neves^a, Milena B. P. Soares^{a,b}, Rosane B. Dias^{a,c}, Ludmila F. Valverde^a, Clarissa A. Gurgel Rocha^{a,c}, Emmanoel V. Costa^d, Felipe M. A. da Silva^d, Waldireny C. Rocha^e, Hector H. F. Koolen^f, Daniel P. Bezerra^{a,*}



Tingenone and 22-hydroxytingenone target oxidative stress through downregulation of thioredoxin, leading to DNA double-strand break and JNK/p38-mediated apoptosis in acute myeloid leukemia HL-60 cells

Ana Carolina B. da C. Rodrigues^a, Larissa M. Bomfim^a, Sara P. Neves^a, Milena B.P. Soares^{a,b}, Rosane B. Dias^{a,c}, Ludmila F. Valverde^a, Clarissa A. Gurgel Rocha^{a,c}, Emmanoel V. Costa^d, Felipe M.A. da Silva^d, Waldireny C. Rocha^e, Hector H.F. Koolen^f, Daniel P. Bezerra^{a,*}

^a Gonçalo Moniz Institute, Oswaldo Cruz Foundation (IGM-FIOCRUZ/BA), Salvador, Bahia 40296-710, Brazil

^b SENAI Institute for Innovation in Advanced Health Systems, SENAI CIMATEC, Salvador, BA 41650-010, Brazil

^c Department of Clinical Propaedeutics and Integrated Clinical, Faculty of Dentistry, Federal University of Bahia (UFBA), Salvador, Bahia 40301-155, Brazil

^d Department of Chemistry, Federal University of Amazonas (UFAM), Manaus, Amazonas 69080-900, Brazil

^e Health and Biotechnology Institute, Federal University of Amazonas (UFAM), Coari, Amazonas 69460-000, Brazil

^f Metabolomics and Mass Spectrometry Research Group, Amazonas State University (UEA), Manaus, Amazonas 690065-130, Brazil

ARTICLE INFO

Keywords:

Tingenone
22-hydroxytingenone
Thioredoxin
Oxidative stress
Apoptosis
AML

ABSTRACT

Acute myeloid leukemia (AML) is the most lethal form of leukemia. Standard anti-AML treatment remains almost unchanged for decades. Tingenone (TG) and 22-hydroxytingenone (22-HTG) are quinonemethide triterpenes found in the Amazonian plant *Salacia impressifolia* (Celastraceae), with cytotoxic properties in different histological types of cancer cells. In the present work, we investigated the anti-AML action mechanism of TG and 22-HTG in the AML HL-60 cell line. Both compounds exhibited potent cytotoxicity in a panel of cancer cell lines. Mechanistic studies found that TG and 22-HTG reduced cell growth and caused the externalization of phosphatidylserine, the fragmentation of internucleosomal DNA and the loss of mitochondrial transmembrane potential in HL-60 cells. In addition, pre-incubation with Z-VAD(OMe)-FMK, a pan-caspase inhibitor, prevented TG- and 22-HTG-induced apoptosis, indicating cell death by apoptosis via a caspase-dependent pathway. The analysis of the RNA transcripts of several genes indicated the interruption of the cellular antioxidant system, including the downregulation of thioredoxin, as a target for TG and 22-HTG. The application of *N*-acetyl-cysteine, an antioxidant, completely prevented apoptosis induced by TG and 22-HTG, indicating activation of the apoptosis pathway mediated by oxidative stress. Moreover, TG and 22-HTG induced DNA double-strand break and phosphorylation of JNK2 (T183/Y185) and p38 α (T180/Y182), and co-incubation with SP 600125 (JNK/SAPK inhibitor) and PD 169316 (p38 MAPK inhibitor) partially prevented apoptosis induced by TG and 22-HTG. Together, these data indicate that TG and 22-HTG are new candidate for anti-AML therapy targeting thioredoxin.

1. Introduction

In 2020, there were an estimated 474,519 new cases and 311,594 deaths from leukemia worldwide [1]. Among the forms of leukemia, acute myeloid leukemia (AML) is the most lethal, and about 19,940 new cases and about 11,180 deaths from AML have been estimated in the United States. The overall ratio of mortality to incidence is 0.56, indicating poor prognosis. The relative 5-year survival rate (2008–2014) is 25% in adults (20 years and over) and 67% in patients aged 0–19 years

[2].

Standard anti-AML treatment remains almost unchanged for decades, which includes cytarabine and anthracyclines (daunorubicin or idarubicin). Although most patients achieve high rates of remission, the rate of recurrence is very high [3]. Therefore, new anti-AML drugs are urgently needed.

Tingenone (TG) and 22-hydroxytingenone (22-HTG) (Fig. 1) are quinonemethide triterpenes found in the Amazonian plant *Salacia impressifolia* (Celastraceae). These compounds have been reported as

* Corresponding author.

E-mail address: daniel.bezerra@fiocruz.br (D.P. Bezerra).

<https://doi.org/10.1016/j.bioph.2021.112034>

Received 28 June 2021; Received in revised form 27 July 2021; Accepted 7 August 2021

Available online 16 August 2021

0753-3322/© 2021 The Author(s).

Published by Elsevier Masson SAS. This is an open access article under the CC BY-NC-ND license

(<http://creativecommons.org/licenses/by-nc-nd/4.0/>).

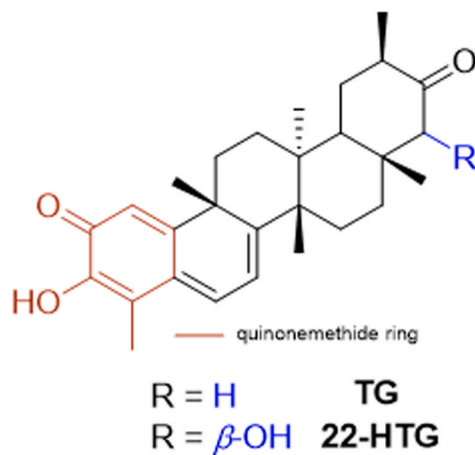


Fig. 1. Chemical structure of TG and 22-HTG.

Table 1
Cytotoxic activity of TG and 22-HTG.

Cells	Histological type	IC ₅₀ and 95% CI (μ M)		
		DOX	TG	22-HTG
Cancer cells				
HL-60	human acute promyelocytic leukemia	0.34	2.09	1.58
		0.23 – 0.48	1.66 – 2.70	1.31 – 1.92
		n.d.	1.50	1.70
Jurkat	human acute T cell leukemia	n.d.	1.50	1.70
			1.17 – 1.80	1.05 – 2.68
			1.76	1.26
THP-1	human acute promyelocytic leukemia	0.25	1.76	1.26
		0.16 – 0.44	1.55 – 2.02	0.94 – 1.72
			2.02	1.72
KG-1a	human acute myelogenous leukemia	0.18	3.68	4.70
		0.17 – 0.22	2.83 – 4.83	3.44 – 6.41
			0.69	1.15
NB4	human acute promyelocytic leukemia	0.46	0.69	1.15
		0.14 – 1.58	0.17 – 2.66	0.53 – 2.43
			2.14	2.27
K-562	human chronic myelogenous leukemia	1.53	2.14	2.27
		0.85 – 2.77	1.83 – 2.52	1.56 – 3.30
			5.45	2.77
MCF-7	human breast adenocarcinoma	1.51	5.45	2.77
		0.96 – 2.38	3.66 – 8.06	1.92 – 4.01
			3.07	1.21
HCT116	human colon carcinoma	0.09	3.07	1.21
		0.05 – 0.16	2.38 – 3.92	0.94 – 1.54
			8.58	2.31
HepG2	human hepatocellular carcinoma	0.32	8.58	2.31
		0.18 – 0.55	6.40 – 11.58	1.51 – 3.55
			1.66	1.26
CAL 27	human tongue squamous cell carcinoma	0.34	1.66	1.26
		1.65 – 0.69	1.12 – 2.45	0.89 – 1.76
			2.07	1.56
HSC-3	human tongue squamous cell carcinoma	0.53	2.07	1.56
		0.39 – 0.73	1.31 – 3.21	1.08 – 2.29
			1.02	1.15
SCC-4	human tongue squamous cell carcinoma	2.1	1.02	1.15
		1.7 – 2.6	0.74 – 1.38	0.92 – 1.44
			2.26	1.97
B16-F10	mouse melanoma	0.15	2.26	1.97
		0.07 – 0.18	1.62 – 3.16	1.33 – 2.93
			2.83	2.82
MRC-5	human lung fibroblast	1.65	2.83	2.82
		1.03 – 2.61	2.26 – 3.57	2.36 – 3.37
			3.28	2.57
BJ	human foreskin fibroblast	3.60	3.28	2.57
		1.15 – 11.22	2.23 – 4.83	1.33 – 3.67
			0.81	n.d.
PBMC	human peripheral blood mononuclear cells	1.21	0.81	n.d.
		0.73 – 1.99	0.62 – 1.05	
			1.05	

cytotoxic agents in different histological types of cancer cells [4–9]. In particular, 22-HTG induced apoptosis and suppressed invasion of melanoma cells by inhibiting the activity of metalloproteinases (MMP-2 and MMP-9) and the expression of the BRAF, NRAS and KRAS genes [7,8]. TG and 22-HTG inhibited tubulin polymerization in vitro [9] and TG has also been identified through in silico study as a pro-apoptotic agent [10]. However, the mechanism of action of these compounds is not yet known. In the present work, we investigated the anti-AML action mechanism of TG and 22-HTG in the AML HL-60 cell line.

2. Material and methods

2.1. Tingenone and 22-hydroxytingenone obtaining

TG and 22-HTG were isolated from the stem bark of *S. impressifolia* using different chromatographic techniques, as previously described [6]. For all experiments, TG and 22-HTG were dissolved in sterile dimethyl sulfoxide (DMSO, Vetec Química Fina Ltda, Duque de Caxias, RJ, Brazil) at a 5 mg/mL stock solution and diluted with culture medium at different concentrations.

2.2. Cells

A total of 13 cancer cell lines, 3 non-cancer cells and 1 mutant and its parent cell line were used in this study and details can be found in Table S1. The American Type Culture Collection (ATCC, Manassas, VA, USA) animal cell culture guide was used for all cell line procedures and mycoplasma test was carried out using a mycoplasma stain kit (Sigma-Aldrich Co., Saint Louis, MO, USA) to validate the use of mycoplasma-free cells. Cells were cultured in RPMI-1640 medium (Gibco-BRL, Gaithersburg, MD, USA) or DMEN-F12 medium (Gibco-BRL) with 10% (or 20% for KG-1a) fetal bovine serum (Life, Carlsbad, CA, USA) and 50 μ g/mL of gentamicin (Life, Carlsbad, CA, USA). Trypsin-EDTA solution (Gibco-BRL) was used to collect adherent cells. All cell lines were grown in flasks at 37 °C in 5% CO₂ and subcultured every 3–4 days to maintain exponential growth. All experiments were carried out at exponential growth phase.

2.3. Alamar blue assay

Cell viability was quantified by Alamar blue assay, as previously described [11–13]. The cells were plated in 96-well culture plates (3×10^4 cells/well for suspension cells and 7×10^3 cells/well for adherent cells) and kept at 37 °C and 5% CO₂ atmosphere. The compounds (0.19–25 μ g/mL) were added to each well and incubated for 72 h. Doxorubicin (0.04–5 μ g/mL) (purity \geq 95%, doxorubicin hydrochloride, Laboratory IMA S.A.I.C., Buenos Aires, Argentina) was used as a positive control. Four (for cell lines) or 24 h (for PBMCs) before the end of incubation, 20 μ L of a stock solution (0.312 mg/mL) of resazurin (Sigma-Aldrich Co.) was added to each well. Absorbances at 570 nm and 600 nm were measured using a SpectraMax 190 Microplate Reader (Molecular Devices, Sunnyvale, CA, USA). Experiments were conducted three times independently.

For subsequent experiments, HL-60 cells (3×10^5 /mL) were seeded in 24-well plate and treated with TG (0.6 and 1.2 μ M) and 22-HTG (1.2 and 2.4 μ M) for 24 and/or 48 h. The negative control was treated with the vehicle (0.2% DMSO) that was used to solubilize and dilute the triterpenes, and doxorubicin (1 μ M) was used as a positive control.

2.4. Trypan blue exclusion assay

After the treatment time, cells were removed from the suspension and added to the trypan blue (0.4%) solution (1:10 dilution). Cells that excluded trypan blue were counted as viable and cells stained in blue, due to membrane damage, were considered non-viable. Cell counting was carried out in a hemocytometer using a light microscope.

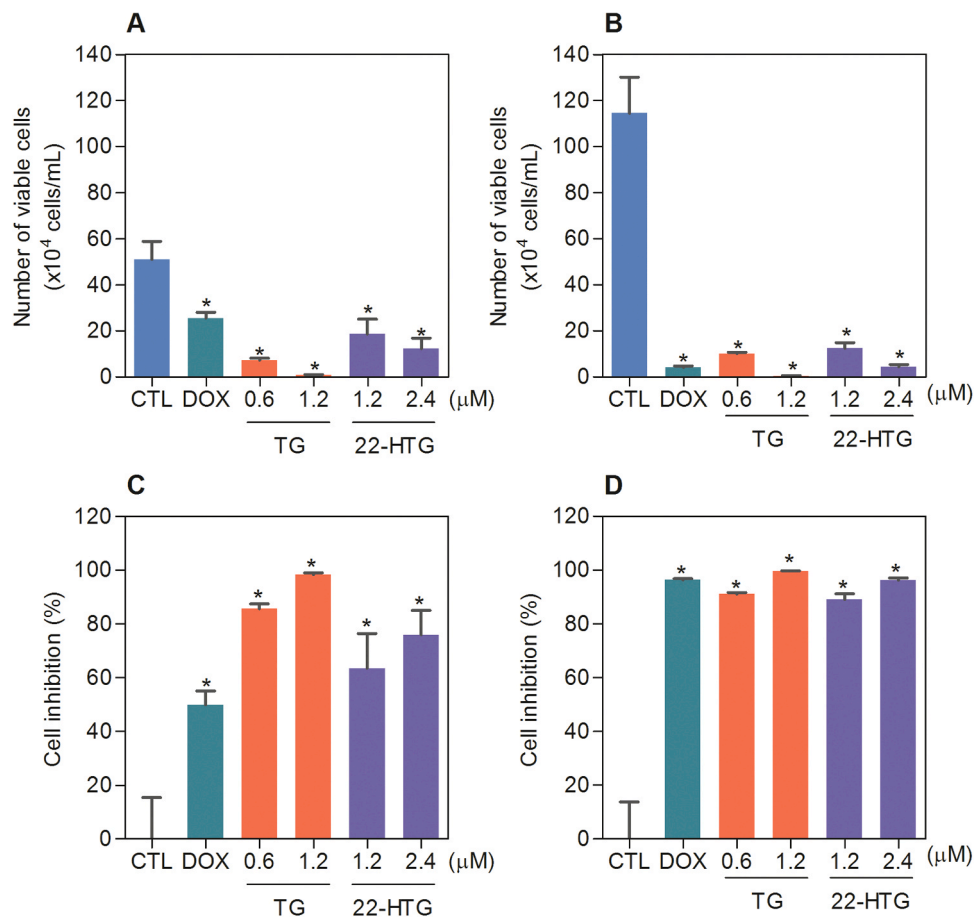


Fig. 2. Trypan blue exclusion assay after 24 (A and C) and 48 (B and D) h of treatment with TG and 22-HTG. The vehicle (0.2% DMSO) was used as a negative control (CTL) and doxorubicin (DOX, 1 μM) was used as a positive control. Data are shown as mean ± S.E.M. of three independent experiments carried out in duplicate. * $p < 0.05$ compared with CTL by ANOVA followed by Student Newman-Keuls test.

Experiments was conducted three times independently.

2.5. Internucleosomal DNA fragmentation and cell cycle distribution

Internucleosomal DNA fragmentation and cell cycle distribution were quantified through DNA content, as previously described [14]. In this assay, HL-60 cells were removed from the plate, washed with PBS and harvested in a permeabilization solution containing 0.1% Triton X-100, 2 μg/mL propidium iodide (PI), 0.1% sodium citrate and 100 μg/mL RNase (all from Sigma-Aldrich Co.), and incubated in the dark at room temperature for 15 min. Cell fluorescence was quantified by flow cytometry. For all flow cytometry analyses, at least 10.000 events/sample were acquired using a BD LSRFortessa cytometer along with BD FACSDiva Software (BD Biosciences, San Jose, CA, EUA) and Flowjo Software 10 (Flowjo LCC, Ashland, OR, USA). Cell debris were excluded from the analysis. Experiments was conducted three times independently.

2.6. Morphological analysis

To evaluate alterations in the morphology, 150 μL of each sample was centrifuged on slides in a cytospin at 2000 rpm for 10 min. Cell fixation was performed with methanol for 1 min, then the slides with a monolayer of cells were stained with hematoxylin and eosin. Morphological alterations were observed and photographed by light microscopy (Leica Microsystems, Wetzlar, Germany). Light scattering features were obtained by flow cytometry, as described above.

2.7. Apoptosis detection

Apoptosis detection was performed using FITC Annexin V Apoptosis Detection Kit I (ID 556547) (BD Biosciences), according to the manufacturer's instructions. HL-60 cells were gently harvested from the plate, washed with PBS, resuspended in binding buffer, and incubated with Annexin V-FITC and PI at room temperature for 15 min. The cell fluorescence was determined by flow cytometry, as described above. Functional assays using pan-caspase inhibitor (Z-VAD(Ome)-FMK, Cayman Chemical; Ann Arbor, MI, USA), antioxidant (*N*-acetyl-cysteine, NAC, Sigma-Aldrich), p38 MAPK inhibitor (PD 169316; Cayman Chemical), JNK/SAPK inhibitor (SP 600125; Cayman Chemical) and MEK inhibitor (U-0126; Cayman Chemical) were also performed. For that, cells were pre-incubated for 2 h with 50 μM Z-VAD(Ome)-FMK, 5 mM NAC, 5 μM PD 169316, 5 μM SP 600125 and 5 μM U-0126, followed by incubation with 1.2 μM TG and 2.4 μM 22-HTG for 48 h. Experiments was conducted three times independently.

2.8. Mitochondrial transmembrane potential

To assess mitochondrial transmembrane potential loss, HL-60 cells were washed twice with PBS, then incubated with rhodamine 123 (5 μg/mL, Sigma-Aldrich Co.) at 37 °C for 15 min in the dark and resuspended with PBS. The mitochondrial transmembrane potential was performed by retention of dye rhodamine 123, as described previously [15]. The cell fluorescence was determined by flow cytometry, as described above. Experiments was conducted three times independently.

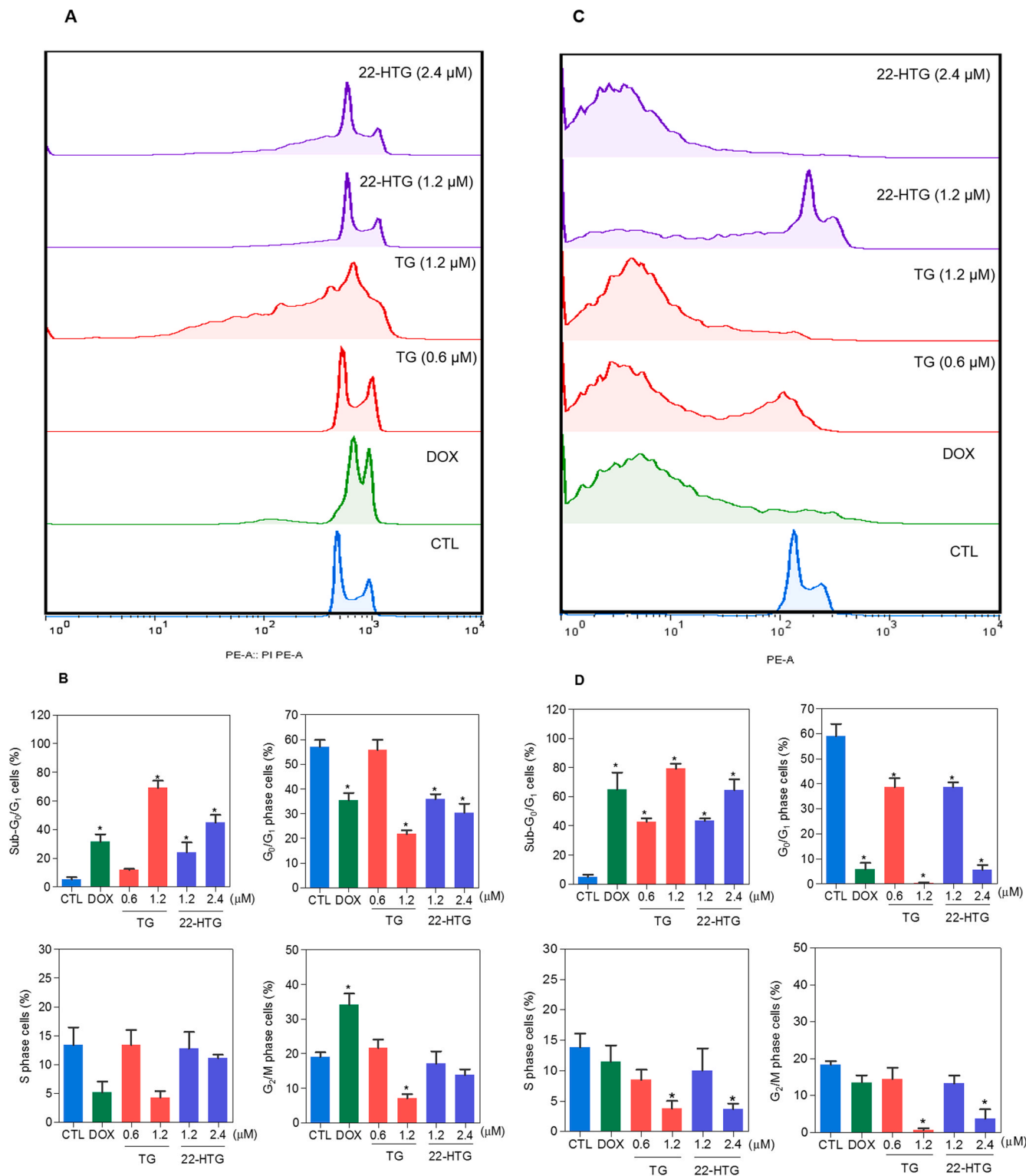


Fig. 3. Cell cycle distribution of HL-60 cells after 24 (A and B) and 48 (C and D) h of incubation with TG and 22-HTG. The vehicle (0.2% DMSO) was used as a negative control (CTL) and doxorubicin (DOX, 1 μ M) was used as a positive control. Data are shown as mean \pm S.E.M. of three independent experiments carried out in duplicate. * p < 0.05 compared with CTL by ANOVA followed by Student Newman-Keuls test.

2.9. RT-qPCR array

HL-60 cells were incubated with 1.2 μ M TG or 2.4 μ M 22-HTG for 12 h and total RNA was isolated from the cells using the RNeasy Plus Mini Kit (Qiagen; Hilden, Germany), according to the manufacturer's instructions. The RNA was analyzed for purity and quantified by a

NanoDrop® 1000 spectrophotometer (Thermo Fisher Scientific, Waltham, Massachusetts, USA). RNA reverse transcription was carried out using a Superscript VIL0™ Kit (Invitrogen Corporation; Waltham, MA, USA). TaqMan® array human cancer drug targets 96-well plate, fast (ID RPRWENH, Applied Biosystems™, Foster City, CA, USA) was used for the gene expression study by qPCR. The reactions were conducted in an

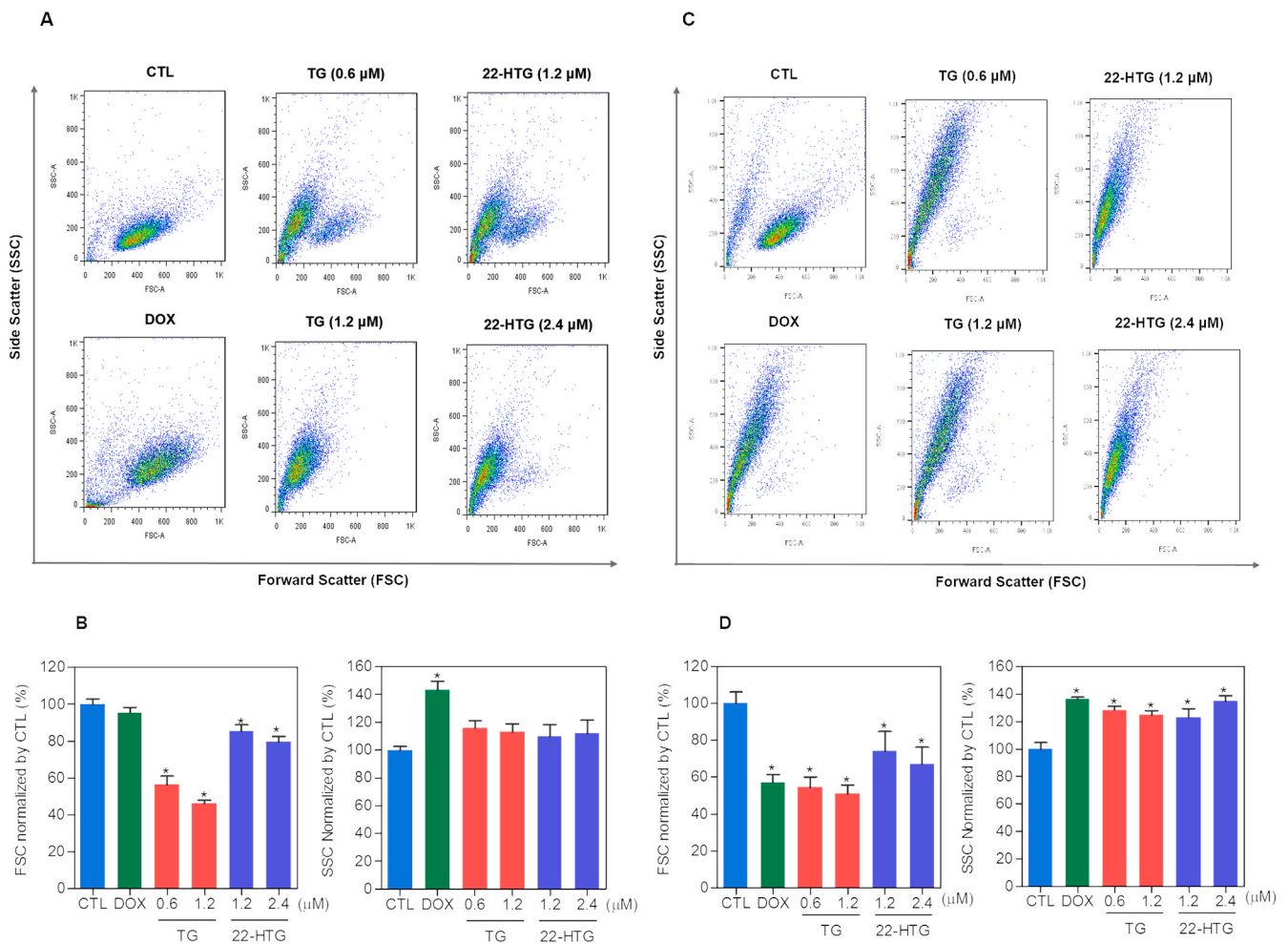


Fig. 4. Light scattering features of HL-60 cells after 24 (A and B) and 48 (C and D) h of treatment with TG and 22-HTG. The vehicle (0.2% DMSO) was used as a negative control (CTL) and doxorubicin (DOX, 1 μM) was used as a positive control. Data are shown as mean ± S.E.M. of three independent experiments carried out in duplicate. * $p < 0.05$ compared with CTL by ANOVA followed by Student Newman-Keuls test.

ABI ViiA7 system (Applied Biosystems™). The cycle conditions comprised 2 min at 50 °C, 10 min at 95 °C, then 40 cycles of 15 s at 95 °C and 1 min at 60 °C. The relative quantification (RQ) of mRNA expression was calculated by the $2^{-\Delta\Delta CT}$ method [16] using Gene Expression Suite™ Software (Applied Biosystems™), and the cells treated with the negative control (0.2% DMSO) were used as a calibrator. The reactions were normalized by the geometric mean of the RQ of the reference genes GAPDH, HPRT1, PGK1 and RLPL0. All experiments were performed in DNase/RNase-free conditions. The genes were considered to be upregulated if the $RQ \geq 2$, which means that the gene expression in TG- and 22-HTG-treated cells were at least twice that of the negative control-treated cells. Similarly, the genes were considered to be downregulated if $RQ \leq 0.5$, which means that the gene expression in TG- and 22-HTG-treated cells were at least half of that of the negative control-treated cells.

2.10. Phospho-specific ELISA

Phosphorylated histone H2AX (S139) (ID DYC2288-2), JNK2 (T183/Y185) (ID DYC2236-2), p38α (T180/Y182) (DYC869B-2) and ERK1 (T202/Y204) (ID DYC1825-2) expression levels were measured in cell lysates using sandwich ELISA kits (all from R&D Systems, Inc. Minneapolis, MN, USA), according to the manufacturer's instructions. HL-60 cells were seeded in a 24-well plate and incubated following treatment with 1.2 μM TG or 2.4 μM 22-HTG for 15 min, 30 min or 24 h, then cells were harvested and suspended in lysis buffer plus phosphatase and

protease inhibitors cocktail and 1 mM PMSF (all from Sigma-Aldrich Co.). Total protein quantification was carried out in each sample by Pierce Protein Assay (Thermo Fisher Scientific, Waltham, MA, USA) using BSA as standard. Absorbance at 450 nm was measured using a SpectraMax 190 Microplate Reader (Molecular Devices, Sunnyvale, CA, USA). Experiments were conducted three times independently.

2.11. DNA interaction assay

DNA interaction was measured in a cell-free system using calf thymus DNA (ctDNA, Sigma-Aldrich Co.), as previously described [17]. The reaction mixture containing 15 μg/mL ctDNA, 1.5 μM ethidium bromide (Sigma-Aldrich Co.) and TG (5 and 10 μM) or 22-HTG (5 and 10 μM) in 100 μL of 0.9% NaCl solution were added to 96-well plates. The vehicle (0.2% DMSO) was used as negative control and doxorubicin (10 μM) was used as positive control. Fluorescence was measured using the excitation and emission wavelengths of 320 and 600 nm, respectively, using a Spectramax Microplate Reader (Molecular Devices).

2.12. Statistical analysis

Data were presented as mean ± S.E.M. or as IC₅₀ values with 95% confidence intervals obtained by nonlinear regressions. The differences between the experimental groups were compared through analysis of variance (ANOVA) followed by Student–Newman–Keuls test ($p < 0.05$). All statistical analyzes were performed using the GraphPad Prism

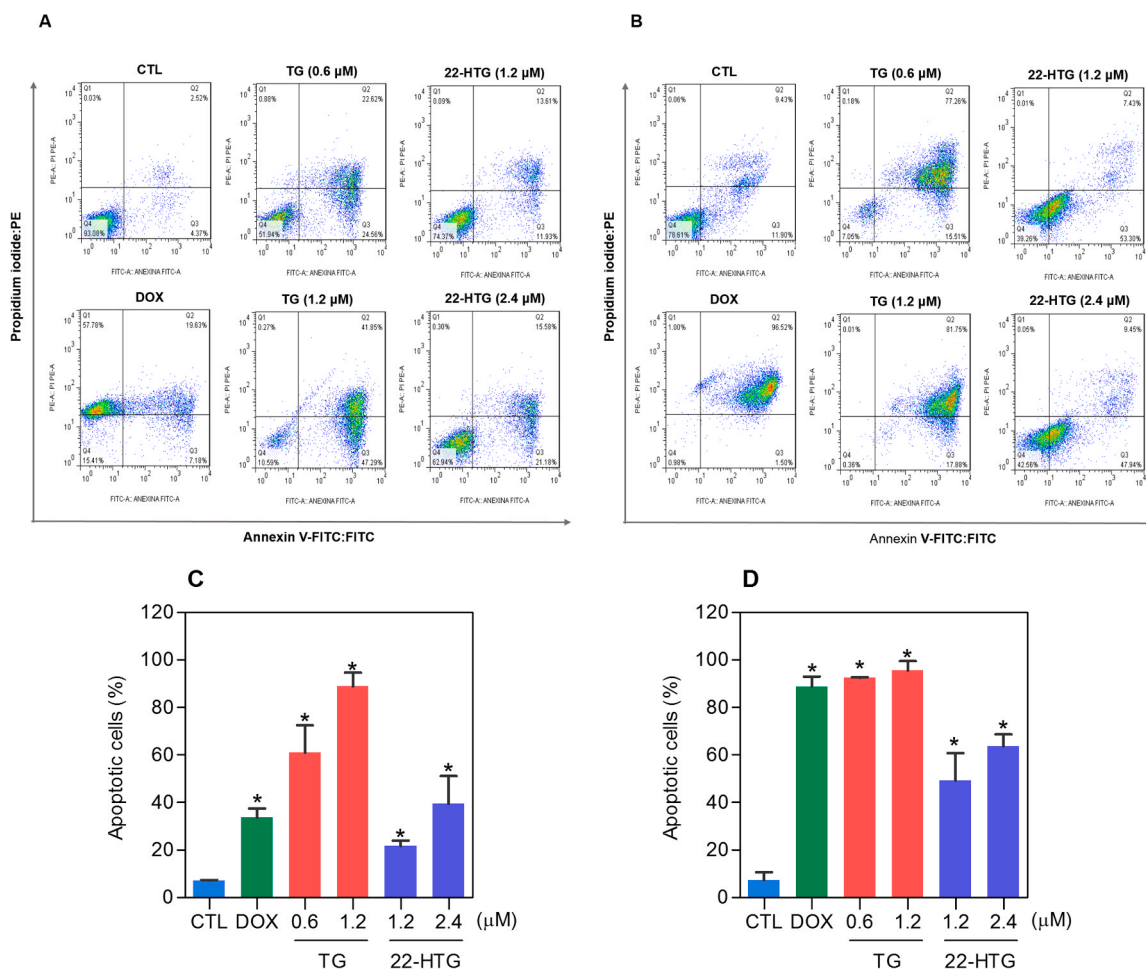


Fig. 5. Induction of apoptosis in HL-60 cells after 24 (A and C) and 48 (B and D) h of treatment with TG and 22-HTG. (A and B) Representative flow cytometric dot plots. (C and D) Quantification of apoptotic HL-60 cells (annexin V-FITC positive cells). The vehicle (0.2% DMSO) was used as a negative control (CTL) and doxorubicin (DOX, 1 μM) was used as a positive control. Data are shown as mean ± S.E.M. of three independent experiments carried out in duplicate. * $p < 0.05$ compared with CTL by ANOVA followed by Student Newman-Keuls test.

(Intuitive Software for Science; San Diego, CA, USA).

3. Results

3.1. Tingenone and 22-hydroxytingenone present potent cytotoxicity in a panel of cancer cells

The cytotoxicity of TG and 22-HTG was evaluated in a panel of 13 different cancer cell lines and 3 non-cancerous cells through the Alamar blue assay after 72 h of incubation. Table 1 shows the data obtained. TG showed IC_{50} values that ranged from 0.69 to 8.58 μM for the cancer cell lines NB4 and HepG2, respectively, while 22-HTG showed IC_{50} values that ranged from 1.15 to 4.70 μM for the cancer cell lines NB4/SCC4 and KG-1a, respectively. Doxorubicin was used as a positive control and showed IC_{50} values ranging from 0.09 to 1.53 μM for the cancer cell lines HCT116 and K562, respectively. Table S2 presents the selectivity index calculated. These data indicated low selectivity of TG and 22-HTG. Doxorubicin also showed potent cytotoxicity to non-cancerous cells.

These data were calculated by nonlinear regression from three independent experiments carried out in duplicate, as quantified by alamar blue assay after 72 h. Doxorubicin (DOX) was used as a positive control. n.d. = not determined.

Next, cell viability was assessed after 24 and 48 h of incubation with TG and 22-HTG with the trypan blue exclusion assay in HL-60 cells (Fig. 2). At concentrations of 0.6 and 1.2 μM, TG reduced the number of viable cells by 85.7% and 98.4% after 24 h and 91.2% and 99.7% after

48 h, respectively. At concentrations of 1.2 and 2.4 μM, 22-HTG reduced the number of viable cells by 63.5% and 76.0% after 24 h and 89.1% and 96.2% after 48 h, respectively. Doxorubicin (1 μM) decreased the number of viable cells by 50.0% and 96.4% after 24 and 48 h of incubation, respectively.

3.2. Tingenone and 22-hydroxytingenone induce caspase-mediated apoptotic cell death in HL-60 cells

In a new set of experiments, DNA content was measured by flow cytometry to quantify the internucleosomal DNA fragmentation and cell cycle distribution in TG- and 22-HTG-treated HL-60 cells (Fig. 3). DNA that was subdiploid (sub- G_0/G_1) was considered fragmented. Both compounds induced DNA fragmentation ($p < 0.05$). At concentrations of 0.6 and 1.2 μM, TG increased the percentage of cells with DNA fragmentation by 12.0% and 69.0% after 24 h and 43.0% and 79.2% after 48 h, respectively. At concentrations of 1.2 and 2.4 μM, 22-HTG increased the percentage of cells with DNA fragmentation by 24.13% and 44.88% after 24 h and 43.5% and 64.5% after 48 h, respectively. Doxorubicin induced cell cycle arrest in G_2/M phase, followed by DNA fragmentation.

Cell morphology was evaluated by light microscopy using hematoxylin & eosin staining after 48 h of treatment (Fig. S1). TG and 22-HTG caused chromatin condensation, cell shrinkage and fragmentation of the nuclei. These morphological features were also observed by flow cytometry through light-scattering where both compounds caused cell

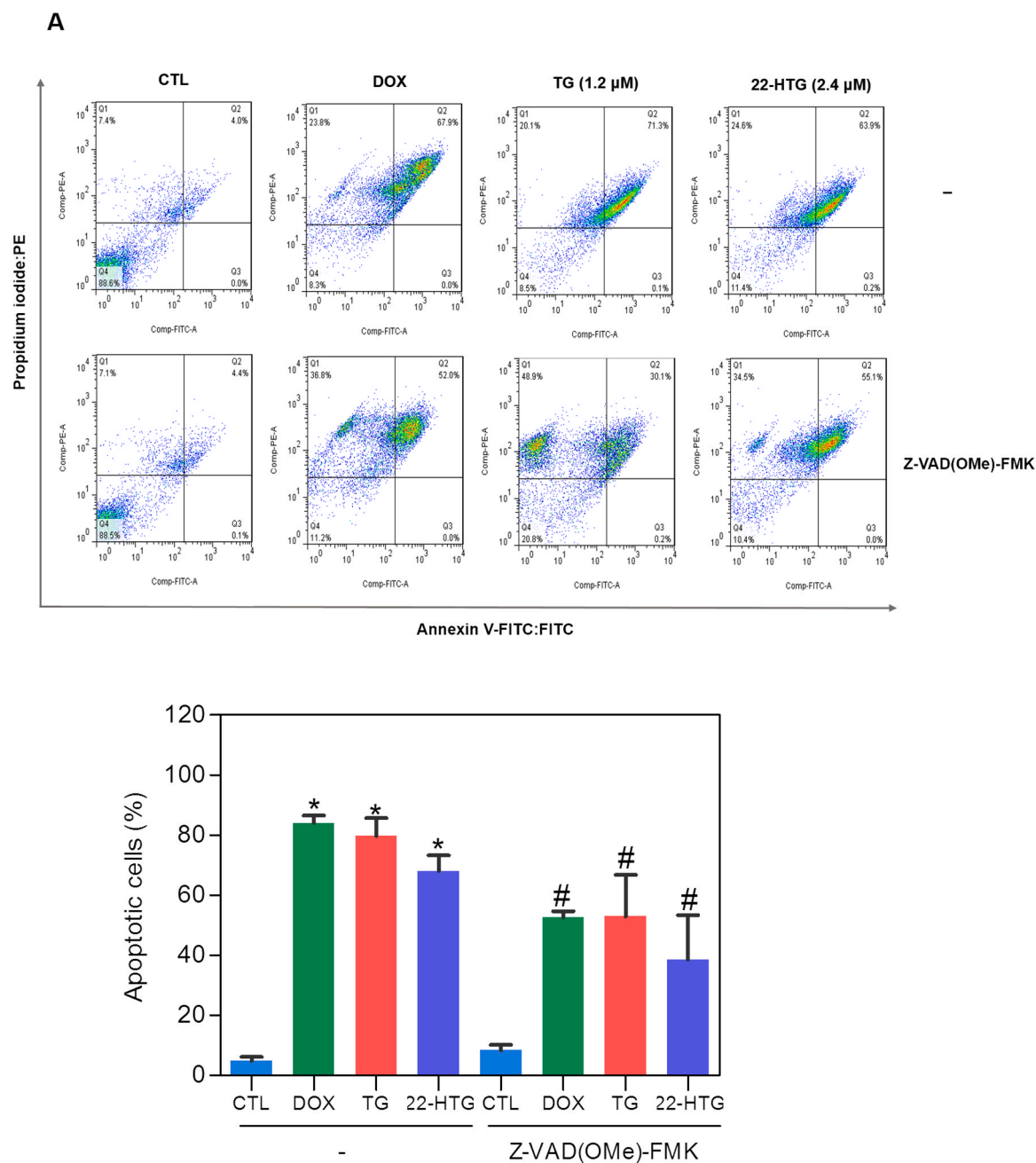


Fig. 6. Action of a pan-caspase inhibitor (Z-VAD(OMe)-FMK) in the apoptosis caused by TG and 22-HTG in HL-60 cells. (A) Representative flow cytometric dot plots. (B) Quantification of apoptotic HL-60 cells (annexin V-FITC positive cells). The cells were pre-treated for 2 h with 50 μ M Z-VAD(OMe)-FMK, then incubated with TG at 1.2 μ M or 22-HTG at 2.4 μ M for 48 h. The vehicle (0.2% DMSO) was used as a negative control (CTL) and doxorubicin (DOX, 1 μ M) was used as a positive control. Data are shown as mean \pm S.E.M. of three independent experiments carried out in duplicate. * p < 0.05 compared with CTL by ANOVA followed by Student Newman-Keuls test. # p < 0.05 compared with the respective treatment without inhibitor by ANOVA followed by Student Newman-Keuls test.

shrinkage, as observed by the decrease in forward-light scatter, and nuclear condensation, as observed by the increase in side scatter (Fig. 4). These morphological changes are associated with apoptotic cell death. Interestingly, doxorubicin also induced morphological changes associated with apoptosis.

Next, annexin V-FITC, a Ca^{2+} -dependent protein with affinity for phosphatidylserine, was used to quantify phosphatidylserine externalization, as an apoptosis marker, and the dye PI was used to assess the loss of membrane integrity, as a necrosis marker. The cells were measured through annexin-V-FITC/PI double staining using flow cytometry after 24 and 48 h. Therefore, viable (those cells that were negative for annexin-V-FITC and PI), early apoptotic (those cells that were positive

for annexin-V-FITC, but negative for PI), late apoptotic cells (those cells that were positive for annexin-V-FITC and PI) and necrotic (annexin-V-FITC negative and PI positive) cells were quantified. Both complexes significantly increased the percentage of apoptotic cells (all cells that were positive for annexin-V-FITC) (Fig. 5). At concentrations of 0.6 and 1.2 μ M, TG increased the percentage of apoptotic cells by 60.9% and 88.8% after 24 h and 92.4% and 95.5% after 48 h, respectively. At concentrations of 1.2 and 2.4 μ M, 22-HTG increased the percentage of apoptotic cells by 21.7% and 39.5% after 24 h and 49.2% and 63.7% after 48 h, respectively. Doxorubicin (1 μ M) also increased the percentage of apoptotic cells by 33.6% and 88.8% after 24 and 48 h, respectively.

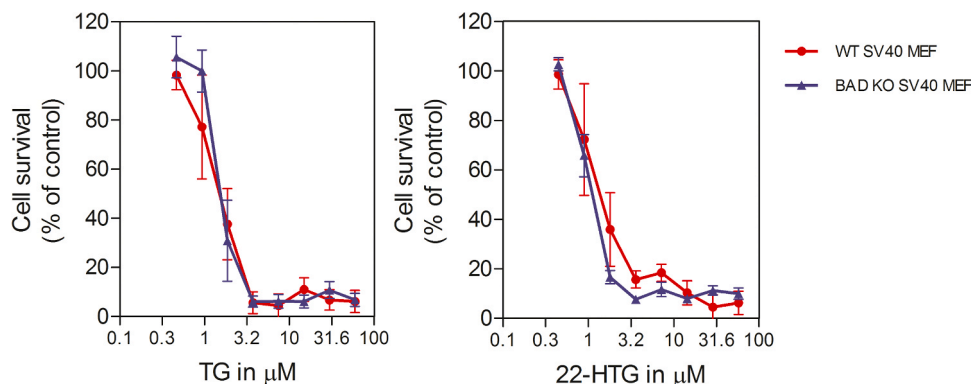


Fig. 7. Survival curves of BAD KO SV40 MEF and WT SV40 MEF cell lines upon treatment with TG and 22-HTG. The curves were obtained from at least three independent experiments carried out in duplicate using Alamar blue assay after 72 h of treatment.

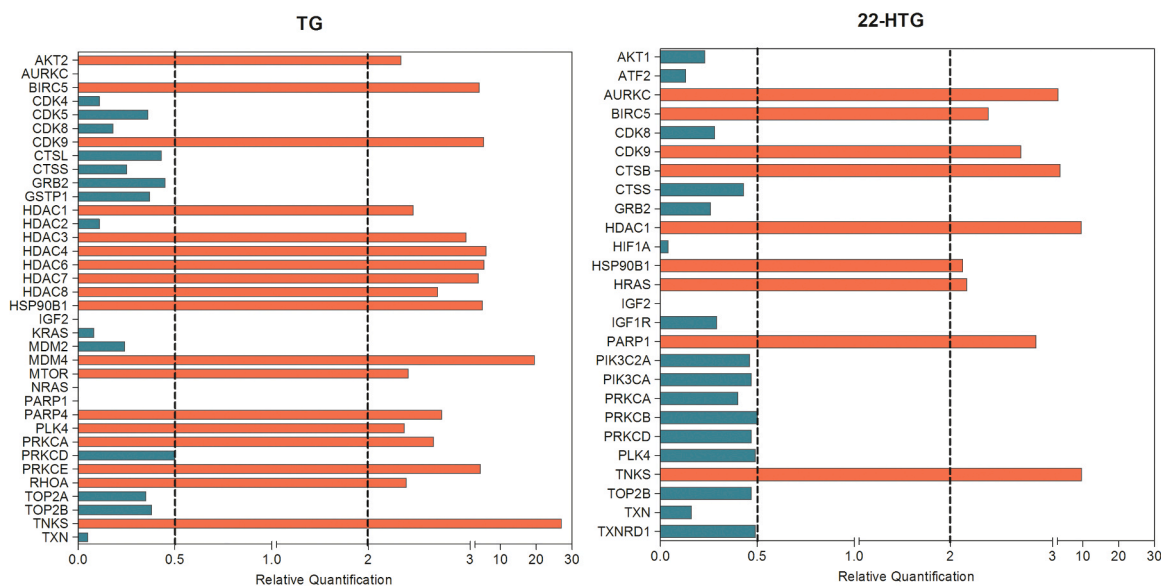


Fig. 8. Genes up- and down-regulated in HL-60 cells after 12 h of treatment with 1.2 μM of TG or 2.4 μM of 22-HTG. The negative control was treated with the vehicle (0.2% DMSO). Values represent the relative quantification (RQ) compared with the calibrator (cells treated with the negative control). The genes were considered to be upregulated if $\text{RQ} \geq 2$ (red bars) and were considered to be downregulated if $\text{RQ} \leq 0.5$ (green bars).

To evaluate the role of caspases in the apoptosis induced by TG and 22-HTG, Z-VAD(OMe)-FMK, a pan-caspase inhibitor, was used. Interestingly, co-treatment with Z-VAD(OMe)-FMK partly decreased the apoptosis induced by TG and 22-HTG (Fig. 6), indicating apoptosis mediated by caspases. The mitochondrial transmembrane potential was also decreased in TG- and 22-HTG-treated cells (Fig. S2).

In additional experiments, we examined the role of BAD gene in the cell death induced by TG and 22-HTG using BAD KO SV40 MEF cell line and in its parental WT SV40 MEF cell line (Fig. 7). The effect of TG and 22-HTG on cell viability was similar in BAD KO SV40 MEF and WT SV40 MEF cell lines, indicating that the BAD gene is not essential for their cytotoxicity.

3.3. Tingenone and 22-hydroxytingenone target oxidative stress through downregulation of thioredoxin leading apoptosis in HL-60 cells

To understand the mechanism of action, the effects of TG and 22-HTG on the expression of 82 genes related to apoptosis, PI3 kinases & phosphatases, growth factors & receptors, drug metabolism, G-protein signaling, hormone receptors, heat shock proteins, receptor tyrosine kinase signaling, cathepsins, cell cycle, topoisomerases type II, transcription factors, protein kinases, RAS signaling, histone deacetylases,

poly ADP-ribose polymerases and structural proteins were detected after 12 h of incubation on HL-60 cells by RT-qPCR array using TaqMan® array human cancer drug targets 96-well plate.

A total of 18 and 9 upregulated genes and 18 and 17 downregulated genes were identified after treatment with TG and 22-HTG, respectively (Fig. 8 and Table S3). Among them, TG downregulated the growth factor gene IGF2, the drug metabolism gene GSTP1 and TXN, the cell cycle genes CDK4, CDK5 and CDK8, the topoisomerases genes TOP2A and TOP2B, the protein kinase gene AURKC, the RAS signaling genes HRAS, KRAS and NRAS, and the poly ADP-ribose polymerase gene PARP1. While downregulation of the growth factor gene IGF2 and its related receptor IGF1R, the drug metabolism genes TXN and TXNRD1, the cell cycle gene CDK8, the topoisomerases gene TOP2B, the transcription factors genes ATF2 and HIF1A, and protein kinases genes PLK4, PRKCA, PRKCB, PRKCC and PRKCD were found after treatment with 22-HTG. Curiously, the gene belongs to the cellular antioxidant system thioredoxin (TXN) was negatively modulated by TG and 22-HTG. Moreover, TG also downregulated the gene expression of glutathione S-transferase pi 1 (GSTP1) and 22-HTG downregulated the gene expression of thioredoxin reductase 1 (TXNRD1) that are important antioxidant enzymes that can protect cells from oxidative stress in various human cancers. These data indicate that the interruption of the cellular antioxidant

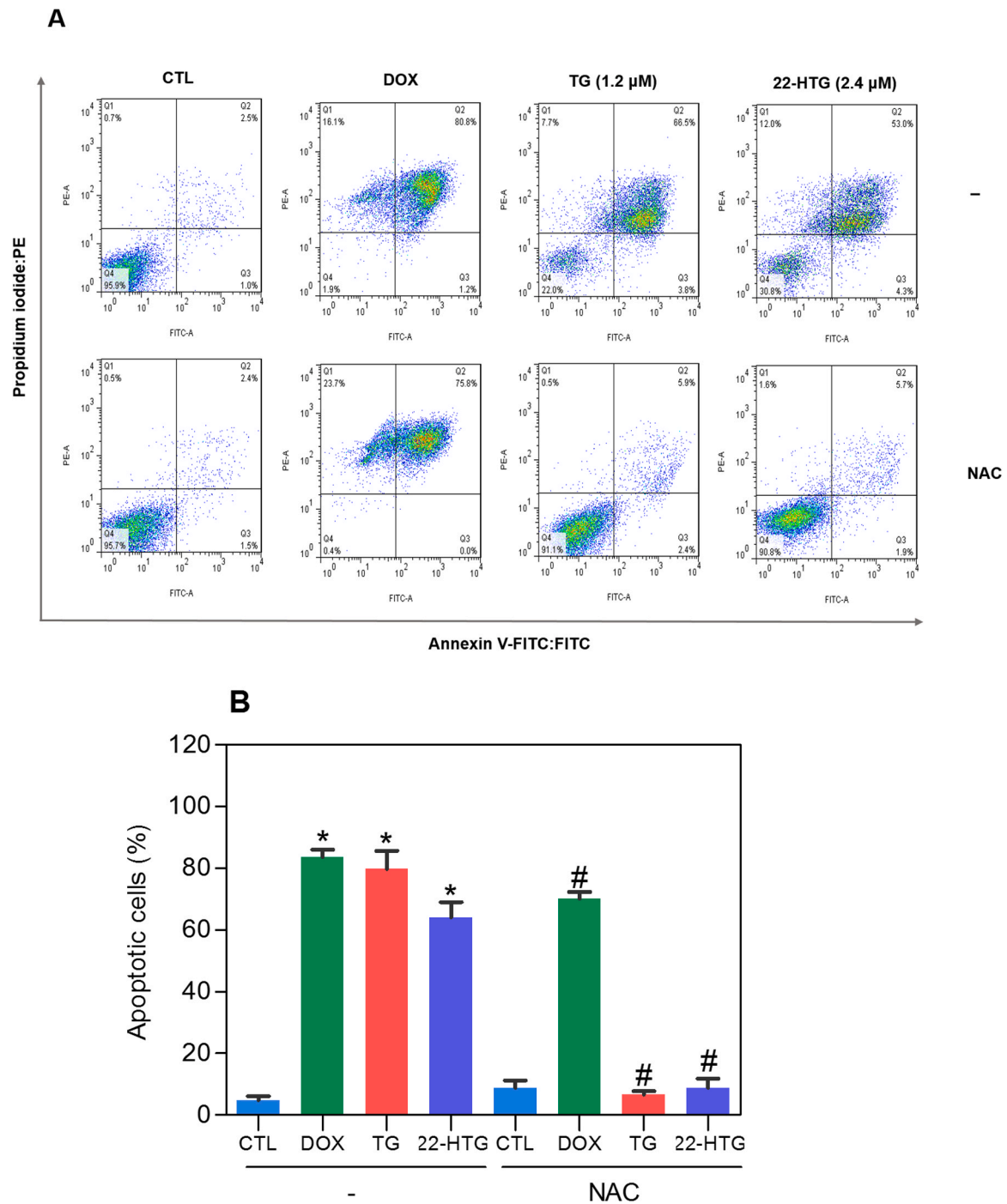


Fig. 9. Action of the antioxidant *N*-acetyl-cysteine (NAC) in the apoptosis induced by TG and 22-HTG in HL-60 cells. (A) Representative flow cytometric dot plots. (B) Quantification of apoptotic HL-60 cells (annexin V-FITC positive cells). The cells were pre-treated for 2 h with 5 mM NAC, and then incubated with TG at 1.2 μ M or 22-HTG at 2.4 μ M for 48 h. The vehicle (0.2% DMSO) was used as a negative control (CTL) and doxorubicin (DOX, 1 μ M) was used as a positive control. Data are shown as mean \pm S.E.M. of three independent experiments carried out in duplicate. * $p < 0.05$ compared with CTL by ANOVA followed by Student Newman-Keuls test. # $p < 0.05$ compared with the respective treatment without inhibitor by ANOVA followed by Student Newman-Keuls test.

system, including downregulation of thioredoxin, as a target of TG and 22-HTG.

Based on the fact of TG and 22-HTG can downregulate the cellular antioxidant system, we decided to study the role of oxidative stress in the cell death induced by these compounds. For that, we measured the apoptotic cells induced by TG and 22-HTG in HL-60 cells that were co-treated with the antioxidant NAC. Interestingly, NAC completely inhibited TG- and 22-HTG-induced apoptosis in HL-60 cells (Fig. 9), indicating that these compounds induce oxidative stress-mediated

apoptotic cell death.

3.4. Tingenone and 22-hydroxytingenone cause DNA damage in HL-60 cells

Induction of oxidative stress can lead to DNA damage. Therefore, we decide to assess DNA double-strand break in HL-60 cells treated with TG and 22-HTG. Phospho-histone H2AX (S139) (also called γ H2AX), a DNA double-strand break marker, expression was measured after 24 h of

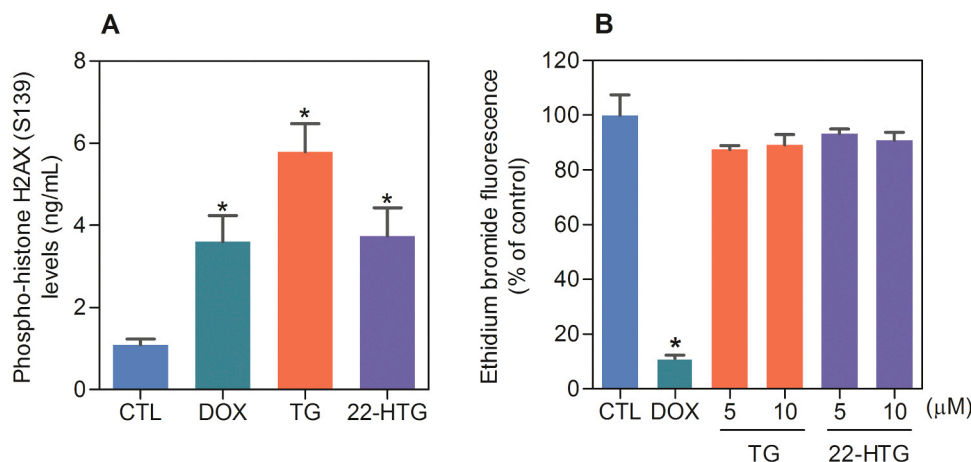


Fig. 10. (A) Phospho-histone H2AX (S139) expression level in HL-60 cells treated with TG at 1.2 μM and 22-HTG at 2.4 μM for 24 h. (B) DNA interaction ability of TG and 22-HTG using ethidium bromide replacement method in a cell-free system with calf thymus DNA. The vehicle (0.2% DMSO) was used as a negative control (CTL) and doxorubicin (DOX, 1 μM) was used as a positive control. Data are shown as mean \pm S.E.M. of three independent experiments carried out in duplicate. * $p < 0.05$ compared with CTL by ANOVA followed by Student Newman-Keuls test.

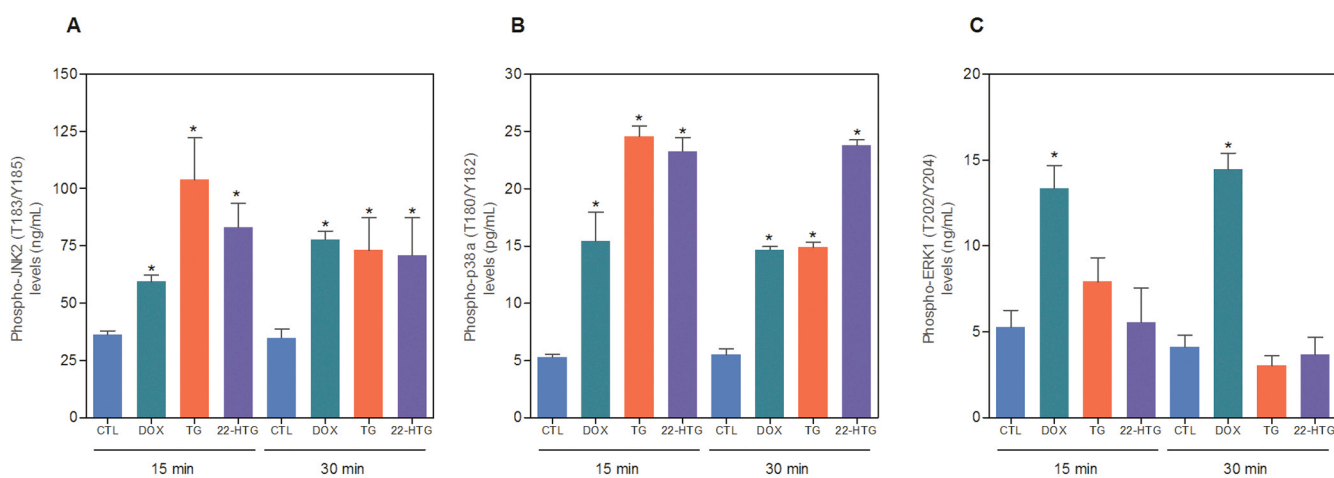


Fig. 11. Phospho-JNK2 (T183/Y185), phospho-p38 α (T180/Y182) and phospho-ERK1 (T202/Y204) expression levels in HL-60 cells treated with TG at 1.2 μM or 22-HTG at 2.4 μM . (A) Quantification of phospho-JNK2 (T183/Y185) expression. (B) Quantification of phospho-p38 α (T180/Y182) expression. (C) Quantification of phospho-ERK1 (T202/Y204) expression. The vehicle (0.2% DMSO) was used as a negative control (CTL) and doxorubicin (DOX, 1 μM) was used as a positive control. Data are shown as mean \pm S.E.M. of three independent experiments carried out in duplicate. * $p < 0.05$ compared with CTL by ANOVA followed by Student Newman-Keuls test.

incubation. Interestingly, treatment with both compounds induced an augment of phosphorylation of histone H2AX, indicating DNA damage (Fig. 10A).

To evaluate whether the DNA damage is caused by a direct DNA-binding ability, TG and 22-HTG were evaluated in a cell-free system using a ctDNA model by ethidium bromide replacement method. In this model, the ability of drugs to displace the ethidium bromide-DNA complex and subsequently reduce the fluorescence is measured. At 5 and 10 μM , neither TG nor 22-HTG significantly decreased the fluorescence intensity, indicating that DNA is not a primary target to these compounds (Fig. 10B). Doxorubicin (10 μM), a known drug that intercalate with DNA, was used as a positive control and decreased the fluorescence intensity by 89.0%.

3.5. Tingenone and 22-hydroxytingenone cause JNK/p38-mediated apoptosis in HL-60 cells

Since mitogen-activated protein kinase (MAPK) signaling is involved in oxidative stress-mediated apoptosis, we decided to evaluate the participation of the MAPK pathway in the apoptosis caused by TG and 22-HTG in HL-60 cells. For that, the levels of expression of phospho-JNK2 (T183/Y185), phospho-p38 α (T180/Y182) and phospho-ERK1 (T202/Y204) were also measured after 15 and 30 min of treatment.

Moreover, the apoptotic cell death caused by TG and 22-HTG was also quantified in HL-60 cells co-incubated with MAPK inhibitors. Interestingly, treatment with TG and 22-HTG increased the phosphorylation of JNK2 (T183/Y185) and phospho-p38 α (T180/Y182), without change phospho-ERK1 (T202/Y204) expression levels (Fig. 11). In addition, co-incubation with a JNK/SAPK inhibitor (SP 600125) and a p38 MAPK inhibitor (PD 169316), but not a MEK (mitogen-activated protein kinase) inhibitor (U-0126) that inhibits the activation of ERK1/2, prevent partially TG and 22-HTG-induced apoptosis, indicating apoptotic cell death through JNK/p38 pathways in HL-60 cells (Fig. 12).

4. Discussion

Herein, we demonstrated that TG and 22-HTG target oxidative stress through downregulation of thioredoxin leading DNA damage and MAPK-mediated apoptosis in AML cell line HL-60. This is the first report on the ability of TG and 22-HTG to inhibit the cellular antioxidant system, including downregulation of thioredoxin, as a target of their cytotoxicity.

Metabolic reprogramming is known as a hallmark of cancer. In this context, aberrant metabolism leads to increased oxidative stress in cancer cells [18]. Interestingly, thioredoxin reductase 1 has been reported to be overexpressed in several types of cancer, including

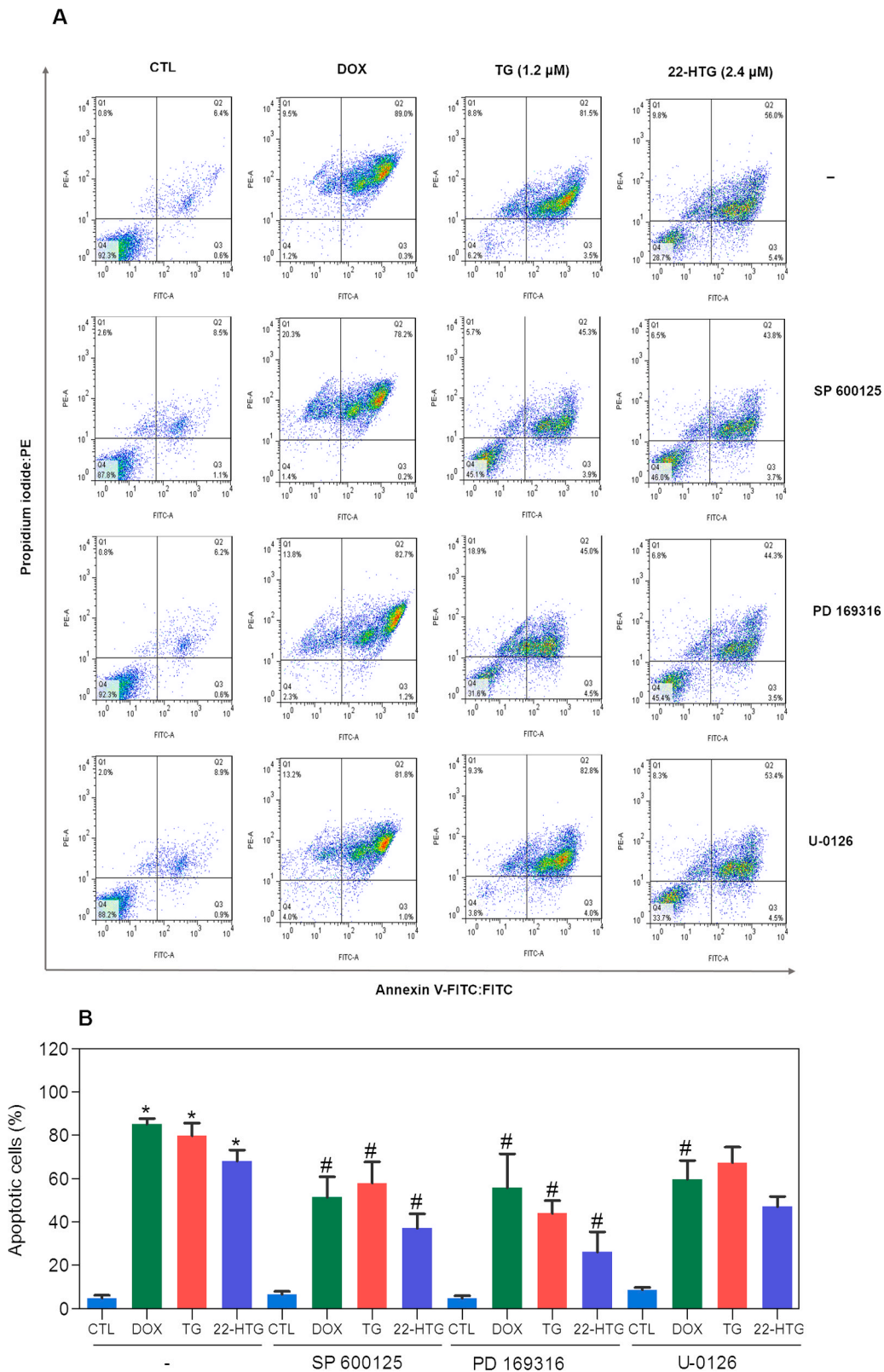


Fig. 12. Action of the JNK/SAPK inhibitor (SP 600125), p38 MAPK inhibitor (PD 169316) and MEK inhibitor (U-0126) on the apoptosis induced by TG and 22-HTG in HL-60 cells. (A) Representative flow cytometric dot plots. (B) Quantification of apoptotic HL-60 cells (annexin V-FITC positive cells). Cells were pretreated for 2 h with 5 μ M U-0126, 5 μ M SP 600125 or 5 μ M PD 169316 and then incubated with TG at 1.2 μ M or 22-HTG at 2.4 μ M for 48 h. The vehicle (0.2% DMSO) was used as a negative control (CTL) and doxorubicin (DOX, 1 μ M) was used as a positive control. Data are shown as mean \pm S.E.M. of three independent experiments carried out in duplicate. * $p < 0.05$ compared with CTL by ANOVA followed by Student Newman-Keuls test. # $P < 0.05$ compared with the respective treatment without inhibitor by ANOVA, followed by the Student-Newman-Keuls test.

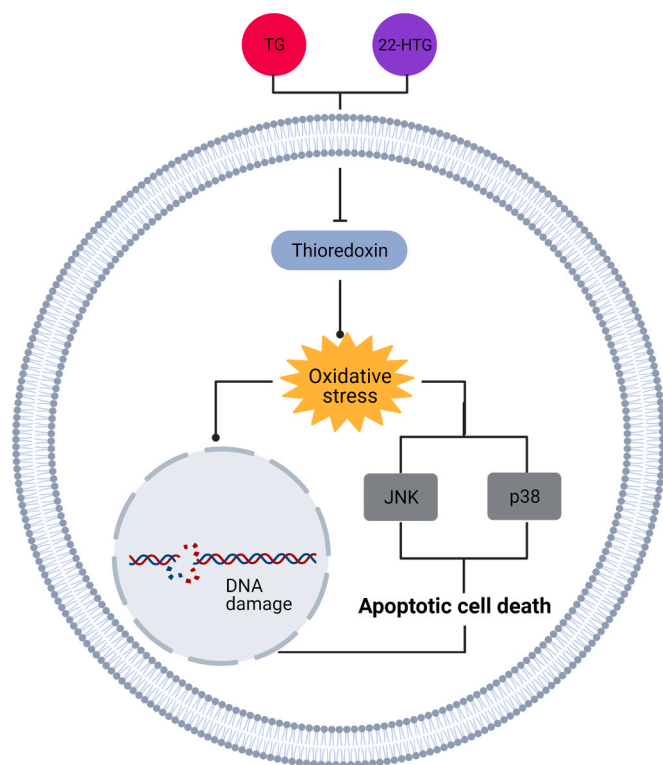


Fig. 13. Molecular mechanism of action proposed for TG and 22-HTG in HL-60 cells.

leukemia. The thioredoxin system is an important class of the mammalian antioxidant system, which scavenges reactive oxygen species to maintain intracellular redox homeostasis. It is composed by thioredoxin, thioredoxin reductase and nicotinamide adenine dinucleotide phosphate (NADPH) [19–24]. Moreover, thioredoxin knockdown with shRNA inhibits the growth of prostate cancer cells [25].

Using a RT-qPCR array, we identified downregulation of thioredoxin as target of TG and 22-HTG. In addition, 22-HTG also downregulated the gene expression of thioredoxin reductase 1. Likewise, TG also downregulated the gene expression of glutathione S-transferase pi 1, another important regulator of oxidative stress, acting by combining glutathione with electrophiles [26]. Furthermore, by functional assay using the antioxidant NAC, we observed that TG and 22-HTG induce oxidative stress-mediated apoptotic cell death.

Pristimerin, a quinonemethide triterpene structurally related to TG and 22-HTG, has been previously reported to inhibit thioredoxin, leading to apoptosis and autophagy through activation of ROS/ASK1/JNK pathway in human breast cancer [27]. Moreover, pristimerin caused apoptosis and autophagy in K562 cells through G₁ phase arrest and produced oxidative stress-inducing JNK activation [28]. Likewise, oxidative stress induced by pristimerin was associated with JNK activation in glioma cells [29], colorectal [30] and cervical [31]. Interestingly, TG and 22-HTG caused DNA damage and MAPK-mediated apoptosis in AML cell line HL-60.

As mentioned above, previous studies using 22-HTG also observed induction of apoptosis and suppression of invasiveness of melanoma cells by inhibiting MMP-2 and MMP-9 activity and expression of BRAF, NRAS and KRAS genes [7,8]. Here, we observed that TG also reduces the expression of the cell cycle genes CDK4, CDK5 and CDK8, topoisomerases type II genes, aurora kinase C (AURKC) gene and the RAS signaling genes HRAS, KRAS and NRAS. While 22-HTG also reduces the expression of the cell cycle gene CDK8, the topoisomerase type II gene and the transcription factors genes ATF2 and HIF1A. These data indicate that cell cycle control proteins, topoisomerases, aurora kinase C, RAS

signaling and transcription factors genes ATF2 and HIF1A can also be targets of TG and 22-HTG.

In summary, we showed the ability of TG and 22-HTG to inhibit the proliferation of AML cell line HL-60 cells by inducing apoptosis. Suppression of the thioredoxin system following treatment with TG and 22-HTG result in oxidative stress, leading to DNA damage and MAPK activation, which contribute to TG and 22-HTG-mediated apoptotic cell death. The molecular mechanism of action proposed for TG and 22-HTG in HL-60 cells is shown in Fig. 13.

CRediT authorship contribution statement

ACBCR: Conceptualization; Formal analysis; Investigation; Methodology. **LMB:** Investigation; Methodology. **SPN:** Investigation; Methodology. **MBPS:** Funding acquisition; Supervision; Visualization. **RBD:** Investigation; Methodology. **LFV:** Investigation; Methodology. **CAGR:** Investigation; Methodology; Funding acquisition; Supervision; Visualization. **EVC:** Investigation; Methodology. **FMAS:** Investigation; Methodology. **WCR:** Investigation; Methodology. **HHFK:** Investigation; Methodology. **DPB:** Conceptualization; Formal analysis; Roles/Writing – original draft; Writing – review & editing.

Conflicts of interest

The authors have declared that there are no conflicts of interest.

Acknowledgments

The authors would like to thanks the flow cytometry core of FIOCRUZ-Bahia for flow cytometry data collection. This work was financially supported by Brazilian agencies: Coordenação de Aperfeiçoamento de Pessoal de Nível Superior (CAPES); Conselho Nacional de Desenvolvimento Científico e Tecnológico (CNPq); Fundação de Amparo à Pesquisa do Estado do Amazonas (FAPEAM); and Fundação de Amparo à Pesquisa do Estado da Bahia (FAPESB).

Appendix A. Supporting information

Supplementary data associated with this article can be found in the online version at doi:10.1016/j.biopha.2021.112034.

References

- [1] H. Sung, J. Ferlay, R.L. Siegel, M. Laversanne, I. Soerjomataram, A. Jemal, F. Bray, Global cancer statistics 2020: GLOBOCAN estimates of incidence and mortality worldwide for 36 cancers in 185 countries, *CA Cancer J. Clin.* (2020), <https://doi.org/10.3322/caac.21660>.
- [2] American Cancer Society. *Cancer Facts & Figures 2020*. Atlanta, Ga: American Cancer Society; 2020.
- [3] H. Dombret, C. Gardin, An update of current treatments for adult acute myeloid leukemia, *Blood* 127 (1) (2016) 53–61, <https://doi.org/10.1182/blood-2015-08-604520>.
- [4] R. Bavovada, G. Blaskó, H.L. Shieh, J.M. Pezzuto, G.A. Cordell, Spectral assignment and cytotoxicity of 22-hydroxytingenone from *Glyptopetalum sclerocarpum*, *Planta Med.* 56 (4) (1990) 380–382, <https://doi.org/10.1055/s-2006-960988>.
- [5] B. Cevatemre, B. Botta, M. Mori, S. Berardozi, C. Ingallina, E. Ulukaya, The plant-derived triterpenoid tingenin B is a potent anticancer agent due to its cytotoxic activity on cancer stem cells of breast cancer in vitro, *Chem. Biol. Interact.* 260 (2016) 248–255, <https://doi.org/10.1016/j.cbi.2016.10.001>.
- [6] A.C.B.D.C. Rodrigues, F.P. Oliveira, R.B. Dias, C.B.S. Sales, C.A.G. Rocha, M.B. P. Soares, E.V. Costa, F.M.A.D. Silva, W.C. Rocha, H.H.F. Koolen, D.P. Bezerra, In vitro and in vivo anti-leukemia activity of the stem bark of *Salacia impressifolia* (Miers) A. C. Smith (Celastraceae), *J. Ethnopharmacol.* 1 (231) (2019) 516–524, <https://doi.org/10.1016/j.jep.2018.11.008>.
- [7] E.S.P. Aranha, E.L. da Silva, F.P. Mesquita, L.B. de Sousa, F.M.A. da Silva, W. C. Rocha, E.S. Lima, H.H.F. Koolen, M.E.A. de Moraes, R.C. Montenegro, M.C. de Vasconcelos, 22 β -hydroxytingenone reduces proliferation and invasion of human melanoma cells, *Toxicol. In Vitro* 66 (2020), 104879, <https://doi.org/10.1016/j.tiv.2020.104879>.
- [8] E.S.P. Aranha, A.J.S. Portilho, L. Bentes de Sousa, E.L. da Silva, F.P. Mesquita, W. C. Rocha, F.M. Araújo da Silva, E.S. Lima, 22 β -hydroxytingenone induces apoptosis

- and suppresses invasiveness of melanoma cells by inhibiting MMP-9 activity and MAPK signaling, *J. Ethnopharmacol.* 267 (2021), 113605, <https://doi.org/10.1016/j.jep.2020.113605>.
- [9] H. Morita, Y. Hirasawa, A. Muto, T. Yoshida, S. Sekita, O. Shirota, Antimitotic quinoid triterpenes from *Maytenus chuchuhuasca*, *Bioorg. Med. Chem. Lett.* 18 (3) (2008) 1050–1052, <https://doi.org/10.1016/j.bmcl.2007.12.016>.
- [10] T.H. Desai, S.V. Joshi, In silico evaluation of apoptogenic potential and toxicological profile of triterpenoids, *Indian J. Pharmacol.* 51 (3) (2019) 181–207, https://doi.org/10.4103/ijp.90_18.
- [11] S.A. Ahmed, R.M.Jr Gogal, J.E. Walsh, A new rapid and simple non-radioactive assay to monitor and determine the proliferation of lymphocytes: an alternative to [³H]thymidine incorporation assay, *J. Immunol. Methods* 170 (1994) 211–224.
- [12] L.S. Santos, V.R. Silva, L.R.A. Menezes, M.B.P. Soares, E.V. Costa, D.P. Bezerra, Xylopin induces oxidative stress and causes G₂/M Phase arrest, triggering caspase-mediated apoptosis by p53-independent pathway in HCT116 cells, *Oxid. Med. Cell. Longev.* 2017 (2017), 7126872.
- [13] V.R. Silva, R.S. Corrêa, L.S. Santos, M.B.P. Soares, A.A. Batista, D.P. Bezerra, A ruthenium-based 5-fluorouracil complex with enhanced cytotoxicity and apoptosis induction action in HCT116 cells, *Sci. Rep.* 8 (1) (2018) 288.
- [14] I. Nicoletti, G. Migliorati, M.C. Pagliacci, F. Grignani, C. Riccardi, A rapid and simple method for measuring thymocyte apoptosis by propidium iodide staining and flow cytometry, *J. Immunol. Methods* 139 (1991) 271–279.
- [15] F.X. Sureda, E. Escubedo, C. Gabriel, J. Comas, J. Camarasa, A. Camins, Mitochondrial membrane potential measurement in rat cerebellar neurons by flow cytometry, *Cytometry* 28 (1997) 74–80.
- [16] K.J. Livak, T.D. Schmittgen, Analysis of relative gene expression data using real-time quantitative PCR and the 2(-Delta Delta C(T)) Method, *Methods* 25 (2001) 402–408.
- [17] L.S. Glass, A. Bapat, M.R. Kelley, M.M. Georgiadis, E.C. Long, Semi-automated high-throughput fluorescent intercalator displacement-based discovery of cytotoxic DNA binding agents from a large compound library, *Bioorg. Med. Chem. Lett.* 20 (2010) 1685–1688.
- [18] D. Hanahan, R.A. Weinberg, Hallmarks of cancer: the next generation, *Cell* 144 (2011) 646–674.
- [19] L. Shao, M.B. Diccianni, T. Tanaka, R. Gribo, A.L. Yu, J.D. Pullen, B.M. Camitta, J. Yu, Thioredoxin expression in primary T-cell acute lymphoblastic leukemia and its therapeutic implication, *Cancer Res.* 61 (19) (2001) 7333–7338.
- [20] H. Li, M. Li, G. Wang, F. Shao, W. Chen, C. Xia, S. Wang, Y. Li, G. Zhou, Z. Liu, EM23, a natural sesquiterpene lactone from *Elephantopus mollis*, induces apoptosis in human myeloid leukemia cells through thioredoxin- and reactive oxygen species mediated signaling pathways, *Front. Pharmacol.* 7 (2016) 77, <https://doi.org/10.3389/fphar.2016.00077>.
- [21] Z. Zheng, S. Fan, J. Zheng, W. Huang, C. Gasparetto, N.J. Chao, J. Hu, Y. Kang, Inhibition of thioredoxin activates mitophagy and overcomes adaptive bortezomib resistance in multiple myeloma, *J. Hematol. Oncol.* 11 (2018) 29, <https://doi.org/10.1186/s13045-018-0575-7>.
- [22] W. Xie, W. Ma, P. Liu, F. Zhou, Overview of thioredoxin system and targeted therapies for acute leukemia, *Mitochondrion* 47 (2019) 38–46, <https://doi.org/10.1016/j.mito.2019.04.010>.
- [23] J.J. Jia, W.S. Geng, Z.Q. Wang, L. Chen, X.S. Zeng, The role of thioredoxin system in cancer: strategy for cancer therapy, *Cancer Chemother. Pharmacol.* 84 (2019) 453–470, <https://doi.org/10.1007/s00280-019-03869-4>.
- [24] E. Clapper, S. Wang, P.V. Ranning, G. Di Trapani, K.F. Tonissen, Cross-talk between Bcr-abl and the thioredoxin system in chronic myeloid leukaemia: implications for CML treatment, *Antioxidants* 9 (2020) 207, <https://doi.org/10.3390/antiox9030207>.
- [25] G.J. Samaranayake, C.I. Troccoli, M. Huynh, R. Lyles, K. Kage, A. Win, V. Lakshmanan, D. Kwon, Y. Ban, S.X. Chen, E.R. Zarco, M. Jorda, K.L. Burnstein, P. Rai, Thioredoxin-1 protects against androgen receptor-induced redox vulnerability in castration-resistant prostate cancer, *Nat. Commun.* 8 (2017) 1204, <https://doi.org/10.1038/s41467-017-01269-x>.
- [26] R.R. Singh, J. Mohammad, M. Orr, K.M. Reindl, Glutathione S-transferase pi-1 knockdown reduces pancreatic ductal adenocarcinoma growth by activating oxidative stress response pathways, *Cancers* 12 (2020) 1501, <https://doi.org/10.3390/cancers12061501>.
- [27] Q. Zhao, Y. Liu, J. Zhong, Y. Bi, Y. Liu, Z. Ren, X. Li, J. Jia, M. Yu, X. Yu, Pristimerin induces apoptosis and autophagy via activation of ROS/ASK1/JNK pathway in human breast cancer in vitro and in vivo, *Cell Death Discov.* 5 (2019) 125, <https://doi.org/10.1038/s41420-019-0208-0>.
- [28] Y. Liu, Z. Ren, X. Li, J. Zhong, Y. Bi, R. Li, Q. Zhao, X. Yu, Pristimerin Induces autophagy-mediated cell death in K562 cells through the ROS/JNK signaling pathway, *Chem. Biodivers.* 16 (8) (2019), 1900325, <https://doi.org/10.1002/cbdv.201900325>.
- [29] H. Zhao, C. Wang, B. Lu, Z. Zhou, Y. Jin, Z. Wang, L. Zheng, K. Liu, T. Luo, D. Zhu, G. Chi, Y. Luo, P. Ge, Pristimerin triggers AIF-dependent programmed necrosis in glioma cells via activation of JNK, *Cancer Lett.* 374 (1) (2016) 136–148, <https://doi.org/10.1016/j.canlet.2016.01.055>.
- [30] Q. Zhao, Y. Bi, J. Guo, Y. Liu, J. Zhong, Y. Liu, L. Pan, Y. Guo, Y. Tan, X. Yu, Effect of pristimerin on apoptosis through activation of ROS/ endoplasmic reticulum (ER) stress-mediated noxa in colorectal cancer, *Phytomedicine* 80 (2021), 153399, <https://doi.org/10.1016/j.phymed.2020.153399>.
- [31] J.Y. Byun, M.J. Kim, D.Y. Eum, C.H. Yoon, W.D. Seo, K.H. Park, J.W. Hyun, Y. S. Lee, J.S. Lee, M.Y. Yoon, S.J. Lee, Reactive oxygen species-dependent activation of Bax and poly(ADP-ribose) polymerase-1 is required for mitochondrial cell death induced by triterpenoid pristimerin in human cervical cancer cells, *Mol. Pharmacol.* 76 (4) (2009) 734–744, <https://doi.org/10.1124/mol.109.056259>.

Supplementary Material

Tingenone and 22-hydroxytingenone target oxidative stress through downregulation of thioredoxin, leading to DNA double-strand break and JNK/p38-mediated apoptosis in acute myeloid leukemia HL-60 cells

Ana Carolina B. da C. Rodrigues¹, Larissa M. Bomfim¹, Sara P. Neves¹, Milena B. P. Soares^{1,2}, Rosane B. Dias^{1,3}, Ludmila F. Valverde¹, Clarissa A. Gurgel Rocha^{1,3}, Emmanoel V. Costa⁴, Felipe M. A. da Silva⁴, Waldireny C. Rocha⁵, Hector H. F. Koolen⁶, Daniel P. Bezerra^{1,*}

¹Gonçalo Moniz Institute, Oswaldo Cruz Foundation (IGM-FIOCRUZ/BA), Salvador, Bahia, 40296-710, Brazil.

²SENAI Institute for Innovation in Advanced Health Systems, SENAI CIMATEC, Salvador, BA, 41650-010, Brazil;

³Department of Clinical Propaedeutics and Integrated Clinical, Faculty of Dentistry, Federal University of Bahia (UFBA), Salvador, Bahia, 40301-155, Brazil.

⁴Department of Chemistry, Federal University of Amazonas (UFAM), Manaus, Amazonas 69077-000, Brazil

⁵Health and Biotechnology Institute, Federal University of Amazonas (UFAM), Coari, Amazonas 69460-000, Brazil

⁶Metabolomics and Mass Spectrometry Research Group, Amazonas State University (UEA), Manaus, Amazonas, 690065-130, Brazil.

*Corresponding authors:

D. P. Bezerra, E-mail: danielpbezerra@gmail.com or daniel.bezerra@fiocruz.br Tel/Fax + 55 71 3176 2272.

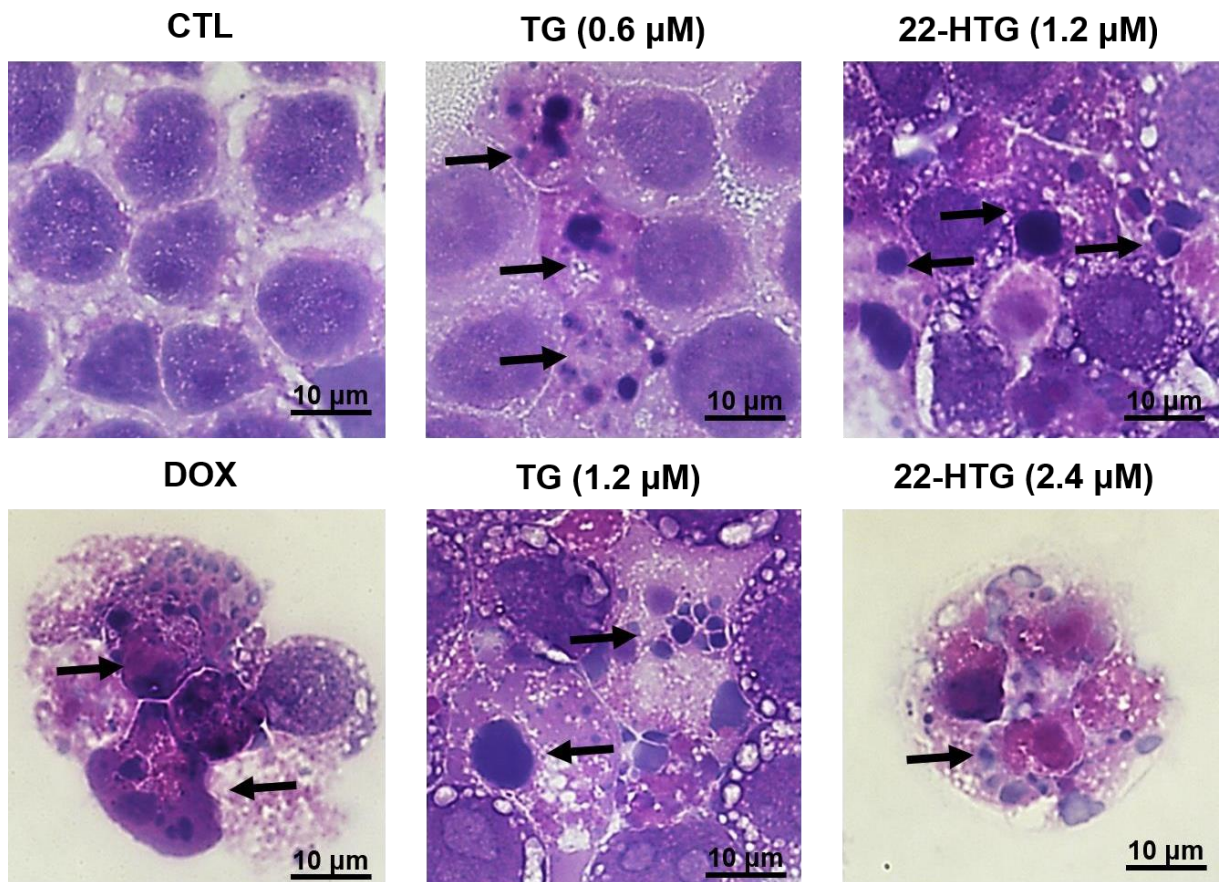


Figure S1. Effect of TG and 22-HTG in the morphological analysis of HL-60 cells, assessed by hematoxylin & eosin staining and examined by light microscopy (bar = 10 μm), after 48 h of treatment. The vehicle (0.2% DMSO) was used as a negative control (CTL) and doxorubicin (DOX, 1 μM) was used as a positive control. Arrows indicated cells with chromatin condensation, fragmented DNA and/or cell shrinkage.

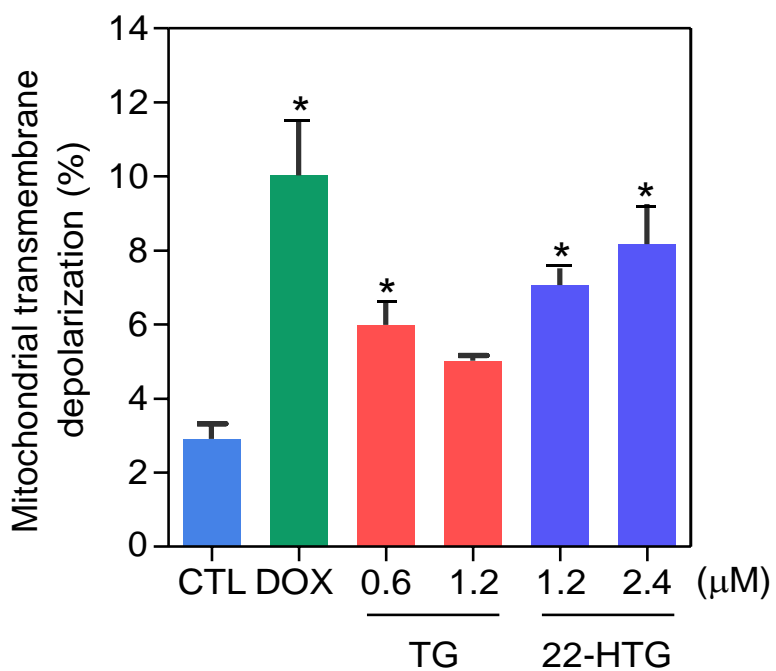


Figure S2. Effect of TG and 22-HTG on the mitochondrial membrane potential of HL-60 cells, as determined by flow cytometry using rhodamine 123 staining after 24 h of incubation. The vehicle (0.2% DMSO) was used as a negative control (CTL) and doxorubicin (DOX, 1 μ M) was used as a positive control. Data are shown as mean \pm S.E.M. of three independent experiments carried out in duplicate. * $p < 0.05$ compared with CTL by ANOVA followed by Student Newman-Keuls test.

Table S1. List of cell lines used

Cells	Histological type	Origin	Source
Cancer cells			
HL-60	acute promyelocytic leukemia	human	ATCC
Jurkat	acute T cell leukemia	human	ATCC
THP-1	acute promyelocytic leukemia	human	ATCC
KG-1a	acute myelogenous leukemia	human	ATCC
NB4	acute promyelocytic leukemia	human	ATCC
K-562	chronic myelogenous leukemia	human	ATCC
MCF-7	breast adenocarcinoma	human	ATCC
HCT116	colon carcinoma	human	ATCC
HepG2	hepatocellular carcinoma	human	ATCC
CAL 27	tongue squamous cell carcinoma	human	ATCC
HSC-3	tongue squamous cell carcinoma	human	ATCC
SCC-4	tongue squamous cell carcinoma	human	ATCC
B16-F10	melanoma	mouse	ATCC
Non-cancerous cells			
MRC-5	human lung fibroblast	human	ATCC
BJ	human foreskin fibroblast	human	ATCC
PBMC	human peripheral blood mononuclear cells	human	primary cell culture
Mutant and its parental cell			

BAD KO SV40 MEF	immortalized mouse embryonic fibroblasts with the BAD gene knocked out	mouse	ATCC
WT SV40 MEF	wild-type immortalized embryonic fibroblasts	mouse	ATCC

ATCC denotes American Type Culture Collection. Primary cell culture of peripheral blood mononuclear cells (PBMC) was obtained from peripheral blood from healthy donors by standard ficoll density protocol. Briefly, PBMC were resuspended in RPMI 1640 medium with 20% fetal bovine serum and 50 µg/mL gentamicin and kept at 37°C with 5% CO₂. Concanavalin A (10 µg/mL, Sigma-Aldrich) was used as a mitogen to trigger cell division in T lymphocytes and was added at the beginning of the culture. The Research Ethics Committee of the Oswaldo Cruz Foundation (Salvador, Bahia, Brazil) approved the experimental protocol (n° 031019/2013).

Table S2. Selectivity index of TG and 22-HTG

Cancer cells	Non-cancerous cells								
	MRC-5			BJ			PBMC		
	DOX	TG	22-	DOX	TG	22-	DOX	TG	22-
	HTG			HTG			HTG		
HL-60	4.8	1.4	1.8	10.5	1.6	1.6	3.5	0.4	n.d.
Jurkat	n.d.	1.9	1.7	n.d.	2.2	1.5	n.d.	0.5	n.d.

THP-1	6.6	1.6	2.2	14.3	1.9	2.0	4.8	0.5	n.d.
KG-1a	n.d.	0.8	0.6	n.d.	0.9	0.6	n.d.	0.2	n.d.
NB4	3.6	4.1	2.5	7.9	4.8	2.2	2.6	1.2	n.d.
K-562	1.1	1.3	1.2	2.4	1.5	1.1	0.8	0.4	n.d.
MCF-7	1.1	0.5	1.0	2.4	0.6	0.9	0.8	0.2	n.d.
HCT116	18.0	0.9	2.3	39.3	1.1	2.1	13.2	0.3	n.d.
HepG2	5.2	0.3	1.2	11.2	0.4	1.1	3.8	0.1	n.d.
CAL 27	4.8	1.7	2.2	10.5	2.0	2.0	3.5	0.5	n.d.
HSC-3	3.1	1.4	1.8	6.8	1.6	1.7	2.3	0.4	n.d.
SCC-4	0.8	2.8	2.5	1.7	3.2	2.3	0.6	0.8	n.d.
B16-F10	14.4	1.3	1.4	31.4	1.5	1.3	10.6	0.4	n.d.

Data are presented the selectivity index (SI) calculated using the following formula: $SI = IC_{50}[\text{non-cancerous cells}] / IC_{50}[\text{cancer cells}]$. Cancer cells: HL-60 (human acute promyelocytic leukemia); Jurkat (human acute T cell leukemia); THP-1 (human acute monocytic leukemia); KG-1a (human acute myelogenous leukemia); NB4 (human acute promyelocytic leukemia); K-562 (human chronic myelogenous leukemia); MCF-7 (human breast adenocarcinoma); HCT116 (human colon carcinoma); HepG2 (human hepatocellular carcinoma); CAL 27 (human tongue squamous cell carcinoma); HSC-3 (human tongue squamous cell carcinoma); SCC-4 (human tongue squamous cell carcinoma); and B16-F10 (mouse melanoma). Non-cancerous cells: MRC-5 (human lung fibroblast); BJ (human foreskin fibroblast); and PBMC (Peripheral blood mononuclear cells). Doxorubicin (DOX) was used as positive control. n.d. = not determined.

Table S3. The effect of on gene expression of TG and 22-HTG in HL-60 cells

Function/Assay ID	Gene symbol	Full name	RQ		
			CTL	TG	22-HTG
Apoptosis					
Hs00608023_m1	BCL2	BCL2, apoptosis regulator	1.0	1.42	1.91
Hs04194392_s1	BIRC5	baculoviral IAP repeat containing 5	1.0	4.14	2.37
PI3 Kinases & Phosphatases					
Hs00234508_m1	MTOR	mechanistic target of rapamycin	1.0	2.39	1.39
Hs00904054_m1	PIK3C2A	phosphatidylinositol-4-phosphate 3-kinase catalytic subunit type 2 alpha	1.0	0.67	0.46
Hs00176908_m1	PIK3C3	phosphatidylinositol 3-kinase catalytic subunit type 3	1.0	1.23	0.84
Hs00907957_m1	PIK3CA	phosphatidylinositol-4,5-bisphosphate 3-kinase catalytic subunit alpha	1.0	0.94	0.47
Growth Factors & Receptors					
Hs01076090_m1	EGFR	epidermal growth factor receptor	n.d.	n.d.	n.d.
Hs01001580_m1	ERBB2	erb-b2 receptor tyrosine kinase 2	n.d.	n.d.	n.d.
Hs00176538_m1	ERBB3	erb-b2 receptor tyrosine kinase 3	n.d.	n.d.	n.d.
Hs01128657_m1	FIGF	c-fos induced growth factor	n.d.	n.d.	n.d.
Hs01052961_m1	FLT1	fms related tyrosine kinase 1	n.d.	n.d.	n.d.
Hs01047677_m1	FLT4	fms related tyrosine kinase 4	n.d.	n.d.	n.d.
Hs01547656_m1	IGF1	insulin like growth factor 1	n.d.	n.d.	n.d.
Hs00609566_m1	IGF1R	insulin like growth factor 1 receptor	1.0	1.73	0.29
Hs04188276_m1	IGF2	insulin like growth factor 2	1.0	n.d.	n.d.
Hs00911700_m1	KDR	kinase insert domain receptor	n.d.	n.d.	n.d.

Hs00174029_m1	KIT	KIT proto-oncogene receptor tyrosine kinase	n.d.	n.d.	n.d.
Hs00998018_m1	PDGFRA	platelet derived growth factor receptor alpha	n.d.	n.d.	n.d.
Hs01019589_m1	PDGFRB	platelet derived growth factor receptor beta	n.d.	n.d.	n.d.
Drug Metabolism					
Hs01561483_m1	ABCC1	ATP binding cassette subfamily C member 1	1.0	1.55	0.88
Hs00943350_g1	GSTP1	glutathione S-transferase pi 1	1.0	0.37	0.77
Hs00153133_m1	PTGS2	prostaglandin-endoperoxide synthase 2	n.d.	n.d.	n.d.
Hs01555214_g1	TXN	thioredoxin	1.0	0.05	0.16
Hs00917067_m1	TXNRD1	thioredoxin reductase 1	1.0	0.53	0.49
G-Protein Signaling					
Hs00357608_m1	RHOA	ras homolog family member A	1.0	2.37	1.76
Hs03676562_s1	RHOB	ras homolog family member B	n.d.	n.d.	n.d.
Hormone Receptors					
Hs01046816_m1	ESR1	estrogen receptor 1	n.d.	n.d.	n.d.
Hs01100353_m1	ESR2	estrogen receptor 2	n.d.	n.d.	n.d.
Hs01556702_m1	PGR	progesterone receptor	n.d.	n.d.	n.d.
Heat Shock Proteins					
Hs00743767_sH	HSP90AA1	heat shock protein 90 alpha family class A member 1	1.0	1.95	0.75
Hs00427665_g1	HSP90B1	heat shock protein 90 beta family member 1	1.0	5.07	2.12
Receptor Tyrosine Kinase Signaling					
Hs00178289_m1	AKT1	AKT serine/threonine kinase 1	1.0	0.65	0.23
Hs01086099_m1	AKT2	AKT serine/threonine kinase 2	1.0	2.32	0.73

Hs00157817_m1	GRB2	growth factor receptor bound protein	1.0	0.45	0.26
2					
Cathepsins					
Hs00947439_m1	CTSB	cathepsin B	1.0	1.33	3.72
Hs00157205_m1	CTSD	cathepsin D	n.d.	n.d.	n.d.
Hs00964650_m1	CTSL	cathepsin L	1.0	0.43	1.71
Hs00175407_m1	CTSS	cathepsin S	1.0	0.25	0.43
Cell Cycle					
Hs00938777_m1	CDK1	cyclin dependent kinase 1	1.0	0.63	1.14
Hs00947994_m1	CDC25A	cell division cycle 25A	n.d.	n.d.	n.d.
Hs01548894_m1	CDK2	cyclin dependent kinase 2	1.0	0.86	0.77
Hs00364847_m1	CDK4	cyclin dependent kinase 4	1.0	0.11	1.01
Hs00358991_g1	CDK5	cyclin dependent kinase 5	1.0	0.36	1.02
Hs00361486_m1	CDK7	cyclin dependent kinase 7	1.0	0.80	1.07
Hs00992501_g1	CDK8	cyclin dependent kinase 8	1.0	0.18	0.28
Hs00977896_g1	CDK9	cyclin dependent kinase 9	1.0	5.38	2.69
Hs00540450_s1	MDM2	MDM2 proto-oncogene	1.0	0.24	1.05
Hs00967238_m1	MDM4	MDM4, p53 regulator	1.0	19.5	0.87
6					
Hs00972650_m1	TERT	telomerase reverse transcriptase	1.0	1.61	0.79
Topoisomerases, Type II					
Hs01032137_m1	TOP2A	topoisomerase (DNA) II alpha	1.0	0.35	0.80
Hs00172259_m1	TOP2B	topoisomerase (DNA) II beta	1.0	0.38	0.47
Transcription Factors					
Hs01095345_m1	ATF2	activating transcription factor 2	1.0	0.81	0.13
Hs00153153_m1	HIF1A	hypoxia inducible factor 1 alpha	1.0	1.16	0.04
subunit					
Hs00158114_m1	IRF5	interferon regulatory factor 5	n.d.	n.d.	n.d.
Hs00765730_m1	NFKB1	nuclear factor kappa B subunit 1	1.0	0.81	1.13

Hs01034249_m1	TP53	tumor protein p53	n.d.	n.d.	n.d.
Protein Kinases					
Hs01582072_m1	AURKA	aurora kinase A	1.0	0.63	1.07
Hs00945858_g1	AURKB	aurora kinase B	1.0	1.40	1.37
Hs00152930_m1	AURKC	aurora kinase C	1.0	n.d.	3.22
Hs00983227_m1	PLK1	polo like kinase 1	1.0	0.94	0.71
Hs00198320_m1	PLK2	polo like kinase 2	n.d.	n.d.	n.d.
Hs00177725_m1	PLK3	polo like kinase 3	n.d.	n.d.	n.d.
Hs00179514_m1	PLK4	polo like kinase 4	1.0	2.35	0.49
Hs00925200_m1	PRKCA	protein kinase C alpha	1.0	2.64	0.40
Hs00176998_m1	PRKCB	protein kinase C beta	1.0	1.70	0.50
Hs01090047_m1	PRKCD	protein kinase C delta	1.0	0.50	0.47
Hs00942886_m1	PRKCE	protein kinase C epsilon	1.0	4.46	0.56
RAS Signaling					
Hs00978050_g1	HRAS	HRas proto-oncogene, GTPase	1.0	n.d.	2.16
Hs00364284_g1	KRAS	KRas proto-oncogene, GTPase	1.0	0.08	0.80
Hs00180035_m1	NRAS	NRas proto-oncogene, GTPase	1.0	n.d.	0.63
Histone Deacetylases					
Hs00978031_g1	HDAC1	histone deacetylase 1	1.0	2.44	9.65
Hs00978031_g1	HDAC11	histone deacetylase 11	n.d.	n.d.	n.d.
Hs00231032_m1	HDAC2	histone deacetylase 2	1.0	0.11	0.63
Hs00187320_m1	HDAC3	histone deacetylase 3	1.0	2.96	1.63
Hs01041648_m1	HDAC4	histone deacetylase 4	1.0	6.02	1.03
Hs00997427_m1	HDAC6	histone deacetylase 6	1.0	5.48	1.88
Hs01045864_m1	HDAC7	histone deacetylase 7	1.0	3.87	0.94
Hs00954353_g1	HDAC8	histone deacetylase 8	1.0	2.68	0.60
Poly ADP-Ribose					
Polymerases					
Hs00242302_m1	PARP1	poly(ADP-ribose) polymerase 1	1.0	n.d.	2.84

Hs00173105_m1	PARP4	poly (ADP-ribose) polymerase family member 4	1.0	2.72	1.63
Hs00186671_m1	TNKS	tankyrase	1.0	27.0	9.73
				6	
Structural Proteins					
Hs00362403_g1	NTN3	netrin 3	n.d.	n.d.	n.d.

4.2 Capítulo II

Neste capítulo, relatamos o efeito antileucêmico de PL através da exploração de modelos celulares de LMA *in vitro* e *in vivo*.

Artigo a ser submetido para publicação.

Piplartine eliminates CD34+ AML stem/progenitor cells by inducing oxidative stress and suppressing NF- κ B signalling.

Ana Carolina B. da C. Rodrigues^{1,4}, Suellen Laila R. Silva¹, Ingrid Rayssa S. B. Dias¹, Rafaela G. A. Costa¹, Maiara de S. Oliveira¹, Milena B. P. Soares^{1,2}, Rosane B. Dias¹, Ludmila F. Valverde¹, Clarissa A. G. Rocha^{1,3}, Emily M. Johnson⁴, Cristina Pina^{4,*,\dagger}, Daniel P. Bezerra^{1,*,\dagger}

Piplartine eliminates CD34+ AML stem/progenitor cells by inducing oxidative stress and suppressing NF- κ B signalling

Ana Carolina B. da C. Rodrigues^{1,4}, Suellen L. R. Silva¹, Ingrid R. S. B. Dias¹, Rafaela G. A. Costa¹, Maiara de S. Oliveira¹, Milena B. P. Soares^{1,2}, Rosane B. Dias¹, Ludmila F. Valverde¹, Clarissa A. G. Rocha^{1,3}, Emily M. Johnson⁴, Cristina C. A. Pina^{4,*, \dagger} , Daniel P. Bezerra^{1,*, \dagger}

¹Gonçalo Moniz Institute, Oswaldo Cruz Foundation (IGM-FIOCRUZ/BA), Salvador, Bahia, 40296-710, Brazil.

²SENAI Institute for Innovation in Advanced Health Systems, SENAI CIMATEC, Salvador, BA, 41650-010, Brazil

³Department of Clinical Propaedeutics and Integrated Clinical, Faculty of Dentistry, Federal University of Bahia (UFBA), Salvador, Bahia, 40301-155, Brazil.

⁴College of Health, Medicine and Life Sciences, Brunel University London, Uxbridge, UB8 3PH, United Kingdom.

\dagger These authors contributed equally to this work.

*Corresponding authors:

D. P. Bezerra, E-mail: danielpbezerra@gmail.com or daniel.bezerra@fiocruz.br Tel/Fax + 55 71 3176 2272.

C. Pina, E-mail: cristina.pina@brunel.ac.uk

Phone number: +44 1895 266676.

Abstract

Acute myeloid leukaemia (AML) is a haematological malignancy characterised by the accumulation of transformed myeloid progenitors in the bone marrow. Piplartine (PL), also known as piperlongumine, is a pro-oxidant small molecule extracted from peppers with demonstrated antineoplastic potential in solid tumours and other haematological malignancies. In this work, we explored the potential of PL against AML using a combination of cellular and molecular analyses of primary and cultured leukaemia cells *in vitro* and *in vivo*. We showed that PL displays *in vitro* cytotoxicity against AML cells, including CD34⁺ leukaemia-propagating cells, but not healthy haematopoietic progenitors, suggesting anti-leukaemia selectivity. Mechanistically, PL treatment increased reactive oxygen species (ROS) and induced ROS-mediated apoptosis in AML cells, which could be prevented by treatment with the antioxidant scavenger N-acetyl-cysteine and the pan-caspase inhibitor Z-VAD(OMe)-FMK. PL treatment reduced *NFKB1* gene transcripts and the expression of NF- κ B p65 (pS536), which was depleted from the nucleus of AML cells, indicating suppression of NF- κ B p65 signalling. Significantly, PL suppressed AML development in a mouse xenograft model, and its combinatorial use with current AML treatments (cytarabine, daunorubicin and azacytidine) showed synergistic activity, indicating translational therapeutic potential. Taken together, these data position PL as a novel anti-AML candidate drug that can target leukaemia stem/progenitors and is amenable to combinatorial therapeutic strategies.

Keywords: Piplartine; Oxidative stress; Stem cells; Acute myeloid leukaemia; Progenitor cells; NF- κ B signalling

Introduction

Acute myeloid leukaemia (AML) comprises a heterogeneous group of diseases with unique molecular and clinical characteristics. It is the most common type of acute leukaemia, and its incidence increases with age, with most patients over the age of 70 (Rodrigues et al., 2021; Döhner et al., 2022; Khoury et al., 2022; Costa et al., 2023). In the United States of America, the estimates for 2023 are approximately 20,380 new cases of AML and approximately 11,310 deaths with a 5-year relative survival rate of only 28% in patients aged 20 years and older. Under age 20, the 5-year relative survival rate is 69% (American Cancer Society, 2023).

The incidence of AML is increasing worldwide; however, the standard therapy has remained nearly unchanged for decades, and there have been few advances, particularly for older AML patients (Newell and Cook, 2021; Bazinet et al., 2021). Current standard cytotoxic regimens combining cytarabine (ARA-C) and an anthracycline (e.g., doxorubicin, DOX, or idarubicin, IDA) have high toxicity, including cardiac side effects, and are not tolerated by most elderly patients (Hwang et al., 2019; Thol and Ganser, 2020). Newer approved treatments such as azacitidine (AZA) and venetoclax have low remission and high relapse rates, particularly in elderly individuals, altogether contributing to poor prognosis (Winters et al., 2019).

AML is sustained by leukaemia-propagating cells with stem-like characteristics (AML-LSCs), which need to be eliminated to achieve clinical remission and are the source of relapse. In the

subset of AML subtypes characterised by expression of the CD34 stem/progenitor marker, AML-LSCs display a CD34⁺CD38⁻ phenotype and can express other markers, including CD123, CD45RA, CD96, CLL-1, TIM-3, CD93, and CD99 (Goardon et al., 2011; Shlush and Feldman, 2021; Rodrigues et al., 2021; Costa et al., 2023). Elimination of AML-LSC is central to achieving long-term remission and preventing relapse and should be specifically monitored in testing new drugs.

Piplartine (PL, **Figure 1A**), also known as piperlongumine, is a plant-based pro-oxidant small molecule with antineoplastic potential (Bezerra et al., 2007; Adams et al., 2012; Bezerra et al., 2013; Baliza et al., 2019; Bezerra et al., 2021; Dartora et al., 2022). It has shown promising results in suppressing cell growth and proliferation of malignant blood cells, including multiple myeloma (Yao et al., 2016), lymphoma (Han et al., 2013) and chronic myelogenous leukaemia (Lan et al., 2023). CD34⁺ AML cells with acquired aberrant glutathione metabolism are sensitive to PL (Pei et al., 2013).

In this work, we explored the anti-AML potential of PL *in vitro* and *in vivo*. We found that PL displays potent cytotoxicity in leukaemia cells, which does not extend to healthy haematopoietic progenitors. PL reduces CD34⁺ LSCs by inducing oxidative stress and suppressing NF- κ B signalling, and displays synergism with ARA-C, suggesting translational value.

Material and Methods

PL preparation

PL was obtained commercially (Cayman Chemical, Ann Arbor, MI, USA). It was dissolved in sterile DMSO (Synth, Diadema, SP, Brazil) as a 5 mg/mL stock solution and stored at -20°C.

PL was diluted in culture medium or PBS, as indicated for individual experiments.

Cell culture

The cell lines used in this work are specified in **Table S1**. Cells were cultured according to the manufacturer's instructions or the ATCC animal cell culture guidelines for each specific cell line or condition, as detailed in **Table S1**. All cell lines were grown in flasks at 37°C in 5% CO₂; assays were run for 3-4 days to sustain exponential growth. A 0.25% trypsin EDTA solution (Sigma–Aldrich Co., Saint Louis, MO, USA) was used to harvest adherent cells. All cell lines were screened for mycoplasma using a mycoplasma stain kit (Sigma Aldrich Co.) to validate their use as mycoplasma-free cells.

Cell viability/proliferation assay

Cell viability/proliferation quantification was performed using the Alamar blue assay (Sigma–Aldrich Co.), MTT assay (Cayman Chemical, Ann Arbor, MI, USA), or live cell counting

under a microscope using trypan blue (Fisher Scientific, UK). For the Alamar blue assay, the cells were plated in 96-well culture plates (3×10^5 cells/well for suspension cells and 7×10^4 cells/well for adherent cells) and kept at 37°C in a 5% CO_2 atmosphere. The drugs were added in specified concentrations to each well in duplicate and incubated for 72 h. DOX (purity $\geq 95\%$, Laboratory IMA S.A.I.C., Buenos Aires, Argentina) was a positive control. Four hours before the end of the incubation period (or 24 h for PBMCs), resazurin was added to each well at a final concentration of $3 \mu\text{M}$. Absorbance values at 570 nm and 600 nm wavelengths were measured using a SpectraMax 190 Microplate Reader (Molecular Devices, Sunnyvale, CA, USA).

The MTT assay was carried out using the MTT Cell Proliferation Assay Kit (Cayman Chemical) according to the manufacturer's instructions. For trypan blue-based cell counts, cells were plated in 24-well culture plates (3×10^5 cells/well for suspension cells and 7×10^4 cells/well for adherent cells) and kept at 37°C in 5% CO_2 . Drugs were added to each well in duplicate and incubated for 72 h. At the end of the incubation period, live and dead cells were counted using a haemocytometer under a light microscope.

Colony-forming assay

MV-4-11, MOLM-13 and OCI-AML-3 cell lines were plated at a density of 500 cells/plate in duplicate in MethoCult H4435 (STEMCELL Technologies), MethoCult H4230 (STEMCELL

Technologies) or StemMACS™ HSC-CFU Media (Miltenyi Biotec). Mouse bone marrow-derived Cas9 Flt3-ITD MLL-AF4 and MLL-AF9 cells (Tzelepis et al., 2016) were plated at a density of 500 cells/plate in duplicate in mouse Methylcellulose Complete Media HSC007 (R&D Systems). C57BL/6 mouse bone marrow cells were plated at a density of 50.000 cells/plate in the same methylcellulose-based medium HSC007. PL was added at different concentrations to the methylcellulose and dispersed by vortexing prior to addition of the cells. PL was used at IC₅₀ concentrations, as described. Colonies were counted/scored by microscopy 6–8 days after plating.

Xenotransplantation of leukaemia cells

A total of 12 NOD. *Cg-Prkdc^{scid} Il2rg^{tm1Wjl}/SzJ* (NSG) mice (male and female, 20-25 g) were supplied and housed under specific pathogen-free conditions by FIOCRUZ-BA animal facilities (Salvador, Bahia, Brazil) following an experimental protocol approved by a local animal ethics committee (#16/2018). All mice were fed a standard pellet diet (with free access to food and water) and kept in an artificially lit room (12 h dark/light cycle).

To achieve a high level of human cell engraftment, busulfan was used as a conditioning agent. The mice were treated with 25 mg/kg busulfan (Sigma–Aldrich Co.) 24 h before receiving KG-1a cells. The following day, mice were intravenously inoculated with 10⁶ cells/mouse by tail vein injection. Animals were monitored every other day for signs of weight loss or lethargy.

After two weeks, flow cytometry confirmed engraftment in peripheral blood using both PE anti-human CD45 (hCD45) and FITC anti-mouse CD45 (mCD45) antibodies. **Table S2** provides a detailed description of all the antibodies used.

After engraftment confirmation, mice were randomly divided into two groups (n=6/per group): negative control (vehicle – DMSO 5%) and the treated group with PL at 20 mg/kg. The treatment was injected into mice intraperitoneally every day for two weeks. Mice were euthanised after two weeks, and cells from the spleen, peripheral blood, and bone marrow were collected. In addition, organs such as the heart, lungs, kidneys, and liver were also collected. The collected cells from the spleen, peripheral blood, and bone marrow were analysed by flow cytometry using hCD45 and mCD45 antibodies.

The heart, lungs, kidneys and liver were also collected for toxicological analyses. These organs were examined for colour change, gross lesion formation, and/or haemorrhaging before being fixed in 4% formaldehyde, dehydrated in a graded alcohol series, cleaned in xylene, and embedded in paraffin wax. The tissue was cut into 5 µm thick slices, stained with haematoxylin-eosin and/or periodic acid-Schiff (liver and kidney), and examined histologically under optical microscopy.

Flow cytometry assays

Cell cycle progression was quantified based on the measurement of DNA content by staining with propidium iodide (PI) (Sigma–Aldrich Co.). Briefly, the cells were diluted with a permeabilisation solution containing 0.1% Triton X-100, 2 g/mL PI, 0.1% sodium citrate, and 100 g/mL RNase (all from Sigma–Aldrich Co.) and incubated for 15 minutes in the dark.

Apoptosis was detected and quantified using annexin V-FITC/PI (FITC Annexin V Apoptosis Detection Kit I, BD Biosciences), annexin V-APC/Hoechst 33258 (Biolegend/Thermo Fisher) or YO-PRO-1/PI (Sigma–Aldrich Co.). Briefly, cells were stained with 200 μ L of Annexin-V buffer (0.01 mol/L HEPES/NaOH, 0.14 mol/L NaCl, 2.5 mmol/L CaCl₂), as per the manufacturers' instructions; cells were washed and resuspended in staining buffer containing 1 μ M Hoechst 33258 or 1.5 μ M PI (incubated at room temperature for 15 minutes). Alternatively, cells were stained with a solution containing 0.1 μ M YO-PRO-1 and 1.5 μ M PI. To examine the involvement of caspases in PL-induced apoptosis, the pancaspase inhibitor Z-VAD(OMe)-FMK (50 μ M) was added to cells one hour prior to PL treatment.

The rhodamine 123 incorporation method was used to determine the mitochondrial transmembrane potential. After 24 h of treatment, the cells were diluted in a solution of rhodamine 1 μ g/mL (Sigma–Aldrich Co.) and incubated at 37°C in the dark for 15 minutes. After this period, the cells were centrifuged and resuspended in PBS.

To detect mitochondrial ROS levels, we used MitoSOX™ Red reagent (Thermo Fisher Scientific, Waltham, MA, USA), and the analysis was performed according to the manufacturer's instructions. Cells were treated with PL and incubated for 1 or 24 hours. Subsequently, the cells were washed and resuspended in a solution containing 5 µM MitoSOX™ Red. Upon entering the mitochondria, the reagent undergoes oxidation by superoxide and emits red fluorescence.

The apoptotic response to oxidative stress was determined upon treatment with the antioxidant N-acetyl-cysteine (NAC). Thus, cells were preincubated for 2 h with 5 mM NAC, incubated with 20 µM PL for 48 h, and then exposed to PL to evaluate the antioxidant's protective effect against oxidative stress-induced apoptosis by PL.

Phenotyping was carried out using antibodies against CD34, CD38, CD123, CD13 and CD33. Cells were washed with incubation buffer (0.5% bovine serum albumin in PBS), stained with PE mouse anti-human CD34, BV421 mouse anti-human CD38, BV605 mouse anti-human CD123, PE-CF594 mouse anti-human CD13 and BV510 mouse anti-human CD33 antibodies and incubated for one hour at room temperature. PE mouse IgG1 κ isotype control was employed as the appropriate isotype control in the experiment, and the analysis excluded apoptotic and dead cells through staining with annexin-V or YO-PRO-1. The gating strategy is detailed in **Figure S1**.

For cleaved PARP-(Asp 214), active caspase-3, and NF- κ B p65 (pS529 and pS536) detection, cells were collected and resuspended in 0.5-1 mL of 4% formaldehyde for 10 minutes at 37 °C. The tubes were then placed on ice for 1 minute. The cells were permeabilised for 30 minutes on ice by slowly adding ice-cold 100% methanol to prechilled cells while gently vortexing to a final concentration of 90% methanol. After washing with incubation buffer (0.5% bovine serum albumin in PBS), FITC rabbit anti-active caspase-3, PE mouse anti-cleaved PARP (Asp214), Alexa Fluor® 488 mouse anti-NF- κ B p65 (pS529) or FITC recombinant rabbit anti-NF- κ B p65 (pS536) antibodies were added and incubated at room temperature for one hour. Finally, the cells were washed with PBS, and the fluorescence of the cells was measured using flow cytometry. DMSO 0.2% was used as the negative control in all experiments. **Table S2** provides a detailed description of all the antibodies used in the flow cytometry experiments.

A minimum of 30,000 events/sample for cell surface staining and 10,000 events/sample for intracellular staining were analysed using a BD LSRFortessa cytometer along with BD FACSDiva Software (BD Biosciences, San Jose, CA, EUA) and Flowjo Software 10 (Flowjo LCC, Ashland, OR, USA). The experiments were performed in duplicate in three independent experiments. Cell doublets and debris were excluded through gating.

Gene expression analysis by qPCR array

KG-1a cells were incubated with 20 μ M PL for 12 h, and total RNA was isolated using the RNeasy Plus Mini Kit (Qiagen; Hilden, Germany) according to the manufacturer's instructions. The RNA was analysed for purity and quantified by a NanoDrop® 1000 spectrophotometer (Thermo Fisher Scientific, Waltham, Massachusetts, USA). RNA reverse transcription was carried out using a Superscript VILO™ Kit (Invitrogen Corporation; Waltham, MA, USA).

Gene expression qPCR analysis was performed on a TaqMan® array plate 96 plus fast (#4413256, Applied Biosystems™, Foster City, CA, USA) in an ABI ViiA7 system (Applied Biosystems™). The PCR cycle conditions were 2 min at 50 °C, 10 min at 95 °C, then 40 cycles of 15 s at 95 °C and 1 min at 60 °C. Relative quantification (RQ) of mRNA expression was calculated using the $2^{-\Delta\Delta CT}$ method (Livak and Schmittgen, 2001) on Gene Expression Suite™ Software (Applied Biosystems™). Cells treated with 0.2% DMSO (negative control) were used as a calibrator; data normalisation used the geometric mean RQ of three reference genes, GUSB, HPRT1 and GAPDH. All experiments were performed in DNase/RNase-free conditions. Genes were called upregulated if the $RQ \geq 2$; similarly, the genes were downregulated if $RQ \leq 0.5$.

Detection of NF- κ B translocation by confocal microscopy

For NF- κ B p65 localisation, cells were plated in 24-well plates and exposed to PL for 24 h. After the incubation period, the cells were washed twice with PBS, placed as a small drop (5 μ L) on a coverslip, permeabilised with Triton X-100 (0.5%), treated with RNase (10 μ g/mL), and incubated overnight with PE mouse anti-NF- κ B p65 antibody. The cells were rinsed with PBS the next day and mounted with Fluoromount-G with DAPI (Invitrogen, Thermo Fisher Scientific). DMSO 0.2% was used as the negative control. A Leica TCS SP8 confocal microscope (Leica Microsystems, Wetzlar, HE, Germany) was used to examine the cells. **Table S2** provides a detailed description of all the antibodies used.

Combination drug analysis

For combinatorial drug treatments, the cells were treated with PL, AZA, daunorubicin (DNR), ARA-C or control vehicle as single agents and in combination in a 96-well plate for 72 h. The doses were established as per the calculated IC₅₀ values for each drug. Cell viability was determined by MTT assay, as described above. We used CompuSyn software (version 1.0; ComboSyn, Paramus, NJ, USA) to evaluate potential synergistic or additive effects through the use of isobolograms and combination-index plots and determination of the drug combination index values (CI). CI values <0.9 indicate a synergistic effect; CI= 0.9-1.1 indicates an additive effect; CI > 1.1 reveals an antagonistic effect (Chou, 2010).

Statistical analysis

The data are shown as the mean of at least three repetitions (done in duplicate) \pm S.E.M. or as IC_{50} values with a 95% confidence interval. Two-tailed unpaired Student's t-test ($P < 0.05$) was used by GraphPad Prism for statistical analyses (Intuitive Software for Science; San Diego, CA, USA).

Results

PL displays potent cytotoxicity to leukaemia cells, sparing healthy haematopoietic progenitor activity

Our initial focus was to explore the cytotoxic effects of PL on different types of cancer and noncancerous cells. We started by treating a panel of 28 cell lines representing 11 tumour types, including solid and haematological malignancies. Cells were treated at serial concentrations for 72 h, after which cell viability was determined by cell counting with trypan blue or through colorimetric viability assays with MTT and Alamar blue (**Figure 1B, Figure S2**).

The IC_{50} values for haematological cancers ranged from 0.96 μ M for the Cas9 Flt3-ITD MLL-AF4 AML cell line to 41.83 μ M for the Jurkat T-acute lymphoblastic leukaemia cell line; for

solid cancers, they ranged from 2.57 μM for the Caco-2 colon cancer cell line to 42.04 μM for the SCC-9 oral squamous cell cancer cell line (**Table S3**). PL treatment at different concentrations showed a remarkable decrease in the cell viability of both haematological and solid tumour cells. Interestingly, AML cells carrying KMT2A rearrangements *in vitro* transformed mouse bone marrow (BM), Cas9 *Flt3-ITD* MLL-AF4 (IC_{50} : 0.96) and Cas9 *Flt3-ITD* MLL-AF9 (IC_{50} : 2.55), and human MV-4-11 (IC_{50} : 2.05) and MOLM-13 (IC_{50} : 2.58), with a mutational spectrum respectively equivalent to the transformed mouse BM lines, were especially sensitive to PL.

PL was also evaluated for its cytotoxicity in noncancerous cell lines, including MRC-5 (derived from normal human lung tissue), and BJ (a human fibroblast cell line), as well as peripheral blood mononuclear cells (PBMCs). The IC_{50} values obtained were 34.19, 21.91, and 20.34 μM for MRC-5 cells, PBMCs, and BJ cells, respectively. These noncancerous cells were included in the study to assess the selectivity and potential toxicity of PL towards normal cells, providing valuable insights into its therapeutic window and safety profile. **Figure 1C** shows the heatmap of the obtained selectivity index. DOX was used as a positive control and showed IC_{50} values ranging from 0.01 μM for the Jurkat cell line to 2.1 μM for the SCC-4 cell line and IC_{50} values of 1.65, 1.21, and 3.60 μM for the noncancerous cells MRC-5, PBMC, and BJ, respectively.

The cell viability was also determined after 12, 24, 48 and 72 h of incubation with PL using the trypan blue exclusion assay in KG-1a cells (**Figure S3**). PL reduced the viability of KG-1a

cells in a time- and concentration-dependent manner. After 12 h and 24 h of treatment, the reduction was 48 and 53.8% (5 μ M), 50.3 and 64.5% (10 μ M) and 67.2 and 53.1% (20 μ M), respectively. A reduction of 70.7 and 94.8%, 72.5 and 94.7%, and 74 and 95.3% was observed after 48 and 72 h of treatment at the same concentrations, respectively.

Since AML models with KMT2A rearrangements were particularly sensitive to PL treatment, we performed colony-forming cell (CFC) assays to determine whether PL would affect the ability of AML cell lines carrying KMT2A rearrangements (MV-4-11, MOLM-13, Cas9 Flt3-ITD MLL-AF4 and MLL-AF9) to initiate colonies, an *in vitro* surrogate for leukemia stem/progenitor activity. In addition, we tested the effects of PL on colony formation in OCI-AML-3, an AML cell line with *DNMT3A* and *NPM1* mutations, which, like the KMT2A rearrangements, also activates a *HOX* oncogenic program. As shown in **Figure 2A-2F**, PL treatment reduced the ability of human AML MV-4-11, MOLM-13 and OCI-AML-3 cells to form colonies. We also observed a significant reduction in CFC number in transformed mouse BM Cas9 Flt3-ITD MLL-AF4 and MLL-AF9 cells, at both 5 and 10 μ M treatments (**Figure 2G-2I**). These data indicate that PL cytotoxicity extends to colony-forming cells, indicating its potential impact on leukaemia-propagating progenitors, particularly *in vitro*.

In contrast, the colony-forming potential of normal primary bone marrow cells from C57BL/6 mice was not affected by PL treatment at 5 and 10 μ M. Mouse CFCs are classified as GEM (granulocyte, erythroid and monocyte), GM (granulocyte-monocyte), G (granulocyte), M

(monocyte) and E (erythroid) colonies to reflect their progenitor of origin. and each type was quantified to assess potential toxic effects of PL on the differentiation or proliferation of different healthy progenitors. As shown in **Figure 2J-2 L**, PL treatment did not cause a significant effect on any type colony type, when compared to the control.

PL targets candidate LSCs and suppresses AML development in a mouse xenograft model

Having demonstrated a specific effect of PL on colony-forming leukaemia progenitors *in vitro*, we tested whether this effect extended to an *in vivo* xenotransplantation setting. For this purpose, we focused on the KG-1a AML cell line, which displays a CD34⁺ phenotype resembling the more clearly defined human AML-LSCs (She et al., 2012). For this purpose, KG-1a cells were grafted in mice to generate a leukemia model. As shown in **Figure 3**, PL treatment significantly inhibited leukemic growth *in vivo*. The number of engrafted human CD45⁺ cells in BM and PB was significantly decreased in the mice treated with PL compared to the negative control group. The mouse CD45-positive cells also showed a reduction in the PB; however, there was no statistically significant difference in the spleen or BM, suggesting selectivity against the leukaemia graft.

In support of low toxicity to normal tissues, no significant change in total body weight or in individual organ weight was observed (**Table S4**). Histopathological analysis of kidneys, heart,

lungs and liver of PL-treated and control animals showed similar alterations in both groups, most of which were mild and/or reversible. Significantly, we did not observe pathological changes in the heart, a critical toxicity target of conventional anti-AML therapies (**Figure S4**).

Compatible with an effect on candidate LSCs, phenotypic analysis of KG-1a AML cells treated with PL for 48h *in vitro* revealed loss of AML stem/progenitor markers CD34 and CD123, as well as myeloid marker CD13, at all doses used (5, 10 and 20 μ M) (**Figures 4 and S5**). Early myeloid marker CD33 was significantly reduced at a concentration of 20 μ M. On the other hand, no changes were observed in CD38, which marks proliferative progenitors, but not LSCs (**Figures S5 and 4**).

PL induces caspase-mediated apoptotic cell death in KG-1a AML cells

To elucidate the mechanism underlying the cytotoxicity associated with PL treatment, we investigated the induction of apoptosis and tested for the presence of caspase activation. First, flow cytometry measured DNA content to quantify internucleosomal DNA fragmentation and cell cycle progression in KG-1a cells after treatment with PL (**Figure 5**). PL treatment was capable of inducing DNA fragmentation ($p < 0.05$). After 48 h of treatment with PL, the highest concentration (20 μ M) significantly increased the percentage (45.15%) of sub-G₀/G₁ compared to the control. At 5, 10 and 20 μ M, DNA fragmentation was significantly increased by 72.73, 71.59 and 80.08%, respectively, after 72 h of treatment. DNA fragmentation is a central feature

of apoptosis and can be used as a marker to identify apoptotic cell death. Doxorubicin also induced DNA fragmentation after 48 and 72 h.

The presence of apoptotic cells was measured in PL-treated KG-1a cells using YO-PRO-1/PI double staining by flow cytometry after 12, 24, 48 and 72 h (**Figure 6**), for quantification of viable (YO-PRO-1/PI-double-negative cells), apoptotic (YO-PRO-1-positive cells PI-negative cells), and dead (YO-PRO-1/PI-double-positive cells). PL treatment at 10 and 20 μM caused a significant increase in the percentage of apoptotic cells after 12 and 24 h. After 48 and 72 h of treatment with PL, the number of dead cells increased at 5, 10 and 20 μM . The positive control, DOX (1 μM), also significantly increased the percentage of apoptotic cells after 12 h of treatment. We also measured apoptosis in PL-treated MOLM-13 cells using annexin V-APC/Hoechst33342 double staining by flow cytometry after 12 h incubation. We observed significant increase in Annexin V-positive cells with 5.2 and 10.4 μM treatments (**Figure S6**).

PL-mediated apoptosis induction, was also tested by activation of the caspase cascade, specifically through quantification of active caspase-3 (**Figures 7A and 7B**) and cleaved PARP (Asp214) (**Figures 7C and 7D**) by flow cytometry. PL treatment at 20 μM induced a significant increase in the levels of active caspase-3 and cleaved PARP (Asp214) after 24 h. Conversely, PL-induced apoptosis was prevented by treatment with the pancaspase inhibitor Z-VAD(OMe)-FMK (**Figures 7E and 7F**).

Given the central role of mitochondria in apoptotic cell death, we also investigated the effects of PL treatment on the mitochondrial membrane potential of KG-1a cells, and observed an increase in the percentage of mitochondrial depolarisation in PL-treated cells (**Figure 7G**).

Finally, we tested the involvement of the mitochondrial anti-apoptotic protein BAD, by treating *BAD* KO SV40 mouse embryonic fibroblast (MEF) cell line versus its parental WT SV40 MEF with PL (**Figure 7H-7K**). PL was able to induce apoptosis in both cell lines, suggesting BAD-independence, at least in this cellular model.

PL induces ROS-mediated apoptotic cell death in KG-1a AML cells

Since PL is a known ROS inducer, we decided to investigate the role of oxidative stress in PL-induced cell death in KG-1a cells. We first observed that PL-induced apoptosis was prevented by the antioxidant NAC (**Figures 8A and 8B**). We then measured mitochondrial ROS using the MitoSOX assay, alone or under NAC pre-treatment. PL increased MitoSOX fluorescence after 1 and 24 h of treatment (**Figures 8C and 8D**). However, MitoSOX levels decreased when KG-1a cells were pretreated with NAC (**Figures 8C and 8D**). Altogether suggesting that PL induces apoptosis through increased oxidative stress.

PL induces ROS-mediated apoptotic cell death in KG-1a AML cells

Since PL is a known ROS inducer, we decided to investigate the role of oxidative stress in PL-induced cell death in KG-1a cells. We observed that PL-induced apoptosis was prevented by the antioxidant N-acetyl-cysteine (NAC) after 48 h (Figures **8A and 8B**). We also performed MitoSOX assays alone or under NAC pre-treatment. PL increased MitoSOX fluorescence after 1 and 24 h of treatment (Figures **8C and 8D**). Conversely, the measurements of MitoSOX were decreased when KG-1a cells were pre-treated with NAC. These data indicate that PL induces apoptosis mediated by oxidative stress.

PL inhibits NF- κ B signalling in KG-1a AML cells

In an attempt to elucidate the molecular mechanism underlying PL-induced apoptosis in KG-1a cells, we measured changes in the relative expression of 92 genes related to important signalling pathways in AML stem/progenitor cells. These included: NF- κ B, WNT/ β -catenin, Hedgehog, NOTCH, EGFR, JAK/STAT, PI3K/Akt/mTOR, TGF- β /SMAD, and PPAR, as well as genes related to oxidative stress, apoptosis, autophagy, necroptosis and epithelial-mesenchymal transition. Gene expression analysis was performed after 12 h of incubation with PL, using the qPCR TaqMan® array plate 96 plus fast.

A total of 41 upregulated genes and 11 downregulated genes were identified after treatment with PL (**Figure 9A and Table S5**). Among them, PL downregulated genes from the NF- κ B pathway (*NFKB1*), Hedgehog pathway (*PTCH1*), NOTCH pathway (*NOTCH1*), JAK/STAT

pathway (*STAT5B* and *STAT6*), and PPAR pathway (*PPARGC1B*), as well as anti-apoptotic genes (*BCL-2* and *PARP1*), necroptosis gene (*RIPK3*) and genes implicated in epithelial-mesenchymal transition (*SNAIL3* and *TWIST1*).

We pursued the putative role of NF- κ B in mediating PL effects in KG-1a cells, and quantified NF- κ B p65 (pS536) and NF- κ B p65 (pS529) protein phosphorylation levels by flow cytometry, as well as the localisation of NF- κ B p65 by confocal microscopy. Both NF- κ B phosphorylation and localisation are central to its activity (Maguire et al., 2015). After 24 h of treatment with PL, although the expression of NF- κ B p65 (pS529) did not change (**Figures 9B and 9C**), the levels of NF- κ B p65 (pS536) were significantly reduced in comparison to the negative control (**Figures 9D and 9E**). In addition, a reduction in nuclear NF- κ B p65 protein was observed in PL-treated KG-1a cells (**Figure 9F**), compatible with reduced activity.

Altogether, our mechanistic analyses suggest that PL impacts NF- κ B activity and ROS production, resulting in apoptosis mediated by oxidative stress.

PL combined with ARA-C or DNR synergistically inhibits AML growth

Having evaluated the anti-AML activity of PL and dissected its mechanisms of action, we tested its translational potential by evaluating the value of its combination with drugs currently used in AML therapy. We specifically tested combinations with ARA-C, DNR and AZA and

focused on cell lines highly responsive to PL, which represent common and/or severe forms of disease. These were KMT2A-rearranged MOLM-13, Cas9 FLT3-ITD MLL-AF4 and Cas9 FLT3-ITD MLL-AF9 cells, and *NPM1* and *DNMT3A* mutant OCI-AML3. Based on the calculated IC_{50} of monotherapy treatments, we used concentrations of PL predicted to inhibit 25, 50 and 75% of cell growth and combined them with IC_{10} and IC_{25} doses of ARA-C and DNR and IC_{25} and IC_{50} doses of AZA. We deliberately assayed lower concentrations of ARA-C and DNR to assess the value of combinatorial use with PL in enabling the use of conventional chemotherapeutic agents, which are not normally tolerated by elderly AML patients. We used the algorithm CompuSyn, which calculates the combination index (CI) and plots it against the inhibitory effect (Chou, 2010). CI is a quantitative measure used to assess the interaction between two or more drugs or treatments. It is calculated based on the concentration–response relationship of individual drugs and their combination. A CI value less than 0.9 indicates a synergistic effect. A CI value in the range of 0.9-1.1 suggests an additive effect. A CI value greater than 1.1 indicates an inhibitory effect.

Figures 10A-10C show the CI plot of the combinations in MOLM-13 cells. The mean CI values for PL/ARA-C and PL/DNR were 0.65 ± 0.02 and 0.88 ± 0.09 , respectively, indicating a synergistic effect of combination therapy on these cells, which was clearer for PL/ARA-C combinations. On the other hand, the mean CI value of the PL/AZA combination was 1.17 ± 0.12 , indicating broadly additive effects.

In the case of OCI-AML3 (**Fig. 10D-10F**), the mean CI values for PL/ARA-C and PL/DNR were 0.87 ± 0.12 and 0.95 ± 0.12 , respectively, which are suggestive of additive effects. The PL/AZA combination displayed an average CI of 1.15 ± 0.18 , which was also additive.

In the mouse primary bone marrow cell lines, Cas9 FLT-ITD MLL-AF4 and MLL-AF9 (**10G - 10J**), only the highest concentrations of ARA-C (50.2 and 32.44 nM, respectively) combined with PL demonstrated a synergistic effect in both cell lines (0.78 ± 0.12 and 0.79 ± 0.25 , respectively). All combinations of DNR and PL in these cell lines were additive. Both cell lines were highly sensitive to AZA treatment, and it was not possible to perform the combinatorial analysis.

Overall, we detected consistent synergisms between PL and ARA-C which were specific to the KMT2A-rearranged cell lines, and may be explored in patients on low ARA-C regimens. No synergisms with DNR or AZA were observed.

4. Discussion

The landscape of AML treatment has shown limited advancement over the years. AML predominantly affects middle-aged and older patients. Despite improvements in therapy, the mortality of AML remains high and is still associated with poor survival particularly in the elderly group (Stubbins et al., 2022). New therapies are urgently needed, focusing on more effective lower-intensity therapy for patients who are unable to tolerate intensive standard chemotherapy regimens (Stanchina et al., 2020).

Herein, we explored the anti-AML potential of PL and found that this molecule displays potent cytotoxicity against leukaemia cells, sparing healthy haematopoietic progenitors, an effect that agrees with prior observations of cytotoxicity against malignant blood cells (Han et al., 2013; Pei et al., 2013; Yao et al., 2016, Lan et al., 2023). At a mechanistic level, PL induced oxidative stress-mediated apoptosis and suppressed NF- κ B signalling. Critically, PL could reduce the CD34⁺ AML stem/progenitor cell subpopulation in KG-1a cells, and hinder leukaemia development in a mouse xenograft model, highlighting its potential to target LSCs.

NF- κ B is constitutively active in 40% of AML cases, and its aberrant activity enables leukemic blasts and AML-LSCs to escape apoptosis and increase cell proliferation (Guzman et al., 2001; di Francesco et al., 2022; Rodrigues et al., 2021). Specifically, it has been reported that NF- κ B is critical in sustaining KMT2A rearrangements in the AML stem/progenitor cell

subpopulation (Kuo et al., 2013), which is compatible with the high sensitivity of *KMT2A*-rearranged cells to the effects of PL. It has also been shown that PL treatment affects breast cancer cell proliferation by suppressing IKK β expression (Jeong et al., 2019). IKK β suppression associates with accumulation of ROS, leading to oxidative damage, thus linking the two mechanisms of action documented for PL. Pei et al. (2013) also demonstrated that PL could cause glutathione depletion in stem cells of primary human AML specimens, leading to leukaemia cell death, but causing less toxicity to normal haematopoietic stem cells. These findings further underline the association between PL and oxidative stress, and the susceptibility of AML to ROS toxicity, defining an avenue of intervention for PL in the disease. Our observation of significant and selective targeting of AML cells in a xenograft model, with limited toxicity to the mouse tissues reinforce these findings. Importantly, they suggest the clinical potential of PL as anti-AML candidate that can eliminate the AML stem/progenitor cell subpopulation, increasing the likelihood of prolonged remission or cure.

We found that the combined treatment of PL with ARA-C has a synergistic effect on AML cells, at least those carrying *KMT2A* rearrangements. Other groups had previously demonstrated that PL can interact synergistically with different anticancer drugs. For example, PL synergises with cisplatin and paclitaxel to inhibit the growth of human ovarian cancer cells (Gong et al., 2014). Similarly, PL and paclitaxel generate a synergistic cytotoxic effect in human intestinal cancer cells (Rawat et al., 2020), and PL can also synergistically enhance oxaliplatin's anticancer effects on human colorectal cancer (Chen et al., 2019). All these

chemotherapy drugs, including ARA-C (Iacobini et al., 2001, Kanno et al., 2007; Kobyakova et al., 2022) cause oxidative stress. Critically, they also activate NF- κ B signalling pathway as a mechanism of chemoresistance (Oiso et al., 2012; Samuel et al., 2014; Yu et al., 2018; Kumbul et al., 2022; Esparza-López et al., 2022; Liu et al., 2022). In the case of ARA-C, this is a likely mechanism behind the failure to eliminate AML-LSCs (Guzman et al., 2001). Conversely, the synergism we observed between ARA-C and PL is likely to result at least in part from the capacity of PL to inhibit NF- κ B signalling, and suggests the putative clinical utility of PL, establishing an avenue for its translational exploitation.

In conclusion, we suggest that PL can be developed as anti-AML drug capable of targeting leukaemia-propagating cells and enhancing the activity of conventional chemotherapy, by targeting resistance mechanisms and allowing the use of lower doses for improved tolerability. Going forward, it will be important to systematically define the AML subtypes that can benefit from PL use by testing against patient cells and PDX models, to compare with current associations of AZA and venetoclax, and to explore possible mechanisms of PL resistance, for optimal and personalized association regimens.

bility to eliminate the AML stem/progenitor cell subpopulation.

Supplementary Materials

Figures S1-S6 and **Tables S1-S5** are available in the supplementary material.

Acknowledgements

The authors would like to thank the FIOCRUZ-Bahia flow cytometry, histotechnology, and electron microscopy cores for collecting flow cytometric data, performing histological techniques, and acquiring confocal microscopy data, respectively. The authors also acknowledge the Biosciences Core Facility at Brunel University London.

Financial support

This work received financial support and fellowships from Brazilian agencies Coordenação de Aperfeiçoamento de Pessoal de Nível Superior (CAPES), Conselho Nacional de Desenvolvimento Científico e Tecnológico (CNPq) and Fundação de Amparo à Pesquisa do Estado da Bahia (FAPESB, Brazil). Work in the Pina lab was funded by a British Society for Haematology Early-stage Research Grant (33932) and a BRIEF award by Brunel University London (2020-2022).

Author contributions

Conceived and designed the experiments: ACBCR, CAGR, MBPS, CP, and DPB. Performed the cellular effect of PL: ACBCR, SLRS, IRSBD, RGAC, MSO, EMJ, and RBD. Performed

the molecular effect of PL: ACBCR, RBD, LFV, and CAGR. Data analysis: ACBCR, RBD, LFV, CAGR, EMJ, CP, and DPB. Contributed reagents/materials/analysis tools: MBPS, CAGR, CP and DPB. Wrote the paper: ACBCR. All authors have read and agreed to the published version of the manuscript.

Conflict of interest

The authors declare that they have no conflicts of interest.

References

Adams DJ, Dai M, Pellegrino G, Wagner BK, Stern AM, Shamji AF, Schreiber SL. Synthesis, cellular evaluation, and mechanism of action of piperlongumine analogs. *Proc Natl Acad Sci U S A*. 2012 Sep 18;109(38):15115-20. doi: 10.1073/pnas.1212802109.

American Cancer Society. Cancer Statistics Center. Accessed on March 28, 2023.

Baliza, I. R. S, Silva, S. L. R., Santos, L. dS. , Neto, J. H. A., Dias, R. B., Sales, C. B. S., Rocha, C. A. G., Soares, M. B. P. Batista, A. A., & Bezerra, D. P. Ruthenium Complexes With Piplartine Cause Apoptosis Through MAPK Signaling by a p53-Dependent Pathway in Human Colon Carcinoma Cells and Inhibit Tumor Development in a Xenograft Model. *Front. Oncol.*, 9:582 (2019). [https://doi: 10.3389/fonc.2019.00582](https://doi.org/10.3389/fonc.2019.00582).

Bazinet, A., Assouline, S. (2021). A review of FDA-approved acute myeloid leukemia therapies beyond '7 + 3'. *Expert review of hematology*, 14(2), 185–197. <https://doi.org/10.1080/17474086.2021.1875814>.

Bezerra DP, Pessoa C, de Moraes MO, Saker-Neto N, Silveira ER, Costa-Lotufo LV. Overview of the therapeutic potential of piplartine (piperlongumine). *Eur J Pharm Sci*. 2013 Feb 14;48(3):453-63. doi: 10.1016/j.ejps.2012.12.003.

Bezerra, D. P. (2021). Chapter 37 - Piplartine (piperlongumine), oxidative stress, and use in cancer. In V. R. Preedy & V. B. Patel (Eds.), *Cancer (Second Edition)* (Second Edition, pp. 417–425). Academic Press. <https://doi.org/https://doi.org/10.1016/B978-0-12-819547-5.00037-7>

Bezerra, D. P., Militão, G. C. G., de Castro, F. O., Pessoa, C., de Moraes, M. O., Silveira, E. R., Lima, M. A. S., Elmiro, F. J. M., & Costa-Lotufo, L. V. (2007). Piplartine induces inhibition of leukemia cell proliferation triggering both apoptosis and necrosis pathways. *Toxicology in Vitro*, 21(1), 1–8. <https://doi.org/10.1016/j.tiv.2006.07.007>

Chen, W. Q., Lian, W. S., Yuan, Y. F., & Li, M. Q. (2019). The synergistic effects of oxaliplatin and piperlongumine on colorectal cancer are mediated by oxidative stress. *Cell Death and Disease*, 10(8). <https://doi.org/10.1038/s41419-019-1824-6>

Chou, T. C. (2010). Drug combination studies and their synergy quantification using the chou-talalay method. In *Cancer Research* (Vol. 70, Issue 2, pp. 440–446). <https://doi.org/10.1158/0008-5472.CAN-09-1947>

Costa RGA, Silva SLR, Dias IRSB, Oliveira MS, Rodrigues ACBDC, Dias RB, Bezerra DP. Emerging drugs targeting cellular redox homeostasis to eliminate acute myeloid leukemia stem cells. *Redox Biol.* 2023 Apr 2;62:102692. doi: 10.1016/j.redox.2023.102692.

Dartora VFC, Salata GC, Passos JS, Branco PC, Silveira E, Steiner AA, Costa-Lotufo LV, Lopes LB. Hyaluronic acid nanoemulsions improve piplartine cytotoxicity in 2D and 3D breast cancer models and reduce tumor development after intraductal administration. *Int J Biol Macromol.* 2022 Oct 31;219:84-95. doi: 10.1016/j.ijbiomac.2022.07.162.

di Francesco, B., Verzella, D., Capece, D., Vecchiotti, D., di Vito Nolfi, M., Flati, I., Cornice, J., di Padova, M., Angelucci, A., Alesse, E., & Zazzeroni, F. (2022). NF- κ B: A Druggable Target in Acute Myeloid Leukemia. In *Cancers* (Vol. 14, Issue 14). MDPI.

<https://doi.org/10.3390/cancers14143557>

Döhner H, Wei AH, Appelbaum FR, Craddock C, DiNardo CD, Dombret H, Ebert BL, Fenaux P, Godley LA, Hasserrjian RP, Larson RA, Levine RL, Miyazaki Y, Niederwieser D, Ossenkoppele G, Röllig C, Sierra J, Stein EM, Tallman MS, Tien HF, Wang J, Wierzbowska A, Löwenberg B. Diagnosis and management of AML in adults: 2022 recommendations from an international expert panel on behalf of the ELN. *Blood.* 2022, 140, 1345-1377. doi: 10.1182/blood.2022016867.

Esparza-López J, Longoria O, De La Cruz-Escobar EN, Garibay-Díaz JC, León-Rodríguez E, De Jesús Ibarra-Sánchez M. Paclitaxel resistance is mediated by NF- κ B on mesenchymal primary breast cancer cells. *Oncol Lett.* 2022 Feb;23(2):50. doi: 10.3892/ol.2021.13168.

Goardon N, Marchi E, Atzberger A, et al. Coexistence of LMPP-like and GMP-like leukemia stem cells in acute myeloid leukemia. *Cancer Cell*. 2011;19(1):138-152. doi:10.1016/j.ccr.2010.12.012

Gong, L. H., Chen, X. X., Wang, H., Jiang, Q. W., Pan, S. S., Qiu, J. G., Mei, X. L., Xue, Y. Q., Qin, W. M., Zheng, F. Y., Shi, Z., & Yan, X. J. (2014). Piperlongumine induces apoptosis and synergizes with cisplatin or paclitaxel in human ovarian cancer cells. *Oxidative Medicine and Cellular Longevity*, 2014. <https://doi.org/10.1155/2014/906804>

Guzman, M. L., Neering, S. J., Upchurch, D., Grimes, B., Howard, D. S., Rizzieri, D. A., Luger, S. M., & Jordan, C. T. (2001). Nuclear factor-B is constitutively activated in primitive human acute myelogenous leukemia cells. *Blood* (2001) 98 (8): 2301–2307. <https://doi.org/10.1182/blood.V98.8.2301>.

Han SS, Son DJ, Yun H, Kamberos NL, Janz S. Piperlongumine inhibits proliferation and survival of Burkitt lymphoma in vitro. *Leuk Res*. 2013 Feb;37(2):146-54. doi: 10.1016/j.leukres.2012.11.009.

Hwang, D., Kim, M., Park, H., Jeong, M. I., Jung, W., & Kim, B. (2019). Natural products and acute myeloid leukemia: A review highlighting mechanisms of action. In *Nutrients* (Vol. 11, Issue 5). MDPI AG. <https://doi.org/10.3390/nu11051010>.

Jeong, C. H., Ryu, H., Kim, D. H., Cheng, W. N., Yoon, J. E., Kang, S., & Han, S. G. (2019). Piperlongumine induces cell cycle arrest via reactive oxygen species accumulation and IKKB suppression in human breast cancer cells. *Antioxidants*, 8(11). <https://doi.org/10.3390/antiox8110553>.

Kobyakova M, Lomovskaya Y, Senotov A, Lomovsky A, Minaychev V, Fadeeva I, Shtatnova D, Krasnov K, Zvyagina A, Odinkova I, Akatov V, Fadeev R. The Increase in the Drug Resistance of Acute Myeloid Leukemia THP-1 Cells in High-Density Cell Culture Is Associated with Inflammatory-like Activation and Anti-Apoptotic Bcl-2 Proteins. *Int J Mol Sci.* 2022 Jul 17;23(14):7881. doi: 10.3390/ijms23147881.

Kanno S, Hiura T, Shouji A, Osanai Y, Ujibe M, Ishikawa M. Resistance to Ara-C up-regulates the activation of NF-kappaB, telomerase activity and Fas expression in NALM-6 cells. *Biol Pharm Bull.* 2007 Nov;30(11):2069-74. doi: 10.1248/bpb.30.2069.

Khoury JD, Solary E, Abla O, Akkari Y, Alaggio R, Apperley JF, Bejar R, Berti E, Busque L, Chan JKC, Chen W, Chen X, Chng WJ, Choi JK, Colmenero I, Coupland SE, Cross NCP, De Jong D, Elghetany MT, Takahashi E, Emile JF, Ferry J, Fogelstrand L, Fontenay M, Germing U, Gujral S, Haferlach T, Harrison C, Hodge JC, Hu S, Jansen JH, Kanagal-Shamanna R, Kantarjian HM, Kratz CP, Li XQ, Lim MS, Loeb K, Loghavi S, Marcogliese A, Meshinchi S, Michaels P, Naresh KN, Natkunam Y, Nejati R, Ott G, Padron E, Patel KP, Patkar N, Picarsic J, Platzbecker U, Roberts I, Schuh A, Sewell W, Siebert R, Tembhare P, Tyner J, Verstovsek S, Wang W, Wood B, Xiao W, Yeung C, Hochhaus A. The 5th edition of the World Health Organization Classification of Haematolymphoid Tumours: Myeloid and Histiocytic/Dendritic Neoplasms. *Leukemia* 2022, 36, 1703–1719. <https://doi.org/10.1038/s41375-022-01613-1>.

Kumbul YÇ, Nazıroğlu M. Paclitaxel Promotes Oxidative Stress-Mediated Human Laryngeal Squamous Tumor Cell Death through the Stimulation of Calcium and Zinc Signaling

Pathways: No Synergic Action of Melatonin. *Biol Trace Elem Res.* 2022 May;200(5):2084-2098. doi: 10.1007/s12011-022-03125-6.

Kuo, H. P., Wang, Z., Lee, D. F., Iwasaki, M., Duque-Afonso, J., Wong, S. H. K., Lin, C. H., Figueroa, M. E., Su, J., Lemischka, I. R., & Cleary, M. L. (2013). Epigenetic Roles of MLL Oncoproteins Are Dependent on NF- κ B. *Cancer Cell*, 24(4), 423–437.

<https://doi.org/10.1016/j.ccr.2013.08.019>.

Iacobini M, Menichelli A, Palumbo G, Multari G, Werner B, Del Principe D. Involvement of oxygen radicals in cytarabine-induced apoptosis in human polymorphonuclear cells. *Biochem Pharmacol.* 2001 Apr 15;61(8):1033-40. doi: 10.1016/s0006-2952(01)00548-2.

Lan X, Hu M, Jiang L, Wang J, Meng Y, Chen X, Liu A, Ding W, Zhang H, Zhou H, Liu B, Peng G, Liao S, Chen X, Liu J, Shi X. Piperlongumine overcomes imatinib resistance by inducing proteasome inhibition in chronic myelogenous leukemia cells. *J Ethnopharmacol.* 2023 Jan 30;301:115815. doi: 10.1016/j.jep.2022.115815.

Livak KJ, Schmittgen TD. Analysis of relative gene expression data using real-time quantitative PCR and the 2(-Delta Delta C(T)) Method. *Methods.* 2001 Dec;25(4):402-8. doi: 10.1006/meth.2001.1262.

Liu B, Wang H. Oxaliplatin induces ferroptosis and oxidative stress in HT29 colorectal cancer cells by inhibiting the Nrf2 signaling pathway. *Exp Ther Med.* 2022 Jun;23(6):394. doi: 10.3892/etm.2022.11321.

Maguire O, O'Loughlin K, Minderman H. Simultaneous assessment of NF- κ B/p65 phosphorylation and nuclear localization using imaging flow cytometry. *J Immunol Methods*. 2015 Aug;423:3-11. doi: 10.1016/j.jim.2015.03.018.

Newell, L. F., & Cook, R. J. (2021). Advances in acute myeloid leukemia. *BMJ*, 375. <https://doi.org/10.1136/bmj.n2026>.

Oiso S, Ikeda R, Nakamura K, Takeda Y, Akiyama S, Kariyazono H. Involvement of NF- κ B activation in the cisplatin resistance of human epidermoid carcinoma KCP-4 cells. *Oncol Rep*. 2012 Jul;28(1):27-32. doi: 10.3892/or.2012.1801.

Pei S, Minhajuddin M, Callahan KP, Balys M, Ashton JM, Neering SJ, Lagadinou ED, Corbett C, Ye H, Liesveld JL, O'Dwyer KM, Li Z, Shi L, Greninger P, Settleman J, Benes C, Hagen FK, Munger J, Crooks PA, Becker MW, Jordan CT. Targeting aberrant glutathione metabolism to eradicate human acute myelogenous leukemia cells. *J Biol Chem*. 2013, 288, 33542-33558. doi: 10.1074/jbc.M113.511170.

Rawat, L., Hegde, H., Hoti, S. L., & Nayak, V. (2020). Piperlongumine induces ROS mediated cell death and synergizes paclitaxel in human intestinal cancer cells. *Biomedicine and Pharmacotherapy*, 128. <https://doi.org/10.1016/j.biopha.2020.110243>

Rodrigues ACBDC, Costa RGA, Silva SLR, Dias IRSB, Dias RB, Bezerra DP. Cell signaling pathways as molecular targets to eliminate AML stem cells. *Crit Rev Oncol Hematol*. 2021, 160, 103277. doi: 10.1016/j.critrevonc.2021.103277.

Samuel T, Fadlalla K, Gales DN, Putcha BD, Manne U. Variable NF- κ B pathway responses in colon cancer cells treated with chemotherapeutic drugs. *BMC Cancer*. 2014 Aug 18;14:599. doi: 10.1186/1471-2407-14-599.

She M, Niu X, Chen X, Li J, Zhou M, He Y, Le Y, Guo K. Resistance of leukemic stem-like cells in AML cell line KG1a to natural killer cell-mediated cytotoxicity. *Cancer Lett*. 2012 May 28;318(2):173-9. doi: 10.1016/j.canlet.2011.12.017.

Shlush, L. I., & Feldman, T. (2021). The evolution of leukaemia from pre-leukaemic and leukaemic stem cells. *Journal of Internal Medicine*, 289(5), 636–649.

<https://doi.org/10.1111/joim.13236>

Stanchina, M., Soong, D., Zheng-Lin, B., Watts, J. M., & Taylor, J. (2020). Advances in acute myeloid leukemia: Recently approved therapies and drugs in development. In *Cancers* (Vol. 12, Issue 11, pp. 1–32). MDPI AG. <https://doi.org/10.3390/cancers12113225>

Stubbins, R. J., Francis, A., Kuchenbauer, F., & Sanford, D. (2022). Management of Acute Myeloid Leukemia: A Review for General Practitioners in Oncology. In *Current Oncology* (Vol. 29, Issue 9, pp. 6245–6259). MDPI. <https://doi.org/10.3390/curroncol29090491>

Thol, F., & Ganser, A. (2020). Treatment of Relapsed Acute Myeloid Leukemia. In *Current Treatment Options in Oncology* (Vol. 21, Issue 8). Springer. <https://doi.org/10.1007/s11864-020-00765-5>

Tzelepis K, Koike-Yusa H, De Braekeleer E, et al. A CRISPR Dropout Screen Identifies Genetic Vulnerabilities and Therapeutic Targets in Acute Myeloid Leukemia. *Cell Rep*. 2016;17(4):1193-1205. doi:10.1016/j.celrep.2016.09.079

- Winters AC, Gutman JA, Purev E, et al. Real-world experience of venetoclax with azacitidine for untreated patients with acute myeloid leukemia. *Blood Adv.* 2019;3(20):2911-2919. doi:10.1182/bloodadvances.2019000243
- Yang L, Shi P, Zhao G, Xu J, Peng W, Zhang J, Zhang G, Wang X, Dong Z, Chen F, Cui H. Targeting cancer stem cell pathways for cancer therapy. *Signal Transduct Target Ther.* 2020 Feb 7;5(1):8. doi: 10.1038/s41392-020-0110-5.
- Yao Y, Sun Y, Shi M, Xia D, Zhao K, Zeng L, Yao R, Zhang Y, Li Z, Niu M, Xu K. Piperlongumine induces apoptosis and reduces bortezomib resistance by inhibiting STAT3 in multiple myeloma cells. *Oncotarget.* 2016 Nov 8;7(45):73497-73508. doi: 10.18632/oncotarget.11988.
- Yu W, Chen Y, Dubrulle J, Stossi F, Putluri V, Sreekumar A, Putluri N, Baluya D, Lai SY, Sandulache VC. Cisplatin generates oxidative stress which is accompanied by rapid shifts in central carbon metabolism. *Sci Rep.* 2018 Mar 9;8(1):4306. doi: 10.1038/s41598-018-22640-y.

Figure legends

Figure 1. (A) Chemical structure of PL. (B) IC₅₀ values of cytotoxicity of PL against haematological (red bars) and solid cancers (blue bars), as well as against noncancerous cells (green bars). (C) Heatmap of selectivity indexes obtained for PL.

Figure 2. Effects of PL on colony formation of human and mouse AML cell lines or normal primary bone marrow cells. Colony-forming ability of (A and B) MV-4-11, (C and D) MOLM-13, (E and F) OCI-AML3 and (G and H) Cas9 FLT3-ITD MLL-AF4 and (G and I) MLL-AF9 cell lines after treatment with PL at different concentrations and representative colony formation microscopy images. (J) Representative colony formation microscopy images of primary mouse bone marrow cells. (K and L) Effects of PL on the total number of colonies and the number of different colony types derived from primary mouse bone marrow cells. Colony-forming cell; M, monocytes; G, granulocyte; GM, granulocyte/macrophage; GEM, granulocyte, erythrocyte, and macrophage. The colony type is indicated by red arrows. The vehicle (0.2% DMSO) was used as a negative control (CTL). Scale bar: 1000 μ m. Data are shown as the mean \pm S.E.M. of three independent experiments carried out in duplicate. * $p < 0.05$ compared to CTL by Student's t test.

Figure 3. PL effect on the growth of xenografts derived from KG-1a cells. A xenograft model was established in NSG mice. After 2 weeks of inoculation of KG-1a cells, mice were randomly

divided into the PL (20 mg/kg) group and the control group (5% DMSO). hCD45-positive cells were quantified by flow cytometry from (A) bone marrow, (C) peripheral blood and (E) spleen. mCD45-positive cells were quantified by flow cytometry from (B) bone marrow, (D) peripheral blood and (F) spleen. Data are shown as the mean \pm S.E.M. of 5-6 animals. * $p < 0.05$ compared with CTL by Student's t test.

Figure 4. Effects of PL treatment on the antigen expression level of AML stem/progenitor cell markers in KG-1a cells. Flow cytometry was used to detect the antigen expression of (A) CD13, (B) CD33, (C) CD34, (D) CD38 and (E) CD123. The vehicle (0.2% DMSO) was used as a negative control (CTL). Data are shown as the mean \pm S.E.M. of three independent experiments carried out in duplicate. * $p < 0.05$ compared to CTL by Student's t test.

Figure 5. Cell cycle progression in KG-1a cells after 12, 24, 48 and 72 h of incubation with PL. Representative histograms after (A) 12, (B) 24, (C) 48 and (D) 72 h of treatment. Percentage of cells in (E) Sub-G₀/G₁, (F) G₀/G₁, (G) S and (H) G₂/M after different incubation periods with PL. Vehicle (0.2% DMSO) was used as a negative control (CTL), and doxorubicin (DOX, 1 μ M) was used as a positive control. Data are shown as the mean \pm S.E.M. of three independent experiments carried out in duplicate. * $p < 0.05$ compared with CTL by Student's t test.

Figure 6. Apoptotic cell death induced by PL in KG-1a cells. **(A)** Representative flow cytometry dot plots. Apoptosis quantification in KG-1a cells after **(B)** 12, **(C)** 24, **(D)** 48 and **(E)** 72 h of treatment with PL. Quantification of live (negative cells for YO-PRO-1 and PI), apoptotic (YO-PRO-1-positive cells) and dead (YO-PRO-1- and PI-positive cells) KG-1a cells. Vehicle (0.2% DMSO) was used as a negative control (CTL), and doxorubicin (DOX, 1 μ M) was used as a positive control. Data are shown as the mean \pm S.E.M. of three independent experiments carried out in duplicate. * $p < 0.05$ compared with CTL by Student's t test.

Figure 7. **(A and B)** PL effect on the levels of active caspase 3 and **(C and D)** cleaved PARP (Asp214) after 24 h of treatment in KG-1a cells. Effect of the pancaspase inhibitor Z-VAD(OMe)-FMK on the apoptosis induced by PL in KG-1a cells. **(E and F)** The cells were pretreated for 2 h with 50 μ M Z-VAD(OMe)-FMK and then incubated with PL at 20 μ M for 48 h. **(G)** PL effect on mitochondrial activity in KG-1a cells. **(H and I)** Induction of cell death in WT SV40 MEF and BAD KO SV40 MEF cell lines after 48 h incubation with 40 μ M 5-FU and 16 μ M PL. **(J and K)** Survival curves of WT SV40 MEF and BAD KO SV40 MEF cell lines upon treatment with 5-FU and PL. The curves were obtained from at least three independent experiments carried out in duplicate using the Alamar blue assay after 72 h of incubation. Vehicle (0.2% DMSO) was used as a negative control (CTL), and doxorubicin (DOX, 1 μ M) was used as a positive control. Data are shown as the mean \pm S.E.M. of three independent experiments carried out in duplicate. * $p < 0.05$ compared with CTL by Student's

t test. # $p < 0.05$ compared with the respective treatment without inhibitor by Student's t test. MFI = Mean fluorescence intensity.

Figure 8. PL induced ROS accumulation in KG-1a cells. **(A and B)** Effect of the antioxidant *N*-acetyl-cysteine (NAC) on the apoptosis induced by PL in KG-1a cells. The cells were pretreated for 2 h with 5 mM NAC and then incubated with PL at 20 μ M for 48 h. **(C and D)** Mitochondrial ROS in KG-1a cells after 1 and 24 h of treatment with PL. Vehicle (0.2% DMSO) was used as a negative control (CTL), and doxorubicin (DOX, 1 μ M) was used as a positive control. Data are shown as the mean \pm S.E.M. of three independent experiments carried out in duplicate. * $p < 0.05$ compared with CTL by Student's t test. # $p < 0.05$ compared with the respective treatment without inhibitor by Student's t test. MFI = Mean fluorescence intensity.

Figure 9. **(A)** Up- and downregulated genes in KG-1a cells after 12 h of treatment with 20 μ M PL. Genes that displayed $RQ \geq 2$ (red bars) were upregulated, and $RQ \leq 0.5$ (green bars) were downregulated. **(B and C)** PL effect on the levels of NF- κ B p65 (pS529) after 24 h of treatment in KG-1a cells. **(D and E)** PL effect on the levels of NF- κ B p65 (pS536) after 24 h of treatment in KG-1a cells. The vehicle (0.2% DMSO) was used as a negative control (CTL). Data are shown as the mean \pm S.E.M. of three independent experiments carried out in duplicate. * $p < 0.05$ compared with CTL by Student's t test. MFI = Mean fluorescence intensity. **(F)**

Representative immunofluorescence images of NF- κ B p65 in KG-1a cells after 24 h of incubation with 20 μ M PL. Scale bar = 25 μ m.

Figure 10. Effect of PL plus ARA-C or DNR or Aza combinatorial treatment on the growth of AML cells *in vitro*. Combination index plot (Fa-CI plot) of the interaction between (A) PL and ARA-C, (B) PL and DNR and (C) PL and AZA in MOLM-13 cells and (D) PL and ARA-C, (E) PL and DNR and (F) PL and AZA in OCI-AML3 cells generated by CompuSyn software. Fa: inhibitory effect, CI: combination index. AML cells were treated for 72 h with control vehicle, individual drugs or the 2-drug combination at different concentrations on the basis of previously established IC₅₀ values, followed by measurement of cell proliferation using the MTT assay. Data are presented as the mean \pm S.E.M. Synergistic, additive, and antagonistic effects of drugs are defined by CI values of < 1.0 , 1.0 , and > 1.0 , respectively.

Fig. 1

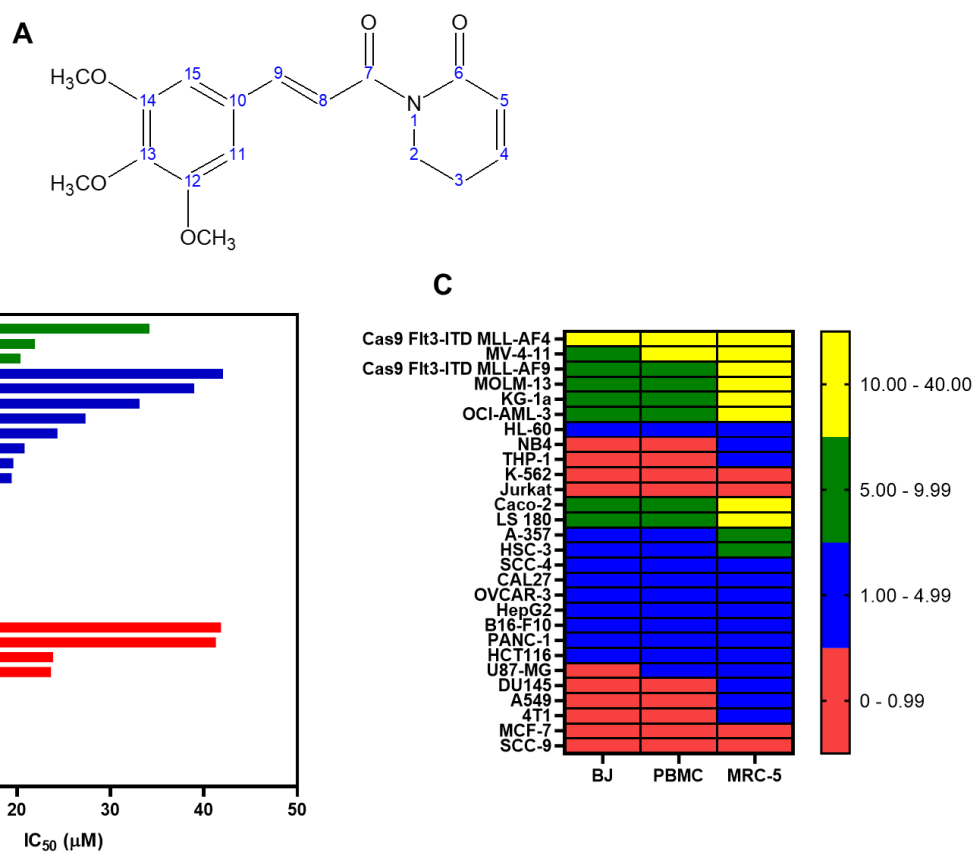


Fig. 2.

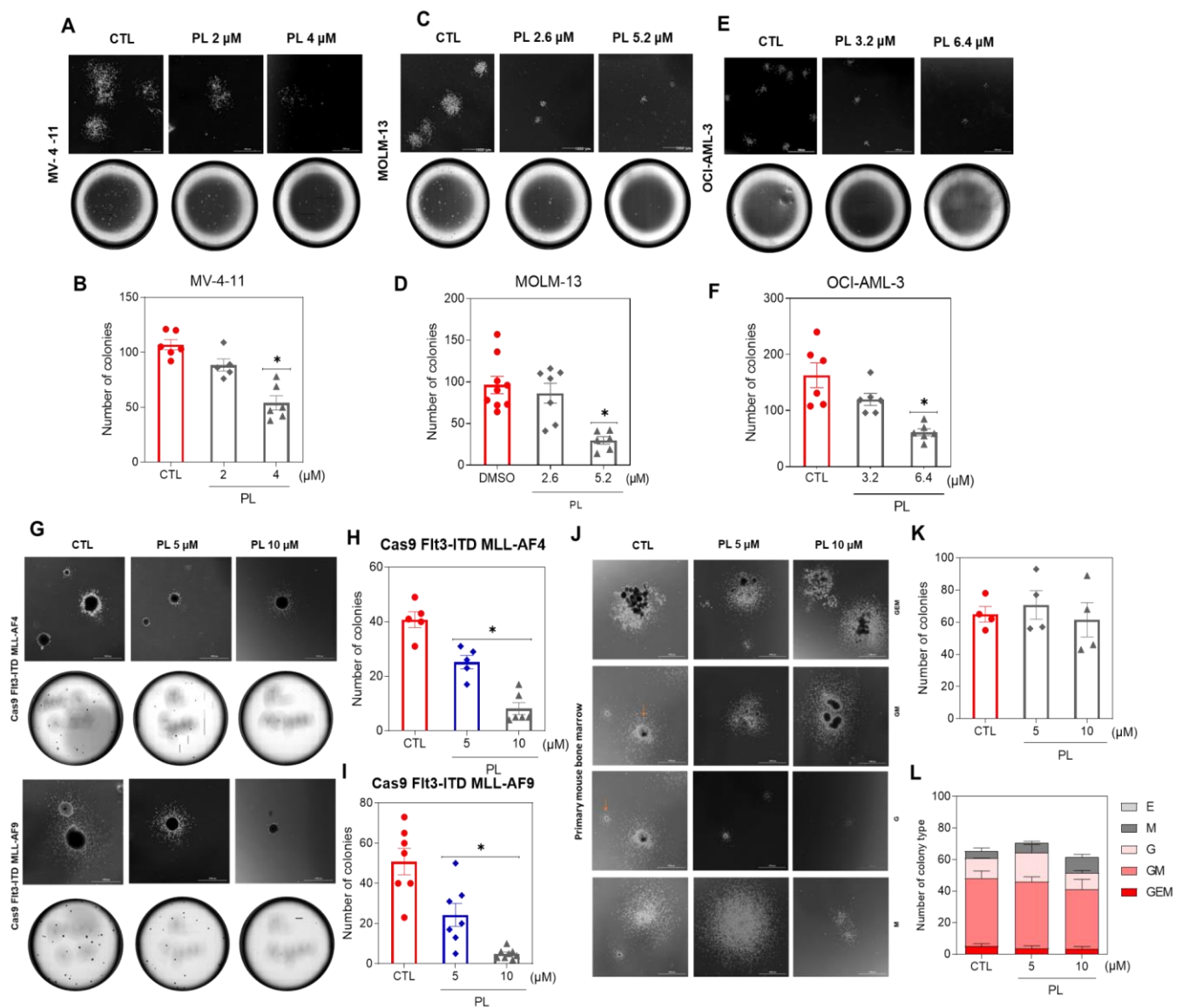


Fig. 3

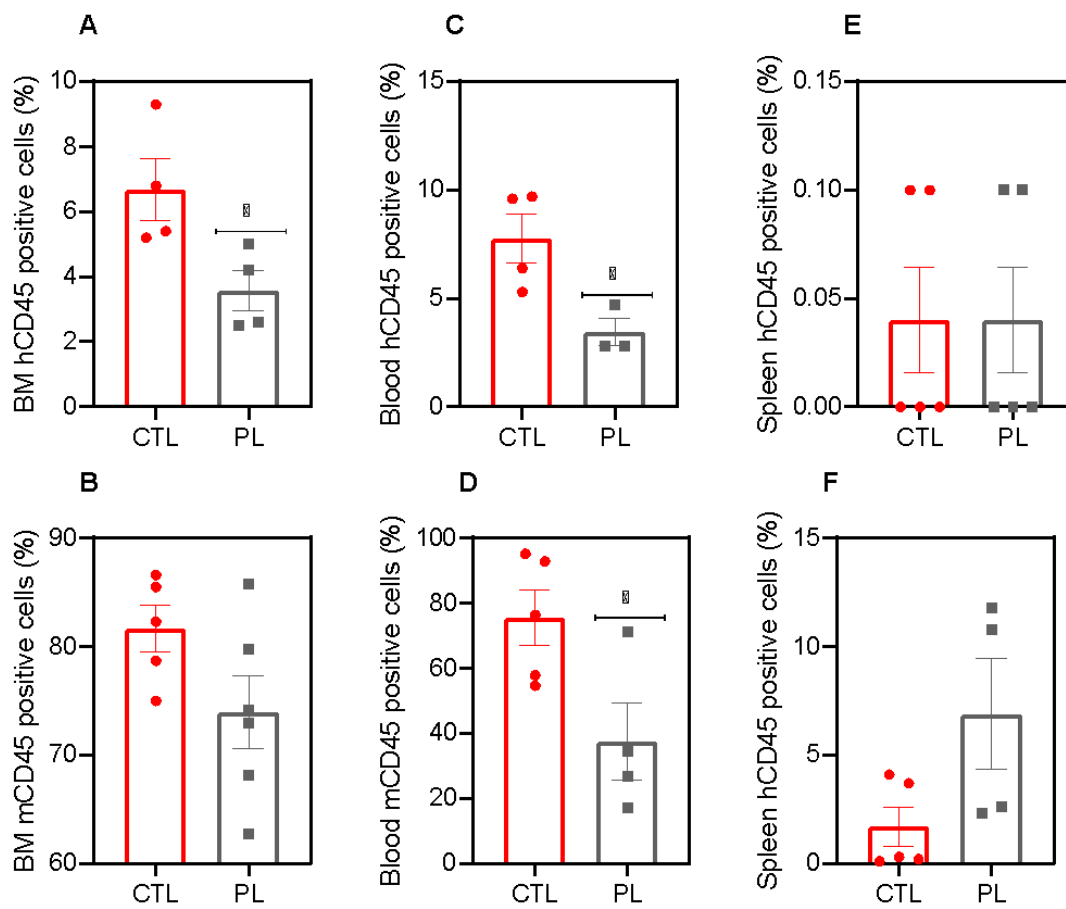


Fig. 4

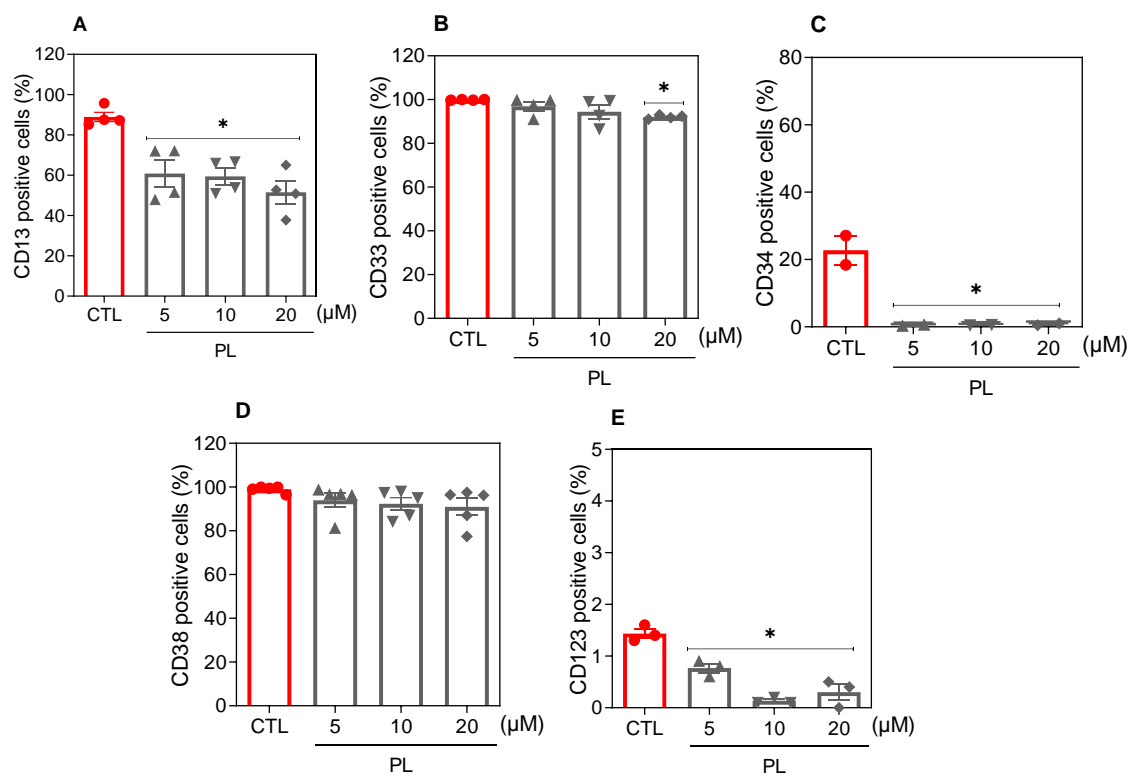


Fig. 5

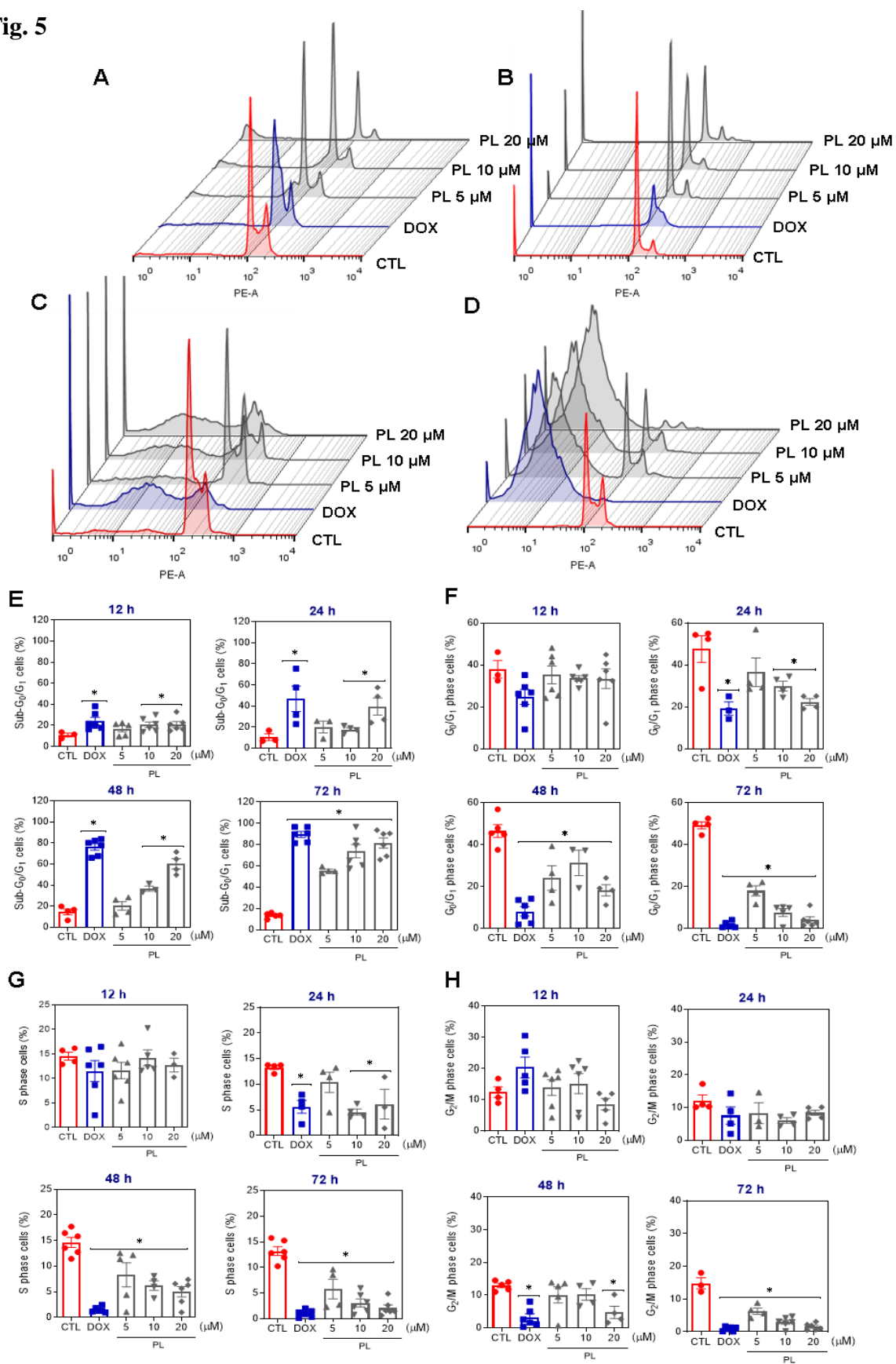


Fig. 6

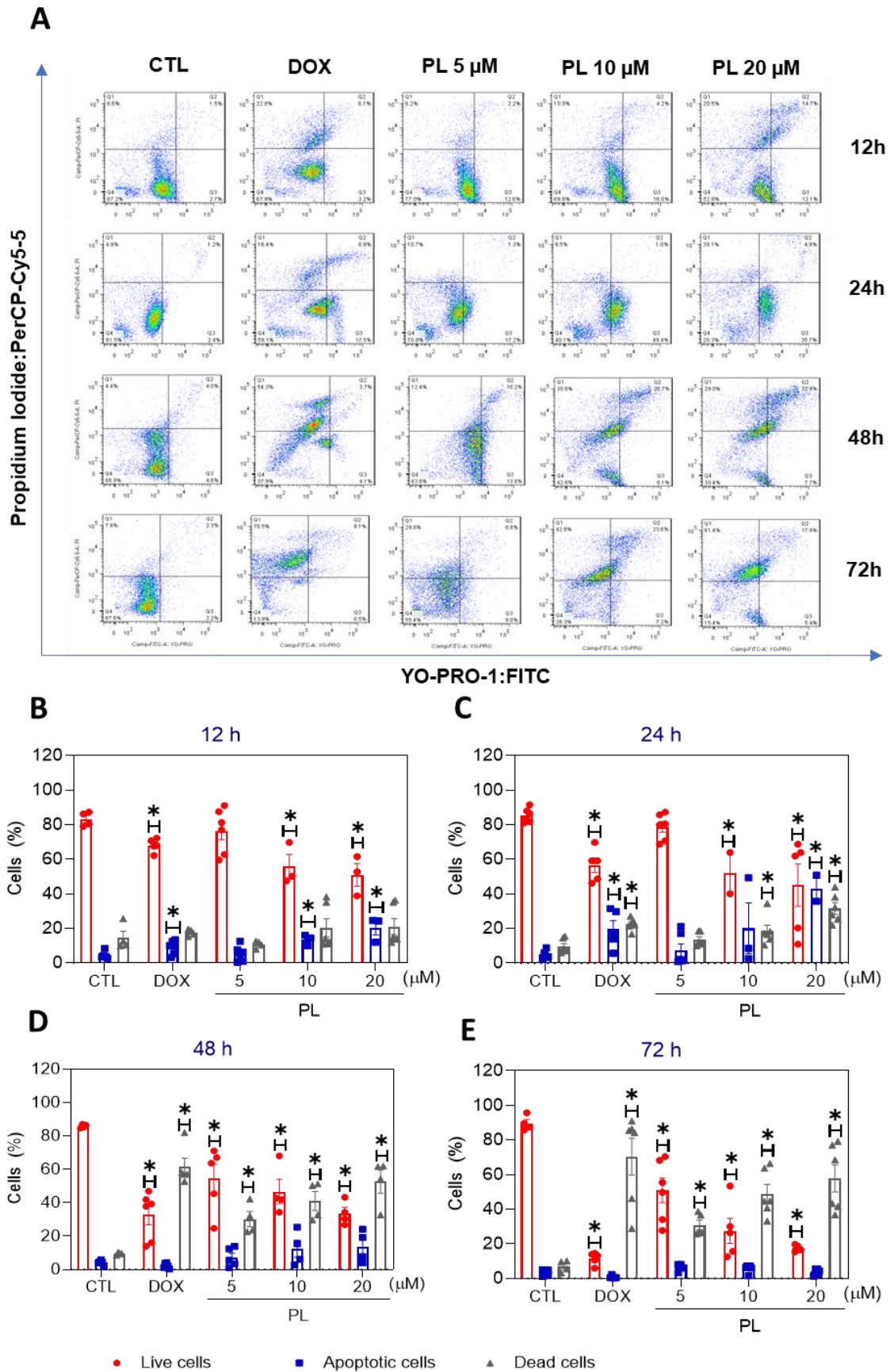


Fig. 7

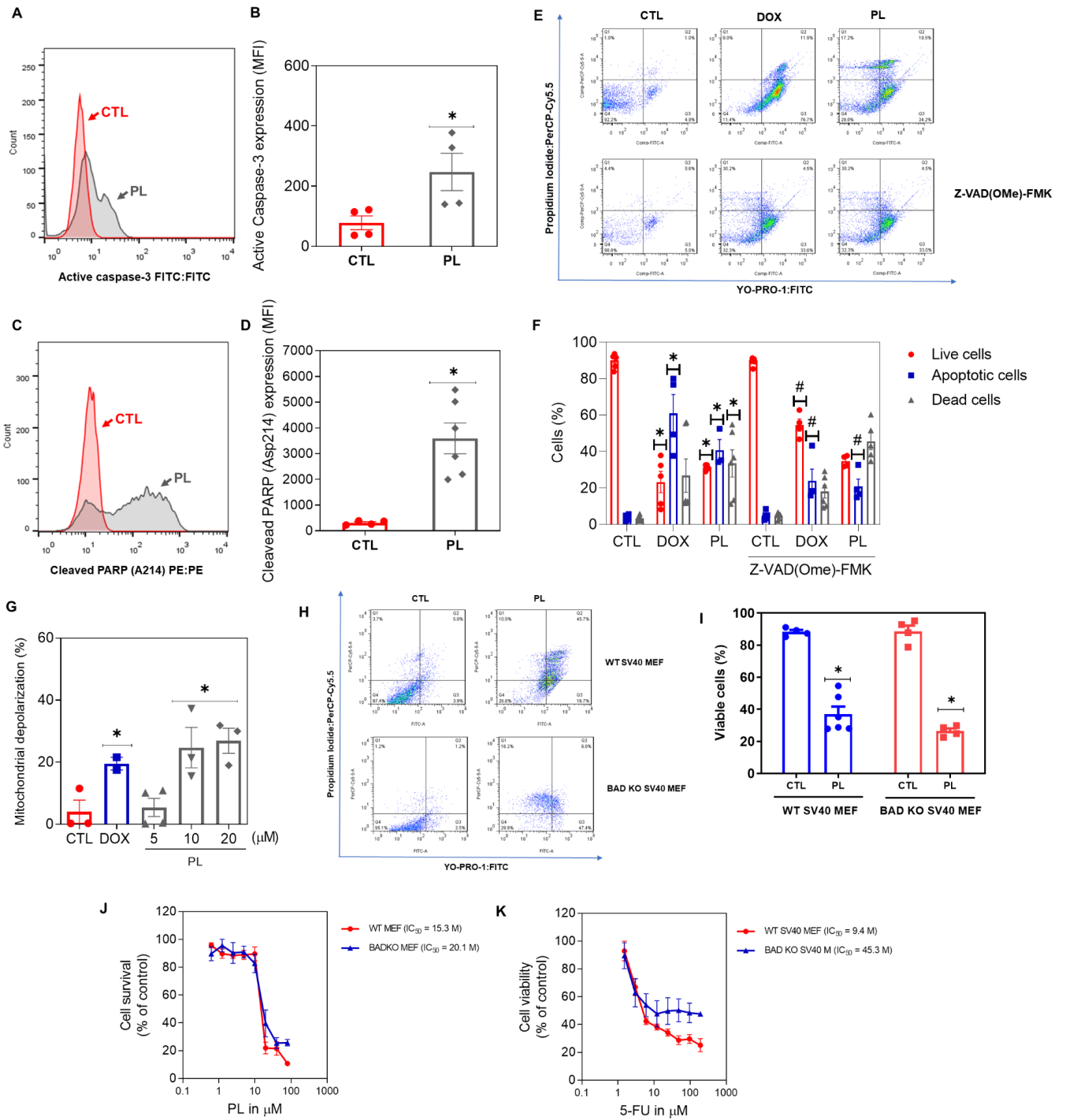


Fig. 8

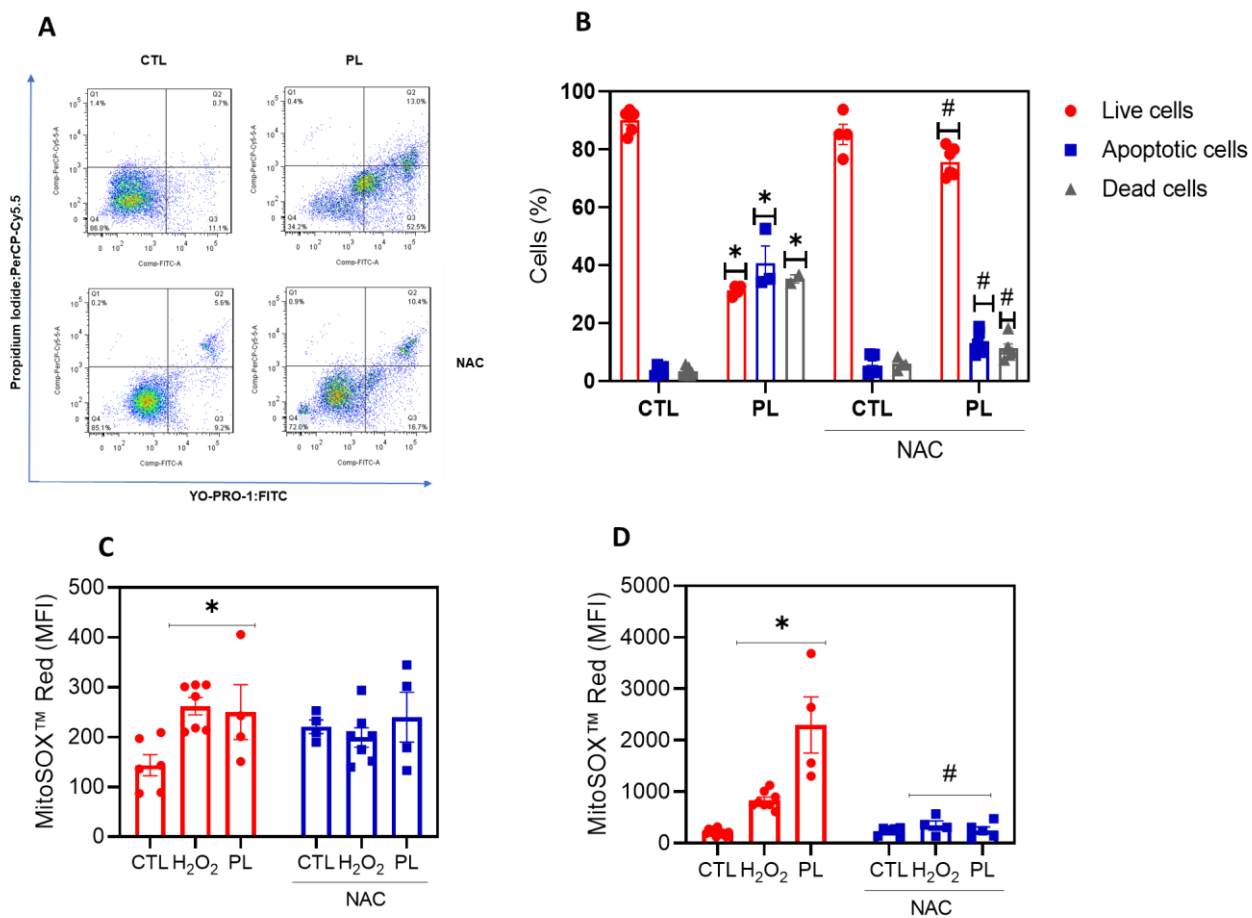


Fig. 9

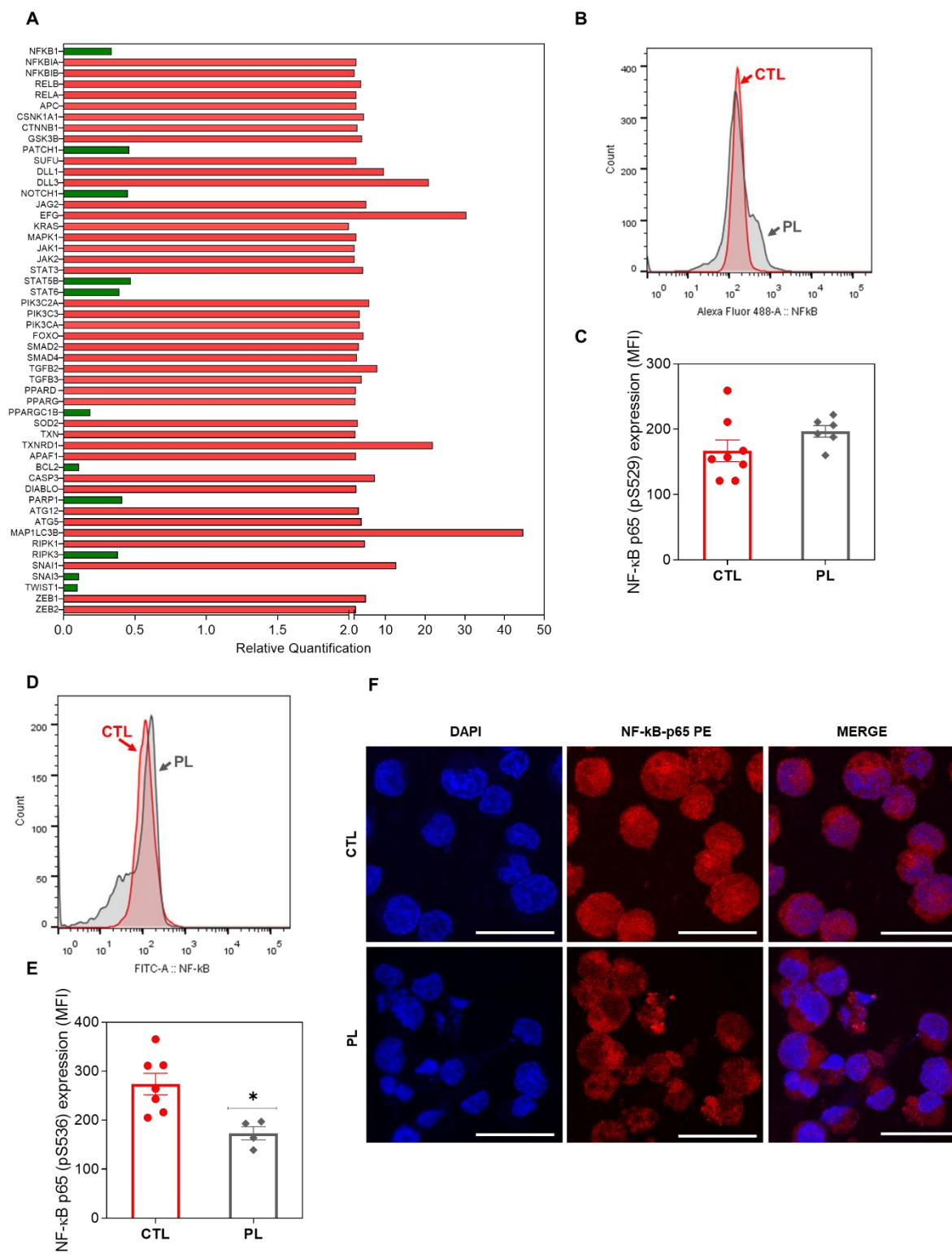
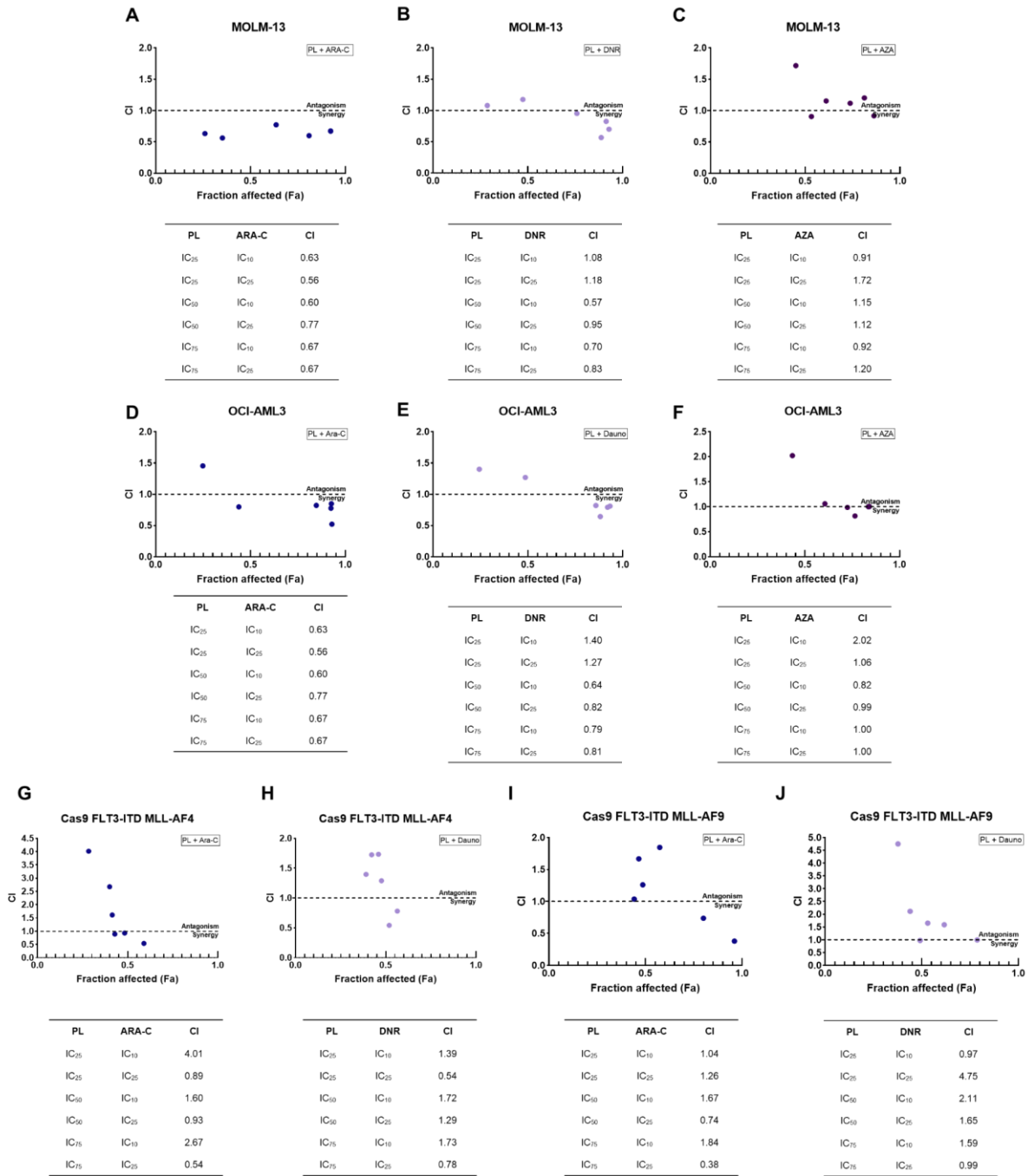


Fig. 10



Supplementary Material

Piplartine eliminates CD34+ AML stem/progenitor cells by inducing oxidative stress and suppressing NF- κ B signaling

Ana Carolina B. da C. Rodrigues^{1,4}, Suellen L. R. Silva¹, Ingrid R. S. B. Dias¹, Rafaela G. A. Costa¹, Maiara de S. Oliveira¹, Milena B. P. Soares^{1,2}, Rosane B. Dias¹, Ludmila F. Valverde¹, Clarissa A. G. Rocha^{1,3}, Emily M. Johnson⁴, Cristina C. A. Pina^{4,* \dagger} , Daniel P. Bezerra^{1,* \dagger}

¹Gonçalo Moniz Institute, Oswaldo Cruz Foundation (IGM-FIOCRUZ/BA), Salvador, Bahia, 40296-710, Brazil.

²SENAI Institute for Innovation in Advanced Health Systems, SENAI CIMATEC, Salvador, BA, 41650-010, Brazil;

³Department of Clinical Propaedeutics and Integrated Clinical, Faculty of Dentistry, Federal University of Bahia (UFBA), Salvador, Bahia, 40301-155, Brazil.

⁴College of Health, Medicine and Life Sciences, Brunel University London, Uxbridge, UB8 3PH, United Kingdom.

\dagger These authors contributed equally to this work.

*Corresponding authors:

D. P. Bezerra, E-mail: danielpbezerra@gmail.com or daniel.bezerra@fiocruz.br Tel/Fax + 55 71 3176 2272.

C. Pina, E-mail: cristina.pina@brunel.ac.uk

Phone number: +44 1895 266676.

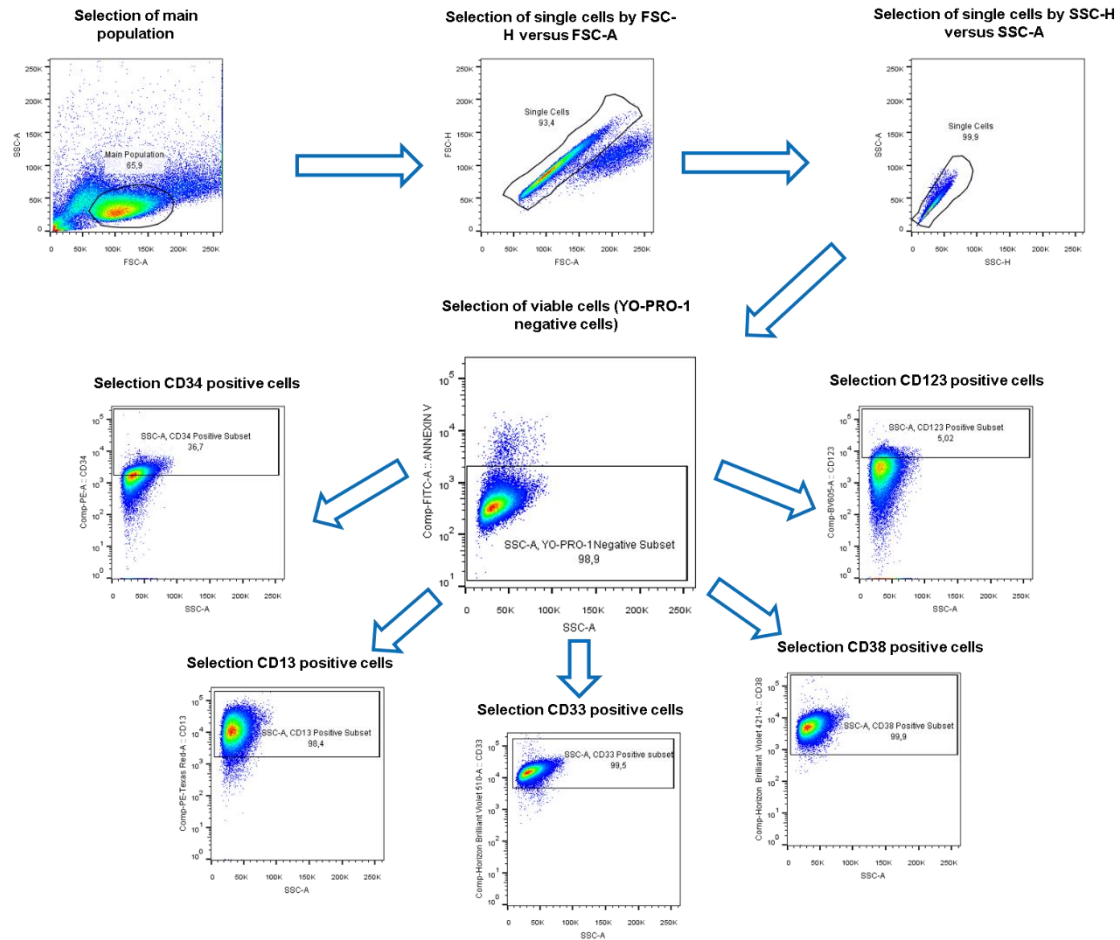


Figure S1. Representative gating strategy for immunophenotyping of KG-1a cells by flow cytometry. PE mouse anti-human CD34, BV421 mouse anti-human CD38, BV605 mouse anti-human CD123, PE-CF594 mouse anti-human CD13 and BV510 mouse anti-human CD33 antibodies were used. PE mouse IgG1, κ isotype control was used as isotype control and annexin V-FITC (BD Biosciences) or YO-PRO-1 were used to select viable cells.

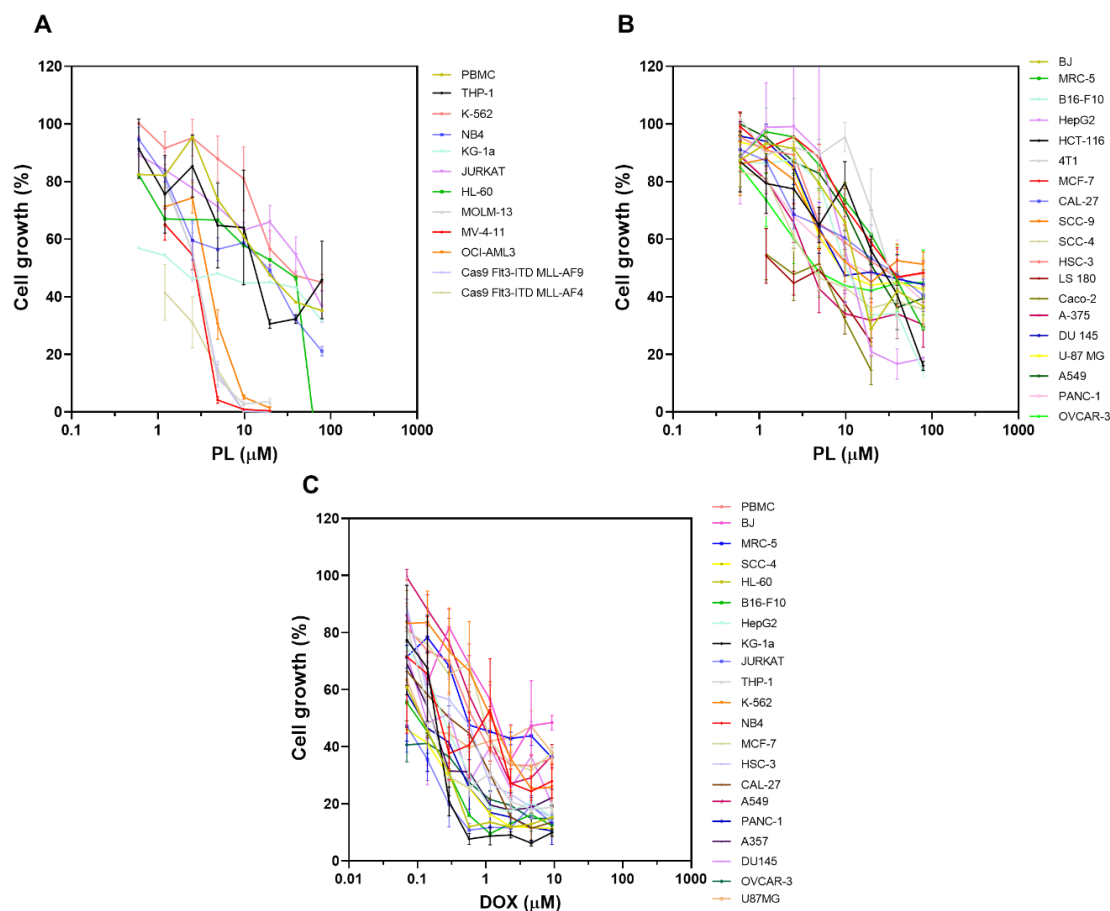


Figure S2. Cell growth curves obtained after 72 h of incubation with PL. **(A)** Cell growth curves of leukemic cells and PBMCs and **(B)** cancer cell lines derived from solid tumours and noncancerous cell lines BJ and MRC-5 after PL treatment. **(C)** Cell growth curve of cancer cells and noncancerous cells after 72 h of incubation with the positive control, doxorubicin. These data were obtained from three independent experiments performed in duplicate and measured either by Alamar blue assay or trypan blue assay after 72 h of incubation.

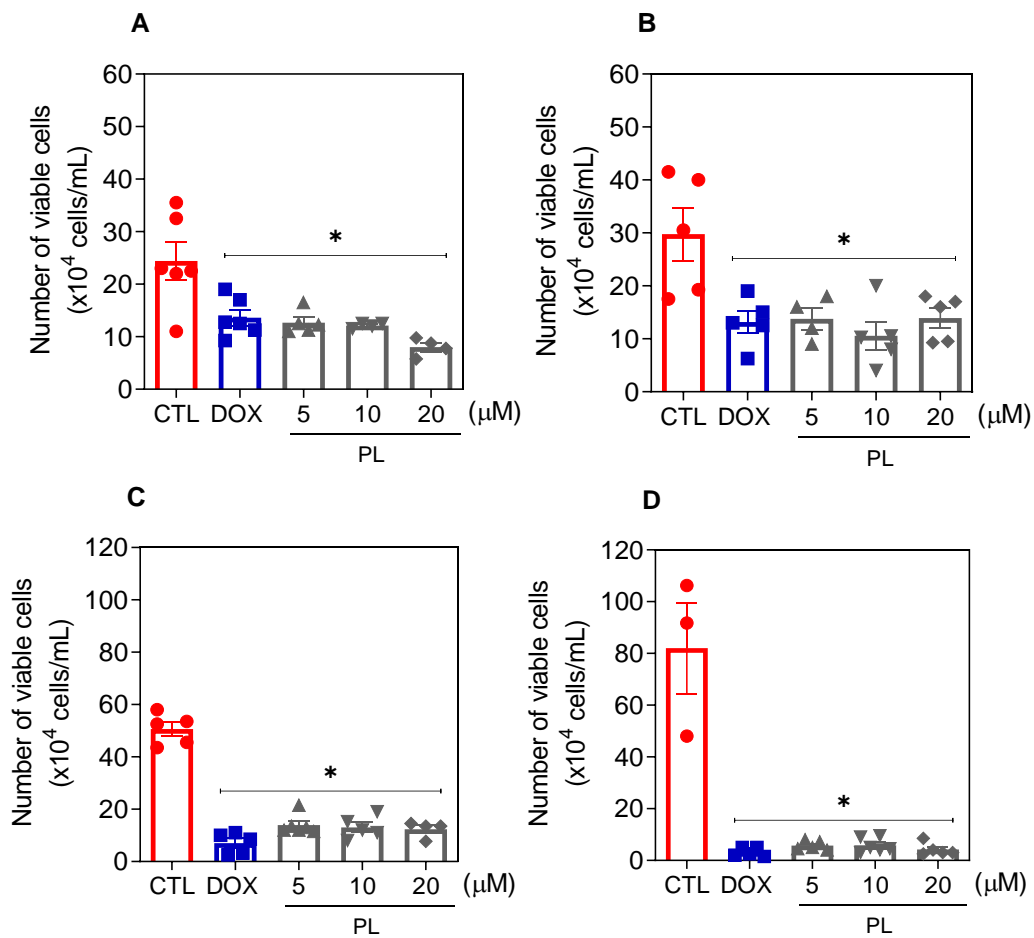


Figure S3. Trypan blue exclusion assay after (A) 12, (B) 24, (C) 48 and (D) 72 h of treatment with PL using KG-1a cells. Vehicle (0.2% DMSO) was used as a negative control (CTL), and doxorubicin (DOX, 1 μM) was used as a positive control. Data are expressed as the mean ± S.E.M. of three independent experiments carried out in duplicate.

* $p < 0.05$ compared with CTL by Student's t test.

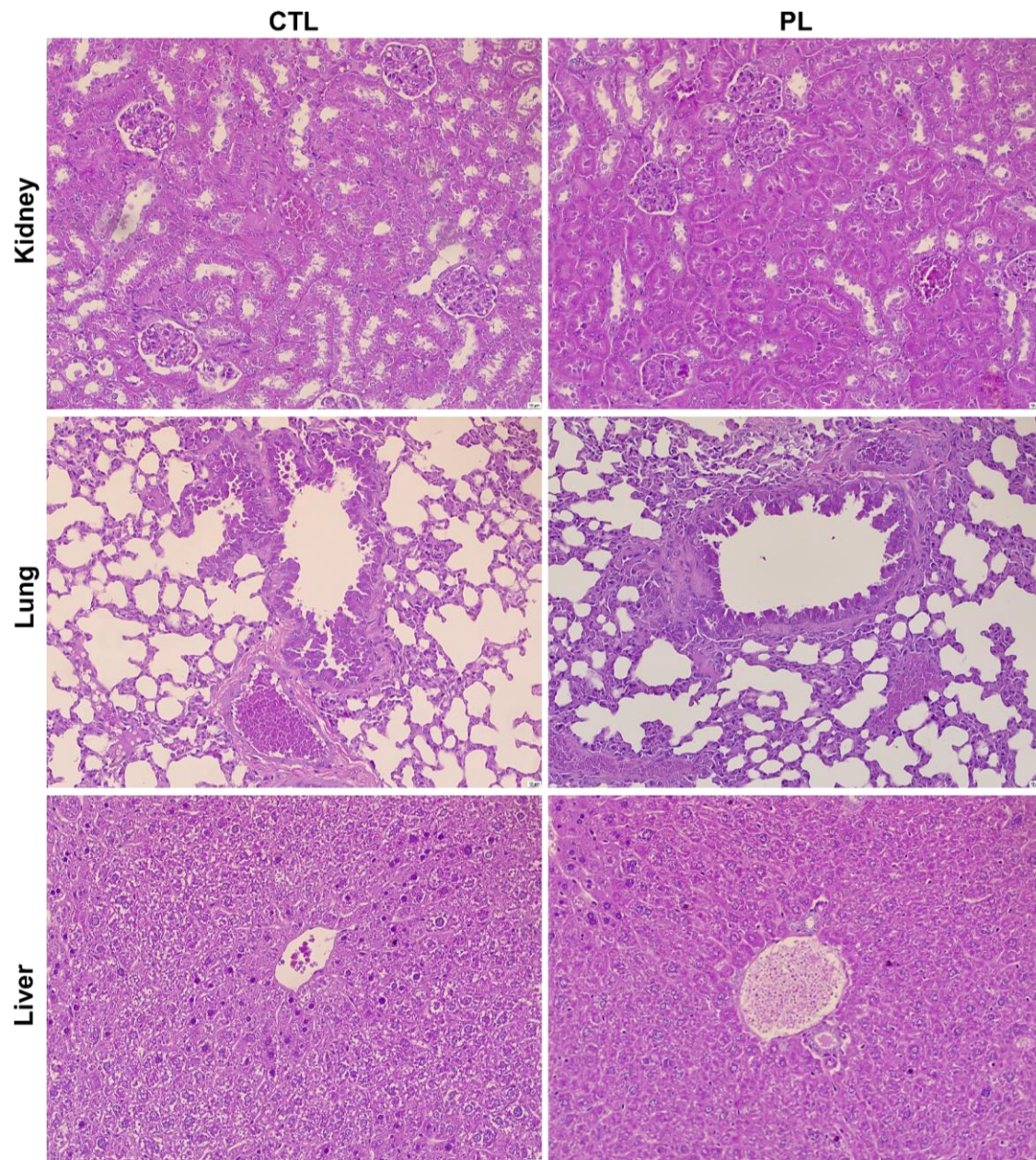


Figure S4. Representative photomicrographs of kidneys, lungs and livers of the NOD. *Cg-Prkdc^{scid} Il2rg^{tm1Wjl}/SzJ* (NSG) mice with AML KG-1a cell xenografts treated with PL. The negative control (CTL) was treated with vehicle (5% DMSO) for dilution. The treatment was injected into mice intraperitoneally every day for two weeks. Histological

analysis of various organs (liver, lung, kidney, and heart) showed histopathological changes in both the CTL and PL experimental groups. Kidneys exhibited mild glomerular hyalinization, decreased urinary space, vascular hyperemia, focal areas of coagulation necrosis, inflammation, and fibrosis. Lungs showed thickened alveolar septa, atelectasis, hyperemia, inflammation, edema, haemorrhage, fibrosis, and focal areas of haemosiderin deposition. The liver displayed vascular hyperemia, tissue inflammation, hydropic degeneration, and hepatocyte coagulation necrosis. However, no significant differences were observed between the two groups, except for certain areas of coagulative necrosis. Notably, the heart showed no remarkable histological changes. These alterations are reversible, except for specific necrotic areas in hepatocytes and renal tubules.

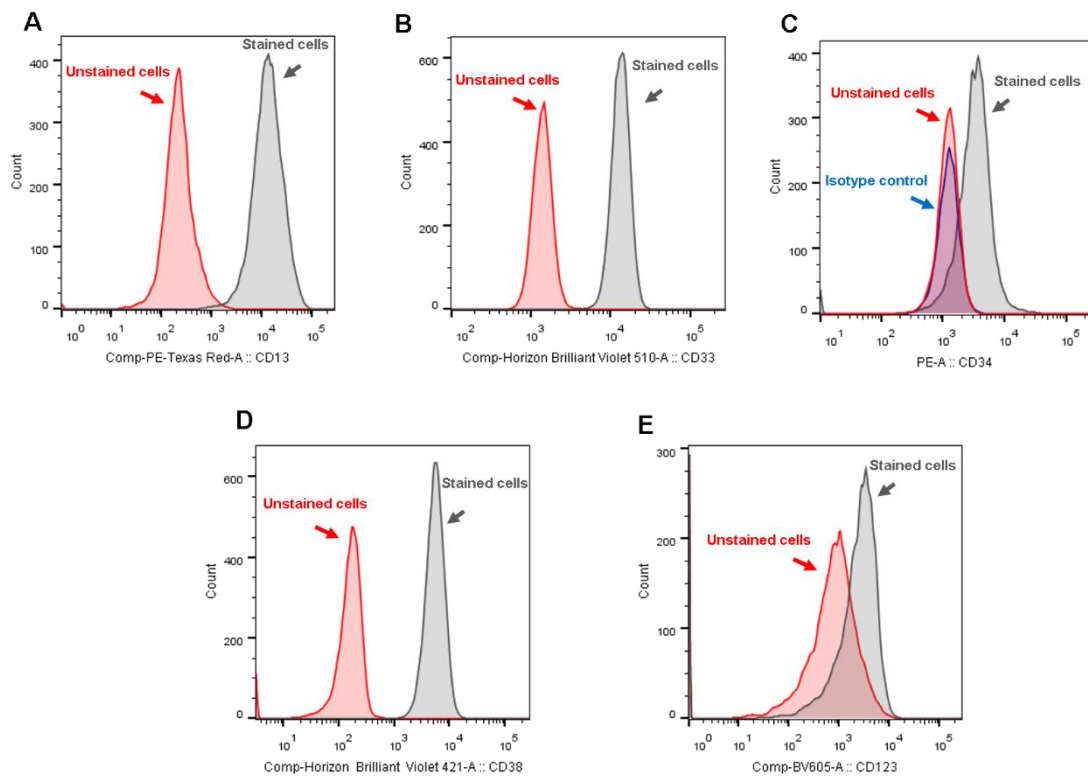


Figure S5. Representative histograms of (A) CD13, (B) CD33, (C) CD34, (D) CD38 and (E) CD123 expression levels in KG-1a cells. PE mouse anti-human CD34, BV421 mouse anti-human CD38, BV605 mouse anti-human CD123, PE-CF594 mouse anti-human CD13 and BV510 mouse anti-human CD33 antibodies were used. PE mouse IgG1, κ isotype control was used as isotype control and annexin V-FITC (BD Biosciences) or YO-PRO-1 were used to select viable cells.

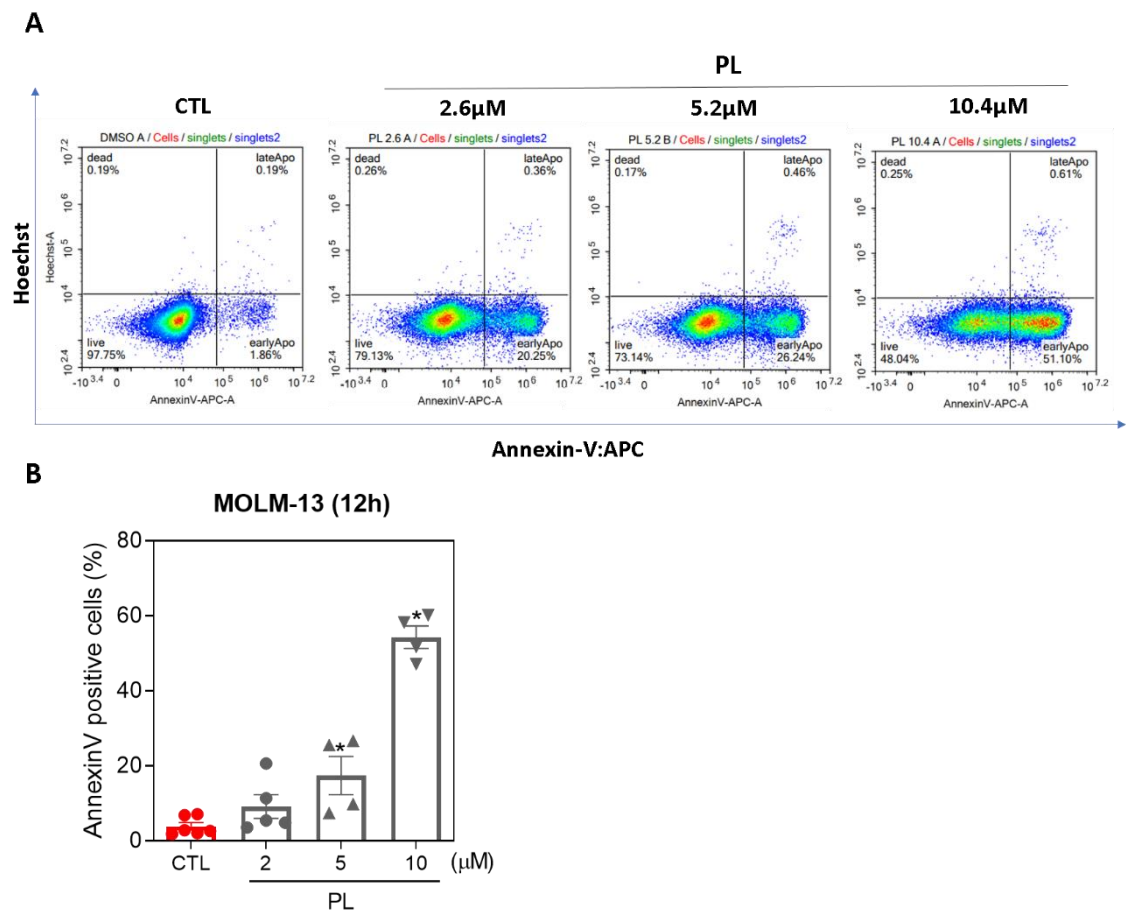


Figure S6. (A) Apoptotic cell death induced by PL in MOLM-13 cells. Representative flow cytometry dot plots. (B) Apoptosis quantification in MOLM-13 cells after 12 h of treatment with PL. The vehicle (0.2% DMSO) was used as a negative control (CTL). Data are shown as the mean \pm S.E.M. of three independent experiments carried out in duplicate. * $p < 0.05$ compared with CTL by Student's t test.

Table S1. List of cells used.

Cells	Histological type	Species	Source^{a,b,c,d,e}
<i>Cancer cell lines</i>			
MV-4-11	acute myelogenous leukemia	human	HL
MOLM-13	acute myelogenous leukemia	human	HL
KG-1a	acute myelogenous leukemia	human	ATCC
OCI-AML-3	acute myelogenous leukemia	human	HL
NB4	acute promyelocytic leukemia	human	ATCC
THP-1	monocytic leukemia	human	ATCC
JUKART	T-cell lymphoid leukemia	human	ATCC
K-562	chronic myelogenous leukemia	human	ATCC
HL-60	acute promyelocytic leukemia	human	ATCC
Caco-2	colorectal adenocarcinoma	human	ABL
LS 180	colorectal adenocarcinoma	human	ABL
HCT116	colorectal carcinoma	human	ATCC
HepG2	hepatocellular carcinoma	human	ATCC
KG-1a	acute myeloid leukemia	human	ATCC
MCF-7	breast adenocarcinoma	human	ATCC
4T1	breast carcinoma	mouse	ATCC
HSC-3	oral squamous cell carcinoma	human	ATCC
CAL 27	oral squamous cell carcinoma	human	ATCC
SCC4	oral squamous cell carcinoma	human	ATCC
SCC-9	oral squamous cell carcinoma	human	ATCC
A549	lung adenocarcinoma	human	BCRJ
PANC-1	pancreas ductal adenocarcinoma	human	BCRJ
OVCAR-3	ovarian carcinoma	human	BCRJ

DU 145	prostate carcinoma	human	BCRJ
U-87 MG	glioblastoma	human	BCRJ
A-375	melanoma	human	BCRJ
B16-F10	melanoma	mouse	ATCC
<i>Noncancer cell lines</i>			
MRC-5	lung fibroblast	human	ATCC
BJ	foreskin fibroblast	human	ATCC
<i>Mutant and its parental cell lines</i>			
BAD KO SV40 MEF	immortalized mouse embryonic fibroblasts with the BAD gene knocked out	mouse	ATCC
WT SV40 MEF	wild-type immortalized embryonic fibroblasts	mouse	ATCC
<i>Primary cells</i>			
Cas9 Flt3-TD MLL-AF4	bone marrow	mouse	primary cell culture
Cas9 Flt3-ITD MLL-AF9	bone marrow	mouse	primary cell culture
C57BL/6	bone marrow	mouse	primary cell culture
PBMC	health peripheral blood mononuclear cells	human	primary cell culture

^aATCC denotes American Type Culture Collection (U.S.) and BCRJ denotes Rio de Janeiro Cell Bank (Brazil). ^bABL denotes cells that were kindly donated by Annabelle Lewis from Brunel University London and were maintained in DMEM (Gibco®) supplemented with 10% FBS and 1% penicillin/streptomycin/amphotericin (Gibco®). ^cPrimary mouse bone marrow

cells from a Roas26-Cas9 Flt3-ITD mouse model transformed in vitro through retroviral transduction with an MLL-AF9 or MLL-AF4 oncogene and serial replating in colony-forming cell assays for leukaemia clone selection were obtained as previously described (Tzelepis et al., 2016). Thus, Cas9 Flt3-ITD MLL-AF9 or MLL-AF4 cells were maintained in XVIVO-15 supplemented with 1% penicillin/streptomycin/amphotericin (Gibco®), 10 ng/mL murine interleukin 3 (mIL-3), 10 ng/mL murine interleukin 6 (mIL-6), and 20 ng/mL murine stem cell factor (mSCF). ^dPrimary cell culture of PBMCs was obtained from peripheral blood from healthy donors by a standard Ficoll density protocol. Then, PBMCs were resuspended in RPMI 1640 or DMEM-F12 medium with 20% FBS and 1% antibiotic. Cells were plated at 5×10^5 cells/well. Concanavalin A (10 μ g/mL, Sigma–Aldrich) was used as a mitogen to trigger cell division in T lymphocytes and was added at the beginning of the culture. The Research Ethics Committee of the Oswaldo Cruz Foundation (Salvador, Bahia, Brazil) approved the protocol (CAAE 16220713.2.0000.0040). ^eMV-4-11, MOLM-13 and OCI-AML3 were either donated by the Huntly Lab or obtained from Sanger Institute. They were verified on the basis of cell surface markers against the DSMZ database.

Table S2. Antibodies used.

Antibody	Fluorochrom e	Reactivity	Clone	Catalogue number	Manufacturer	Dilution
Active caspase-3	FITC	Human/Mouse	C92-605	559341	BD Pharmingen™	1:20
Cleaved PARP (Asp214)	PE	Human	F21-852	552933	BD Pharmingen™	1:10
NFκB (pS529)	p65 AF488	Human	K1089512 50	558421	BD Phosflow™	1:20
NFκB (pS536)	p65 FITC	Human	NFκBp65 S536-B7	MA5-37157	Thermo Scientific	1:20
NFκB p65	PE	Human	14G10A2 1	653004	BioLegend	1:20
CD13	PE-CF594	Human	WM15	562491	BD Horizon™	1:400
CD33	BV510	Human	WM53	563257	BD Horizon™	1:400
CD123	BV605	Human	7G3	564197	BD Horizon™	1:100
CD34	PE	Human	8G12	348057	BD™	1:10
CD38	BV421	Human	HIT2	562444	BD Horizon™	1:400

IgG1, κ Isotype Control	PE	-	MOPC-21	556650	BD Pharmingen™	1:100
CD45 (hCD45)	PE	Human	2D1	368509	BioLegend	1:1000
CD45 (mCD45)	FITC	Mouse	30-F11	103107	BioLegend	1:1000

Table S3. Cytotoxicity of PL

Cells	IC ₅₀ and 95% CI (μ M)	
	PL	DOX
<i>Cancer cells</i>		
Cas9 Flt3-ITD MLL-AF4	0.96 0.60 - 1.54	N.D.
MV-4-11	2.05 1.76 - 2.40	N.D.
Cas9 Flt3-ITD MLL-AF9	2.55 2.15 - 3.02	N.D.
MOLM-13	2.58 2.32 - 2.87	N.D.
KG-1a	2.83 0.5 - 14.7	0.17 0.13 - 0.22
OCI-AML-3	3.21 2.66 - 3.89	N.D.
HL-60	8.25 2.42 - 28.1	0.34 0.23 - 0.48
NB4	23.66	0.46

	11.86 – 47.21	0.14 – 1.58
THP-1	23.87	0.25
	7.88 – 72.28	0.016 – 0.44
K-562	41.29	1.53
	27.91 – 61.09	0.85 – 2.77
Jurkat	41.83	0.01
	26.66 – 65.61	0.007 – 0.54
Caco-2	2.57	N.D.
	1.36 - 4.88	
LS 180	2.23	N.D.
	1.03 – 4.81	
HSC-3	4.69	0.53
	3.32 – 6.61	0.39 – 0.73
A-375	6.8	0.16
	4.50 – 10.30	0.08 - 0.30
SCC-4	8.90	2.1
	5.74 – 13.8	1.7 – 2.6
CAL27	10.88	0.34
	7.31 – 16.20	1.65 – 0.69
HepG2	11.96	0.32
	6.20 – 23.09	0.18 -0.55
OVCAR-3	12.95	0.03
	5.35 – 31.32	0.01 - 0.08
B16-F10	14.50	0.15
	10.22 – 20.53	0.07 – 0.18
PANC-1	19.44	0.12

	6.57 – 57.53	0.05 – 0.26
HCT116	19.61	0.09
	11.59 – 33.16	0.05 – 0.16
U87-MG	20.82	0.17
	11.5 – 37.8	0.01 – 1.64
DU 145	24.34	0.24
	14.20 – 41.80	0.07 – 0.85
A549	27.34	1.17
	19.53 – 38.25	0.74 – 1.83
4T1	33.11	1.62
	23.18 – 47.34	1.10 – 2.35
MCF-7	38.99	1.51
	26.12 – 58.20	0.96 – 2.38
SCC-9	42.04	1.01
	15.39 – 114.9	0.60 – 1.73
<i>Noncancerous cells</i>		
BJ	20.34	3.60
	11.95 – 34.62	1.15 – 11.22
PBMC	21.91	1.21
	12.01 – 39.98	0.73 – 1.99
MRC-5	34.19	1.65
	21.48 – 54.42	1.03 – 2.61

These data were calculated by nonlinear regression from three independent experiments carried out in duplicate. Doxorubicin (DOX) was used as a positive control. N.D. = not determined.

Table S4. Effect of PL on body and relative organ weights from NSG mice with KG-1a cell xenografts.

Parameters	CTL	PL
Dose (mg/kg)	-	20 mg/kg
Initial body weight (g)	22 ± 0.51	24.8 ± 1.32
Final body weight (g)	20.7 ± 1.00	24.13 ± 0.67
Liver (g/100 g body weight)	5.34 ± 0.51	5.60 ± 0.30
Kidney (g/100 g body weight)	1.25 ± 0.16	1.47 ± 0.10
Heart (g/100 g body weight)	0.47 ± 0.04	0.52 ± 0.01
Lung (g/100 g body weight)	0.74 ± 0.03	0.66 ± 0.01
Spleen (g/100 g body weight)	0.28 ± 0.02	0.15 ± 0.02

After engraftment confirmation, mice were randomly divided into two groups (n=6/per group): negative control (5% DMSO) and the group treated with PL at 20 mg/kg. The treatment was injected into mice intraperitoneally every day for 2 weeks. Data are presented as the mean ± S.E.M. of 5-6 animals. * $p < 0.05$ compared to CTL (negative control) by Student's *t* test.

Table S5. The effect of PL on gene expression in KG-1a cells.

Function/Assay ID	Gene Symbol	Gene Name	RQ	
			CTL	PL
NFkB pathway				
Hs00765730_m1	NFKB1	nuclear factor kappa B subunit 1	1.00	0.34
Hs00174517_m1	NFKB2	nuclear factor kappa B subunit 2	1.00	1.17
Hs00153283_m1	NFKBIA	NFkB inhibitor alpha	1.00	2.60
Hs00182115_m1	NFKBIB	NFkB inhibitor beta	1.00	2.19
Hs00153294_m1	RELA	RELA proto-oncogene, NF-kB subunit	1.00	2.64
Hs00232399_m1	RELB	RELB proto-oncogene, NF-kB subunit	1.00	3.86
WNT/β-catenin pathway				
Hs00181051_m1	APC	APC, WNT signaling pathway regulator	1.00	2.67
Hs00793391_m1	CSNK1A1	casein kinase 1 alpha 1	1.00	4.60
Hs00170025_m1	CTNNB1	catenin beta 1	1.00	2.88
Hs00275656_m1	GSK3B	glycogen synthase kinase 3 beta	1.00	4.08
Hs00228741_m1	WNT10A	Wnt family member 10A	n.d.	n.d.
Hs00559664_m1	WNT10B	Wnt family member 10B	1.00	n.d.
Hs00257131_m1	WNT2B	Wnt family member 2B	n.d.	n.d.
Hs00362452_m1	WNT6	Wnt family member 6	n.d.	n.d.
Hedgehog pathway				
Hs00368306_m1	DHH	desert hedgehog	n.d.	n.d.

Hs00171790_m1	GLI1	GLI family zinc finger 1	1.00	1.30
Hs00257977_m1	GLI2	GLI family zinc finger 2	n.d.	n.d.
Hs00181117_m1	PTCH1	patched 1	1.00	0.46
Hs00179843_m1	SHH	sonic hedgehog	n.d.	n.d.
Hs00170665_m1	SMO	smoothened, frizzled class receptor	n.d.	n.d.
Hs00171981_m1	SUFU	SUFU negative regulator of hedgehog signaling	1.00	2.66
NOTCH pathway				
Hs00194509_m1	DLL1	delta like canonical Notch ligand 1	1.00	9.59
Hs01085096_m1	DLL3	delta like canonical Notch ligand 3	1.00	21.01
Hs00164982_m1	JAG1	jagged 1	1.00	1.55
Hs00171432_m1	JAG2	jagged 2	1.00	5.14
Hs01062014_m1	NOTCH1	notch 1	1.00	0.45
Hs01050702_m1	NOTCH2	notch 2	1.00	0.99
EGFR pathway				
Hs01099999_m1	EGF	epidermal growth factor	1.00	30.45
Hs01076078_m1	EGFR	epidermal growth factor receptor	n.d.	n.d.
Hs00364282_m1	KRAS	KRAS proto-oncogene, GTPase	1.00	2.00
Hs01046830_m1	MAPK1	mitogen-activated protein kinase 1	1.00	2.66
Hs00234119_m1	RAF1	Raf-1 proto-oncogene, serine/threonine kinase	1.00	1.77
Hs00269660_s1	RHOB	ras homolog family member B	n.d.	n.d.
JAK/STAT pathway				
Hs01026983_m1	JAK1	Janus kinase 1	1.00	2.16

Hs01078136_m1	JAK2	Janus kinase 2	1.00	2.12
Hs00169663_m1	JAK3	Janus kinase 3	n.d.	n.d.
Hs01013989_m1	STAT1	signal transducer and activator of transcription 1	1.00	1.33
Hs00374280_m1	STAT3	signal transducer and activator of transcription 3	1.00	4.28
Hs00273500_m1	STAT5B	signal transducer and activator of transcription 5B	1.00	0.47
Hs00598625_m1	STAT6	signal transducer and activator of transcription 6	1.00	0.39
PI3K/AKT/MTOR pathway				
Hs00178289_m1	AKT1	AKT serine/threonine kinase 1	1.00	0.57
Hs01086102_m1	AKT2	AKT serine/threonine kinase 2	1.00	0.94
Hs00234508_m1	MTOR	mechanistic target of rapamycin	1.00	1.52
Hs00904054_m1	PIK3C2A	phosphatidylinositol-4-phosphate 3-kinase catalytic subunit type 2 alpha	1.00	5.88
Hs00176908_m1	PIK3C3	phosphatidylinositol 3-kinase catalytic subunit type 3	1.00	3.46
Hs00907957_m1	PIK3CA	phosphatidylinositol-4,5-bisphosphate 3-kinase catalytic subunit alpha	1.00	3.54
Hs02621230_s1	PTEN	phosphatase and tensin homolog	1.00	0.51

TGF-beta/SMAD pathway

Hs01054576_m1	FOXO1	forkhead box O1	1.00	4.51
Hs00183425_m1	SMAD2	SMAD family member 2	1.00	3.31
Hs00929647_m1	SMAD4	SMAD family member 4	1.00	2.81
Hs00178696_m1	SMAD7	SMAD family member 7	1.00	0.54
Hs00998133_m1	TGFB1	transforming growth factor beta 1	1.00	0.75
Hs00234244_m1	TGFB2	transforming growth factor beta 2	1.00	7.89
Hs01086000_m1	TGFB3	transforming growth factor beta 3	1.00	3.97

PPAR pathway

Hs00947536_m1	PPARA	peroxisome proliferator activated receptor alpha	1.00	1.74
Hs04187066_g1	PPARD	peroxisome proliferator activated receptor delta	1.00	2.50
Hs01115513_m1	PPARG	peroxisome proliferator activated receptor gamma	1.00	2.39
Hs01016719_m1	PPARGC1A	PPARG coactivator 1 alpha	n.d.	n.d.
Hs00991677_m1	PPARGC1B	PPARG coactivator 1 beta	1.00	0.19

Oxidative stress

Hs00943350_g1	GSTP1	glutathione S-transferase pi 1	1.00	0.97
Hs00178247_m1	OXS1	oxidative stress responsive 1	1.00	1.91
Hs00167309_m1	SOD2	superoxide dismutase 2, mitochondrial	1.00	2.98

Hs01555214_g1	TXN	thioredoxin	1.00	2.47
Hs00917067_m1	TXNRD1	thioredoxin reductase 1	1.00	21.94
Apoptosis				
Hs00559441_m1	APAF1	apoptotic peptidase activating factor 1	1.00	2.55
Hs00188930_m1	BAD	BCL2 associated agonist of cell death	1.00	0.97
Hs00180269_m1	BAX	BCL2 associated X, apoptosis regulator	1.00	0.70
Hs99999018_m1	BCL2	BCL2, apoptosis regulator	1.00	0.11
Hs00609632_m1	BID	BH3 interacting domain death agonist	1.00	0.77
Hs00234387_m1	CASP3	caspase 3	1.00	7.36
Hs00169152_m1	CASP7	caspase 7	1.00	1.04
Hs00219876_m1	DIABLO	diablo IAP-binding mitochondrial protein	1.00	2.66
Hs00538709_m1	FADD	Fas associated via death domain	1.00	1.71
Hs00531110_m1	FAS	Fas cell surface death receptor	1.00	1.13
Hs00242302_m1	PARP1	poly(ADP-ribose) polymerase 1	1.00	0.41
Autophagy				
Hs01047860_g1	ATG12	autophagy related 12	1.00	3.20
Hs00223937_m1	ATG3	autophagy related 3	1.00	0.90
Hs00169468_m1	ATG5	autophagy related 5	1.00	3.94

Hs00186838_m1	BECN1	beclin 1	1.00	1.18
Hs01076567_g1	MAP1LC3A	microtubule associated protein 1 light chain 3 alpha	1.00	1.93
Hs00797944_s1	MAP1LC3B	microtubule associated protein 1 light chain 3 beta	1.00	44.71
Necroptosis				
Hs00169407_m1	RIPK1	receptor interacting serine/threonine kinase 1	1.00	4.82
Hs01572686_m1	RIPK2	receptor interacting serine/threonine kinase 2	1.00	0.69
Hs01011177_g1	RIPK3	receptor interacting serine/threonine kinase 3	1.00	0.38
Epithelial-mesenchymal transition				
Hs00170423_m1	CDH1	cadherin 1	n.d.	n.d.
Hs00195591_m1	SNAI1	snail family transcriptional repressor 1	1.00	12.69
Hs00950344_m1	SNAI2	snail family transcriptional repressor 2	n.d.	n.d.
Hs01018996_m1	SNAI3	snail family transcriptional repressor 3	1.00	0.11
Hs00361186_m1	TWIST1	twist family bHLH transcription factor 1	1.00	0.10
Hs00185584_m1	VIM	vimentin	1.00	1.95

Hs00232783_m1	ZEB1	zinc finger E-box binding homeobox	1.00	5.02
---------------	------	------------------------------------	------	------

1

Hs00207691_m1	ZEB2	zinc finger E-box binding homeobox	1.00	2.50
---------------	------	------------------------------------	------	------

2

KG-1a cells were treated with 20 μ M PL for 12 h. The negative control (CTL) was treated with the vehicle (0.2% DMSO) used for diluting the compound tested. After treatment, total RNA was isolated and reverse transcribed. Gene expression was detected using TaqMan® array plate 96 plus fast (#4413256). The GUSB, HPRT1 and GAPDH genes were used as endogenous genes for normalisation. Values represent the relative quantitation (RQ) compared with the calibrator (cells treated with the negative control). The genes were considered to be upregulated if $RQ \geq 2$ and downregulated if $RQ \leq 0.5$. N.d. Not determine.

5 DISCUSSÃO

O tratamento eficaz da LMA é muito desafiador. Devido à imensa heterogeneidade desta doença, tratá-la usando uma abordagem única é ineficaz e beneficia apenas um subconjunto de pacientes. A taxa de sobrevida de 5 anos após o diagnóstico para pessoas com 20 anos ou mais com LMA é de 27%, e nenhuma melhoria notável na sobrevida global de indivíduos com mais de 65 anos de idade foi observada desde 1968 (AMERICAN CANCER SOCIETY, 2022). Uma razão para a falta de sucesso da terapia antileucêmica nas últimas décadas é devido ao esquema de indução padrão “7 + 3” praticamente inalterado. O sucesso limitado deste tratamento, especialmente na população idosa, pode ser atribuído não somente ao fato de que essas drogas são altamente tóxicas, mas também à heterogeneidade da doença, onde existe uma variabilidade considerável entre e dentro de cada paciente (NAIR et al., 2021; DE LEEUW et al., 2022).

Deste modo, faz-se necessário desenvolver novas estratégias terapêuticas anti-LMA, possibilitando selecionar a terapia mais adequada para cada paciente. O presente estudo investiga o efeito antileucêmico de três moléculas à base de plantas, que exercem seus efeitos através da indução do estresse oxidativo, atuando na inibição de vias de sinalização que servem como condutores da leucemogênese, levando à indução de morte celular apoptótica.

Inicialmente investigamos o efeito de TG e 22-HTG num painel de linhagens celulares cancerosas de diferentes tipos histológicos e identificamos uma potente atividade citotóxica para ambos compostos. Dentre as linhagens estudadas nesse trabalho, podemos destacar, câncer de cólon, mama, fígado, língua, da pele e hematológicos, salientando um efeito potente sobre as linhagens leucêmicas, como a HL-60, que foi foco deste estudo. Em concordância com nossos resultados, outros autores também demonstraram o efeito citotóxico desses compostos em células de carcinoma hepatocelular humano e de rato, melanoma humano, adenocarcinoma cervical, carcinoma esofágico, adenocarcinoma de mama, leucemia linfocítica murina, mieloma humano e em células-tronco de câncer de mama (SHIROTA et al., 1994; SETZERL et al., 1998; MORITA et al., 2008; YELANI et al., 2010; CEVATEMRE et al., 2016; ARANHA et al., 2020).

Após identificarmos a atividade citotóxica desses triterpenos, decidimos investigar *in vitro* o mecanismo de ação por trás da morte celular induzida por estes compostos em células HL-60. Através da citometria de fluxo, avaliamos o ciclo celular, a indução de morte celular

apoptótica usando Anexina V/IP e o efeito destes compostos em um ensaio de reversão com um inibidor de pan-caspase, Z-VAD(OMe)-FMK. Ambos compostos aumentaram significativamente a população de células na fração sub-G0/G1, indicando fragmentação do DNA. TG e 22-HTG induziram também a externalização de fosfatidilserina e, quando as células foram tratadas previamente com um inibidor de pan-caspase, o efeito (apoptose) foi revertido após 48 h de incubação com os triterpenos. A desregulação da apoptose facilita o desenvolvimento e a progressão da LMA, permitindo a sobrevivência contínua de células com oncogenes ativados. Além disso, vários componentes da via apoptótica em células leucêmicas já foram destacados como potenciais alvos terapêuticos (KRAWIEC et al., 2022).

Nossos achados demonstram que TG e 22-HTG foram capazes de induzir apoptose nas células leucêmicas. Aranha e colaboradores (2021) também demonstraram que a 22-HTG induziu alterações morfológicas condizentes com morte celular apoptótica, como encolhimento celular, condensação da cromatina, fragmentação nuclear, além de induzir um aumento na exposição de fosfatidilserina em células de melanoma humano (ARANHA et al., 2021). Em um outro estudo, a 22-HTG demonstrou citotoxicidade em células de adenocarcinoma de mama humano através da indução de apoptose (CEVATEMRE et al., 2016). Adicionalmente, também investigamos o papel do gene BAD na morte induzida por TG e 22-HTG utilizando as linhagens celulares BAD KO SV40 MEF e WT SV40 MEF e nossos resultados indicam que o gene BAD não é necessário para a indução de morte celular apoptótica.

A fim de elucidar os mecanismos envolvidos na indução do apoptose por estes compostos, realizamos ensaios funcionais para avaliação do potencial transmembrânico mitocondrial, qPCR para investigação da expressão gênica e utilização do antioxidante NAC para avaliar o efeito dos compostos sobre o estresse oxidativo. A mitocôndria é uma organela celular que desempenha um papel importante na ativação apoptose (WANG E YOULE, 2009) e os resultados obtidos a partir da análise do potencial de membrana mitocondrial demonstram que os triterpenos estudados, alteraram a integridade da mitocôndria, sugerindo indução de apoptose através da via intrínseca. Resultados similares para 22-HTG também foram observados em células-tronco de câncer de mama e melanoma humano (CEVATEMRE et al., 2016; ARANHA et al., 2021).

A indução do estresse oxidativo é considerada um alvo interessante na terapia anticâncer, podendo ser induzido pelo aumento de ERO e/ou inibição do sistema antioxidante protetor. Além disso, as espécies reativas de oxigênio desempenham papéis críticos na

patogênese do câncer e nos mecanismos subjacentes de várias modalidades terapêuticas, como a quimioterapia (VAN LOENHOUT et al., 2020; KHAN et al., 2021). Com a análise da expressão gênica através de qPCR observamos uma regulação negativa da tioredoxina, como também na expressão do gene da tioredoxina redutase 1, particularmente pós-tratamento com 22-HTG. De maneira similar, a expressão gênica da glutathione S-transferase pi 1 também foi afetada por TG. Ao pré-tratar as células com o antioxidante NAC, demonstramos que este pré-tratamento reverteu quase completamente a morte induzida pelos triterpenos, indicando que a apoptose é mediada pelo estresse oxidativo. No entanto, a apoptose induzida por 22-HTG não foi associada a produção de ERO em células de melanoma humano (ARANHA et al., 2021).

A via de sinalização das MAPKs desempenha um papel importante na regulação da expressão gênica, crescimento celular e sobrevivência. A sinalização anormal de MAPK pode resultar em proliferação celular aumentada ou descontrolada e resistência à apoptose (LEE et al., 2020). Finalmente, ensaios funcionais utilizando inibidores dos principais componentes da via em questão, demonstrou que TG e 22-HTG exercem seus efeitos através das vias JNK/p38 em células HL-60. Interessantemente, a 22-HTG induziu apoptose e foi capaz de inibir a expressão gênica de BRAF, NRAS e KRAS. As proteínas codificadas por esses genes têm um papel importante na via de sinalização MAPK (ARANHA et al., 2021).

Nos apresentamos aqui pela primeira vez, a capacidade de TG e 22-HTG de inibir o sistema antioxidante celular, incluindo a regulação negativa da tioredoxina, como alvo de sua citotoxicidade.

Em seguida, direcionamos nossos esforços para investigar o efeito antileucêmico da PL. Como mencionado anteriormente, a PL tem sido alvo de diversos estudos, com foco em sua atividade anticâncer, devido a relatos relacionados aos seus alvos moleculares, a atividade farmacológica caracterizada por uma boa seletividade, indicativos de um bom perfil de segurança e até mesmo relatos evidenciando sua boa disponibilidade (PISKA et al., 2018; PARAMA et al., 2021).

Com base nisso, inicialmente realizamos uma triagem com PL em diferentes tipos de câncer a fim de investigar o potencial citotóxico desta molécula e identificar se um possível efeito mais direcionado poderia ser observado para as células leucêmicas. Ao realizar ensaios em diferentes linhagens celulares de LMA, pudemos elucidar o efeito desta molécula em relação a variação genética e molecular da doença. Os modelos utilizados para essa avaliação incluem, KG-1a (FGFR1OP2-FGFR1), MOLM-13 (MLL-AF9 e FLT3-ITD), MV4-11 (MLL-

AF4 e FLT3-ITD), OCI-AML3 (mutante NPM1c e DNMT3A), HL-60 e NB4 (PML-RAR α), THP-1 (MLL-AF9), K-562 (BCR:ABL) e Jurkat (linfócitos T imortalizados). Utilizamos também modelos equivalentes ao humano (MOLM-13 e MV4-11), utilizando cultura primária de camundongo com rearranjo de MLL e FLT3-ITD (Cas9 Flt3-ITD MLL-AF4 e Cas9 Flt3-ITD MLL-AF9). Observamos uma pequena variação nos valores de CI₅₀ nas células leucêmicas, com maior sensibilidade nos modelos celulares com rearranjo em KMT2a.

Após a determinação da CI₅₀, elegemos a linhagem celular KG-1a para dar continuidade aos estudos, uma vez que estava entre uma das linhagens que se apresentou mais sensível ao tratamento e como um modelo celular relevante para investigar o efeito de PL em células-tronco e progenitoras hematopoiéticas, devido ao seu fenótipo CD34⁺ (O'REILLY et al., 2021). Realizamos o primeiro ensaio utilizando KG-1a a fim detectar a viabilidade celular pós-tratamento com PL e os resultados se mostraram em concordância com resultados prévios de citotoxicidade. Dando seguimento a investigação do efeito antileucêmico de PL, performamos estudos para identificar os mecanismos subjacentes a citotoxicidade induzida pelo composto. Primeiramente, realizamos uma sequência de experimentos para avaliar o tipo de morte celular envolvida na ação de PL. Através da citometria de fluxo, investigamos a morte celular apoptótica utilizando YO-PRO-1/IP e anticorpos para detectar caspase-3 ativada e PARP1 clivada, proteínas importantes na indução de morte celular por apoptose, uma vez que durante a apoptose dependente de caspase, a PARP1 é clivada pela caspase-3 (MASHIMO et al., 2021). Diversos estudos evidenciam a indução de morte celular apoptótica por PL e associam esse resultado a diversos mecanismos moleculares e bioquímicos, como ativação de caspases, vias de sinalização como PI3K/Akt/mTOR, NF- κ B, JAK/STAT3 e ERK e indução do estresse oxidativo (KONG et al., 2008; LI et al., 2015; YAO et al., 2016; ZHANG et al., 2019).

Assim como TG e 22-HTG, a PL induz apoptose das células leucêmicas através da indução do estresse oxidativo. Descobertas recentes também destacam a importância terapêutica de ERO para melhores resultados clínicos em pacientes com câncer, pois induzem apoptose e autofagia. Adicionalmente, ERO desempenham um papel crítico nas ações anticâncer de produtos naturais (KHAN et al., 2021). Através de citometria de fluxo, nossos achados demonstram que o pre-tratamento com NAC (antioxidante) foi capaz de reverter completamente a apoptose induzida por PL. Ao utilizar o MitoSOX Red, uma sonda capaz de detectar ERO mitocondrial, observamos um aumento na intensidade de fluorescência após o tratamento com PL. Resultados similares foram encontrados por outros grupos de pesquisa.

Chen et al (2015) atribuiu o efeito citotóxico e a inibição da invasão por PL em carcinoma hepatocelular a ativação do eixo ERO-ER-MAPKs-CHOP (CHEN et al., 2015). Outros relatos evidenciam o envolvimento das espécies reativas de oxigênio na morte induzida por PL (RAWAT et al., 2020; XIONG et al., 2015), bem como também a inibição da tioredoxina redutase 1 (TrxR1), uma importante enzima antioxidante, e indução do apoptose mediado por ERO em células do de carcinoma hepatocelular humano (ZHANG et al., 2019).

PL também foi testado quanto à sua capacidade de afetar o potencial de membrana mitocôndrial e os resultados indicam que o tratamento foi capaz de reduzir o potencial de membrana das mitocôndrias, sugerindo ativação da via intrínseca, o que pode ser atribuído pelo aumento dos níveis de ERO. Similarmente, outros estudos também constataram que a via mitocondrial estava envolvida na apoptose induzida por PL (BEZERRA et al., 2007, 2008).

Em resposta a vários eventos celulares, o aumento de ROS nas células cancerosas, leva à ativação mediada pelo estresse oxidativo de vários fatores de transcrição sensíveis ao estado redox como, por exemplo, NF- κ B (KHAN et al., 2021). PL têm demonstrado capacidade em modular a expressão de genes associados à sobrevivência, invasão e decisão de destino celular, como heme oxigenase 1 (HMOX1), membro 1A da família de proteínas de choque térmico (HSPA1A), caspase-3 (CASP3), inibidor de quinase dependente de ciclina 1A (CDKN1A), MYC, fosfatidilinositol-4,5-bifosfato 3-quinase subunidade catalítica gama (PIK3CG), linfoma de células B 2 (Bcl-2), NF- κ B subunidade 1 (NF- κ B1), AKT3, matriz metaloproteinase-9 (MMP-9) e Twist (PARAMA et al., 2021).

Tendo em vista a modulação da expressão gênica por PL, nós realizamos um qPCR array no intuito de mapear os mecanismos moleculares envolvidos no efeito do composto. PL modulou negativamente a expressão NFKB1 e Bcl-2. A ativação da via NF- κ B geralmente atua como um promotor do câncer, estando ativado em grande parte dos casos de LMA, e está associado a regulação de Bcl-2 (LI et al., 2020).

Os resultados de citometria de fluxo reforçam os achados do qPCR, onde observamos que PL diminuiu a expressão de p-NF- κ B p65 (S536). Outros autores também demonstraram que a inibição mediada por PL da atividade de NF- κ B diminui as características de crescimento agressivo de células de câncer de próstata *in vitro* (GINZBURG et al., 2014). Como citado anteriormente, as células de LMA com rearranjo em KMT2A apresentaram valores de CI₅₀ mais baixos quando comparado com as outras linhagens leucêmicas, isso possivelmente se deve ao fato de NF- κ B ser um dos alvos de PL, uma vez que as leucemias que exibem esse rearranjo

são dependentes de NF- κ B (KUO et al., 2013). Coletivamente, esses achados indicam que o PL possivelmente induz a apoptose por uma via dependente de caspase, através da regulação negativa de NF κ B1 e consequentemente da regulação negativa de Bcl-2. Curiosamente, proteínas da família Bcl-2 são conhecidas como os principais reguladores do apoptose celular mediado pela mitocôndria, o que reforça o envolvimento da mitocôndria na morte celular induzida por PL.

Como as CTPLs são a causa da recaída da leucemia e da resistência aos medicamentos, a eliminação efetiva dessa subpopulação de células é um aspecto muito importante do tratamento antileucêmico bem-sucedido. Desse modo, decidimos então investigar os marcadores de superfície presentes nas células-tronco e progenitoras leucêmicas, como CD34, CD38 e CD123. Observamos uma redução de células positivas para esses marcadores, indicando um efeito direcionado de PL nas CTPLs, possivelmente devido ao fato da regulação negativa de NF- κ B pelo composto. A partir do ensaio de formação de colônia também foi possível detectar uma diminuição na iniciação do tumor, uma vez que houve uma redução na formação de colônias quando as células foram tratadas com PL, como também na proliferação celular, já que as colônias também se apresentavam em tamanho menores. Por outro lado, esse efeito não foi observado em células de cultura primária da medula óssea de camundongos, indicando seletividade do composto. Pei e colaboradores (2013) também evidenciaram que PL é capaz de induzir a depleção de glutathione em células-tronco de amostras primárias de LMA humana, resultando em apoptose das células leucêmicas, ao passo que exibe menor toxicidade às células-tronco hematopoéticas normais (PEI et al., 2013).

PL também suprimiu o crescimento de células de LMA em um modelo de leucemia de xenoinxerto e sua atividade antileucemia *in vivo* sem qualquer sinal de toxicidade em camundongos suporta os relatos anteriores que destacam seu efeito antitumoral em diferentes tipos de câncer e a segurança associada ao seu uso (BEZERRA, 2021).

A terapia combinada baseia-se nos efeitos positivos das interações farmacodinâmicas (sinérgicas ou aditivas) entre dois ou mais medicamentos, com interações sinérgicas resultando em tratamentos mais eficazes. Na terapia de combinação, ambos os compostos são administrados em doses mais baixas e interagem com múltiplas vias moleculares; portanto, tratamentos combinados baseados em compostos que exibem um efeito sinérgico ou aditivo geralmente têm menos toxicidade do que a monoterapia (MOKHTARI et al., 2017). Esses esquemas terapêuticos têm mostrado várias vantagens sobre a monoterapia, incluindo a

diminuição da concentração e toxicidade do fármaco, aumento da eficácia, direcionamento de várias vias moleculares e sensibilização das células ao tratamento. E diversos estudos tem mostrado um potencial promissor de PL em combinação com quimioterápicos utilizados atualmente na clínica, como placitaxel, cisplastina e oxaliplatina (GONG et al., 2014; CHEN et al., 2019; YAO et al., 2016; RAWAT et al., 2020).

A combinação de PL e oxaliplatina teve um efeito sinérgico na indução de estresse oxidativo em células de câncer colorretal, conforme demonstrado por Chen et al. (2019). Além disso, Gong e colaboradores (2014) obtiveram um efeito anticrescimento sinérgico em células de câncer de ovário humano ao utilizar baixas doses de cisplatina ou paclitaxel em conjunto com PL. No presente estudo, testamos PL em combinação com fármacos da terapia padrão anti-LMA, como citarabina, daunorrubicina e azacitidina. O tratamento combinado de PL com Ara-C ou daunorrubicina demonstrou efeito sinérgico nas linhas celulares de LMA MOLM-13 e OCI-AML3. A combinação PL + azacitidina mostrou-se aditiva apenas na linhagem celular OCI-AML3. Este regime terapêutico combinado pode oferecer uma oportunidade para reduzir a dosagem efetiva desses medicamentos e diminuir sua toxicidade indesejada. Isso é especialmente importante para adultos mais velhos com LMA, que representam uma população vulnerável ao tratamento intensivo padrão.

6 CONCLUSÃO

O presente trabalho fornece uma compreensão do mecanismo de citotoxicidade induzido por TG, 22-HTG e PL em células de leucemia mieloide aguda. Demonstramos que TG e 22-HTG exercem efeito antileucêmico por meio da indução de estresse oxidativo, inibindo a enzima tioredoxina e levando ao dano do DNA e apoptose via MAPK JNK/p38. Além disso, a PL inibe a proliferação celular e induz apoptose por meio de estresse oxidativo, suprimindo a sinalização de NF- κ B, reduz a subpopulação de células tronco/progenitoras CD34⁺ em células KG-1a e inibe o desenvolvimento de LMA em modelos de xenotransplante em camundongos. A combinação de PL com quimioterápicos utilizados na terapia convencional de LMA apresentou efeito sinérgico, especificamente com citarabina, indicando que PL pode ser desenvolvido como um medicamento anti-LMA capaz de direcionar células propagadoras de leucemia e potencializar a atividade da quimioterapia convencional. Em resumo, evidenciamos que TG, 22-HTG e PL apresentam um promissor efeito antileucêmico e potencial terapêutico para o tratamento da LMA.

REFERÊNCIAS

- ALI ABDALLA, Y. O. et al. Natural Products for Cancer Therapy: A Review of Their Mechanism of Actions and Toxicity in the Past Decade. **Journal of Tropical Medicine**, v. 2022, 2022.
- AMERICAN CANCER SOCIETY. Cancer Facts & Figures 2023. Atlanta, Ga: **American Cancer Society**; 2023.
- ARANHA, E. S. P. et al. 22 β -hydroxytingenone reduces proliferation and invasion of human melanoma cells. **Toxicology in Vitro**, v. 66, p. 104879, 2020.
- ARANHA, E. S. P. et al. 22 β -hydroxytingenone induces apoptosis and suppresses invasiveness of melanoma cells by inhibiting MMP-9 activity and MAPK signaling. **Journal of Ethnopharmacology**, v. 267, p. 113605, 2021.
- ARBER, D. A. et al. International Consensus Classification of Myeloid Neoplasms and Acute Leukemias: integrating morphologic, clinical, and genomic data. **Blood**, v. 140, n. 11, p. 1200-1228, 2022.
- ATANASOV, A. G. et al. Natural products in drug discovery: advances and opportunities. **Nature Reviews Drug Discovery**, v. 20, n. 3, p. 200-216, 2021.
- ATASHZAR, M. R. et al. Cancer stem cells: A review from origin to therapeutic implications. **Journal of Cellular Physiology**, v. 235, n. 2, p. 790-803, 2020.
- BAI, Dong; UENO, Lynn; VOGT, Peter K. Akt-mediated regulation of NF κ B and the essentialness of NF κ B for the oncogenicity of PI3K and Akt. **International journal of cancer**, v. 125, n. 12, p. 2863-2870, 2009.
- BALIZA, I. R. S. et al. Ruthenium Complexes With Piplartine Cause Apoptosis Through MAPK Signaling by a p53-Dependent Pathway in Human Colon Carcinoma Cells and Inhibit Tumor Development in a Xenograft Model. **Frontiers in Oncology**, v. 9, p. 582, 2019.
- BAVOVADA, Rapepol et al. Spectral assignment and cytotoxicity of 22-hydroxytingenone from *Glyptopetalum sclerocarpum*. **Planta medica**, v. 56, n. 04, p. 380-382, 1990.
- BERNASCONI, P.; BORSANI, O. Eradication of measurable residual disease in aml: A challenging clinical goal. **Cancers**, v. 13, n. 13, p. 3170, 2021.
- BEWERSDORF, J. P.; ABDEL-WAHAB, O. Translating recent advances in the pathogenesis of acute myeloid leukemia to the clinic. **Genes & Development**, v. 36, n. 5-6, p. 259-277, 2022.
- BEZERRA, D. P. et al. Piplartine induces inhibition of leukemia cell proliferation triggering both apoptosis and necrosis pathways. **Toxicology in vitro**, v. 21, n. 1, p. 1-8, 2007.

BEZERRA, D. P. et al. Overview of the therapeutic potential of piplartine (piperlongumine). **European Journal of Pharmaceutical Sciences**, v. 48, n. 3, p. 453-463, 2013.

BEZERRA, D. P. Piplartine (piperlongumine), oxidative stress, and use in cancer. In: **Cancer. Academic Press**, 2021. p. 417-425.

BONNET, Dominique; DICK, John E. Human acute myeloid leukemia is organized as a hierarchy that originates from a primitive hematopoietic cell. **Nature medicine**, v. 3, n. 7, p. 730-737, 1997.

BOURS, Vincent et al. Nuclear factor- κ B, cancer, and apoptosis. **Biochemical pharmacology**, v. 60, n. 8, p. 1085-1089, 2000.

BRAICU, Cornelia et al. A Comprehensive Review on MAPK: A Promising Therapeutic Target in Cancer. **Cancers**, v. 11, n. 10, p. 1618, 2019.

BRAUN, Thorsten et al. NF- κ B constitutes a potential therapeutic target in high-risk myelodysplastic syndrome. **Blood**, v. 107, n. 3, p. 1156-1165, 2006.

CEVATEMRE, B. et al. The plant-derived triterpenoid tingenin B is a potent anticancer agent due to its cytotoxic activity on cancer stem cells of breast cancer in vitro. **Chemico-Biological Interactions**, v. 260, p. 248-255, 2016.

CHEN, W. Q. et al. The synergistic effects of oxaliplatin and piperlongumine on colorectal cancer are mediated by oxidative stress. **Cell death & disease**, v. 10, n. 8, p. 600, 2019.

CHEN, Y. et al. Piperlongumine selectively kills hepatocellular carcinoma cells and preferentially inhibits their invasion via ROS-ER-MAPKs-CHOP. **Oncotarget**, v. 6, n. 8, p. 6406, 2015.

CHUNG, Stephen S. et al. CD99 is a therapeutic target on disease stem cells in myeloid malignancies. **Science translational medicine**, v. 9, n. 374, 2017.

CI, T. et al. Delivery strategies in treatments of leukemia. **Chem. Soc. Rev.**, v. 51, n. 6, p. 2121–2144, 2022.

COSTA, C. O. S. et al. Novel piplartine-containing ruthenium complexes: synthesis, cell growth inhibition, apoptosis induction and ROS production on HCT116 cells. **Oncotarget**, v. 8, n. 61, p. 104367, 2017.

DAVER, N. et al. New directions for emerging therapies in acute myeloid leukemia: the next chapter. **Blood cancer journal**, v. 10, n. 10, p. 107, 2020.

DE LEEUW, D. C.; OSSENKOPPELE, G. J.; JANSSEN, J. J. W. M. Older Patients with Acute Myeloid Leukemia Deserve Individualized Treatment. **Current oncology reports**, p. 1-14, 2022.

DOLCET, Xavier et al. NF- κ B in development and progression of human cancer. **Virchows archiv**, v. 446, n. 5, p. 475-482, 2005.

EPPERT, Kolja et al. Stem cell gene expression programs influence clinical outcome in human leukemia. **Nature medicine**, v. 17, n. 9, p. 1086-1093, 2011.

GHOSH, Sourav et al. Essential role of tuberous sclerosis genes TSC1 and TSC2 in NF- κ B activation and cell survival. **Cancer cell**, v. 10, n. 3, p. 215-226, 2006.

GILL, Balraj Singh; KUMAR, Sanjeev. Differential algorithms-assisted molecular modeling-based identification of mechanistic binding of ganoderic acids. **Medicinal Chemistry Research**, v. 24, n. 9, p. 3483-3493, 2015.

GILL, Balraj Singh et al. Triterpenes in cancer: significance and their influence. **Molecular biology reports**, v. 43, n. 9, p. 881-896, 2016.

GINZBURG, S. et al. Piperlongumine inhibits NF- κ B activity and attenuates aggressive growth characteristics of prostate cancer cells. **Prostate**, v. 74, n. 2, p. 177–186, fev. 2014.

GONG, L. H. et al. Piperlongumine induces apoptosis and synergizes with cisplatin or paclitaxel in human ovarian cancer cells. **Oxidative Medicine and Cellular Longevity**, v. 2014, 2014.

GREEN, Steven D.; KONIG, Heiko. Treatment of acute myeloid leukemia in the Era of genomics—achievements and persisting challenges. **Frontiers in Genetics**, v. 11, 2020.

GROSJEAN-RAILLARD, J. et al. ATM mediates constitutive NF- κ B activation in high-risk myelodysplastic syndrome and acute myeloid leukemia. **Oncogene**, v. 28, n. 8, p. 1099-1109, 2009.

GUIMARÃES, Adriana G.; SERAFINI, Mairim R.; QUINTANS-JÚNIOR, Lucindo J. Terpenes and derivatives as a new perspective for pain treatment: a patent review. **Expert opinion on therapeutic patents**, v. 24, n. 3, p. 243-265, 2014.

GUO, Yan-Jun et al. ERK/MAPK signalling pathway and tumorigenesis. **Experimental and therapeutic medicine**, v. 19, n. 3, p. 1997-2007, 2020.

GUPTA, Subash C. et al. Inhibiting NF- κ B activation by small molecules as a therapeutic strategy. **Biochimica et Biophysica Acta (BBA)-Gene Regulatory Mechanisms**, v. 1799, n. 10-12, p. 775-787, 2010.

GUZMAN, Monica L. et al. Nuclear factor- κ B is constitutively activated in primitive human acute myelogenous leukemia cells. **Blood**, The Journal of the American Society of Hematology, v. 98, n. 8, p. 2301-2307, 2001.

GUZMAN, Monica L. et al. The sesquiterpene lactone parthenolide induces apoptosis of human acute myelogenous leukemia stem and progenitor cells. **Blood**, v. 105, n. 11, p. 4163-4169, 2005.

GUZMAN, Monica L. et al. An orally bioavailable parthenolide analog selectively eradicates acute myelogenous leukemia stem and progenitor cells. **Blood, The Journal of the American Society of Hematology**, v. 110, n. 13, p. 4427-4435, 2007.

GUZMAN, Monica L. et al. The sesquiterpene lactone parthenolide induces apoptosis of human acute myelogenous leukemia stem and progenitor cells. **Blood**, v. 105, n. 11, p. 4163-4169, 2005.

HANEKAMP, Diana et al. Leukaemic stem cell load at diagnosis predicts the development of relapse in young acute myeloid leukaemia patients. **British journal of haematology**, v. 183, n. 3, p. 512-516, 2018.

HANSEN, Q. et al. Characteristics of leukemic stem cells in acute leukemia and potential targeted therapies for their specific eradication. **Cancer Drug Resistance**, v. 5, n. 2, p. 344, 2022.

HAUBNER, S. et al. Coexpression profile of leukemic stem cell markers for combinatorial targeted therapy in AML. **Leukemia**, v. 33, n. 1, p. 64–74, 1 jan. 2019.

HERNANDES, Camila; MARIA SOARES PEREIRA, Ana; SEVERINO, Patricia. Compounds from Celastraceae targeting cancer pathways and their potential application in head and neck squamous cell carcinoma: a review. **Current genomics**, v. 18, n. 1, p. 60-74, 2017.

HERRMANN, H. et al. Delineation of target expression profiles in CD34+/CD38- and CD34+/CD38+ stem and progenitor cells in AML and CML. **Blood Advances**, v. 4, n. 20, p. 5118–5132, 21 out. 2020.

HOU, H. A.; TIEN, H. F. Genomic landscape in acute myeloid leukemia and its implications in risk classification and targeted therapies. **Journal of biomedical science**, v. 27, p. 1-13, 2020.

HWANG, S. M. Classification of acute myeloid leukemia. **Blood research**, v. 55, n. S1, p. S1-S4, 2020.

HOSEN, Naoki et al. CD96 is a leukemic stem cell-specific marker in human acute myeloid leukemia. **Proceedings of the National Academy of Sciences**, v. 104, n. 26, p. 11008-11013, 2007.

INSTITUTO NACIONAL DE CÂNCER (BRASIL). Estimativa 2023: incidência de câncer no Brasil / Instituto Nacional de Câncer. – Rio de Janeiro: INCA, 2022.

INSTITUTO NACIONAL DE CÂNCER JOSÉ ALENCAR GOMES DA SILVA. Leucemia. Rio de Janeiro: INCA, 2012. Disponível em: <https://www.gov.br/inca/pt-br/assuntos/cancer/tipos/leucemia>.

IWASAKI, Masayuki et al. CD93 marks a non-quiescent human leukemia stem cell population and is required for development of MLL-rearranged acute myeloid leukemia. **Cell stem cell**, v. 17, n. 4, p. 412-421, 2015.

Ji, Qing et al. Antineoplastic effects and mechanisms of micheliolide in acute myelogenous leukemia stem cells. **Oncotarget**, v. 7, n. 40, p. 65012, 2016.

JIMENEZ, J. J. et al. Acute promyelocytic leukemia (APL): a review of the literature. **Oncotarget**, v. 11, n. 11, p. 992, 2020.

JIN, Yanli et al. Antineoplastic mechanisms of niclosamide in acute myelogenous leukemia stem cells: inactivation of the NF- κ B pathway and generation of reactive oxygen species. **Cancer research**, v. 70, n. 6, p. 2516-2527, 2010.

JORDAN, C. T. et al. The interleukin-3 receptor alpha chain is a unique marker for human acute myelogenous leukemia stem cells. **Leukemia**, v. 14, n. 10, p. 1777-1784, 2000.

KAMATH, G. R. et al. Comparing the epidemiology, clinical characteristics and prognostic factors of acute myeloid leukemia with and without acute promyelocytic leukemia. **Carcinogenesis**, v. 40, n. 5, p. 651–660, 2019.

KAMRAN, S. et al. Therapeutic Potential of Certain Terpenoids as Anticancer Agents: A Scoping Review. **Cancers**, v. 14, n. 5, p. 1100, 2022.

KARIN, Michael. Nuclear factor- κ B in cancer development and progression. **Nature**, v. 441, n. 7092, p. 431-436, 2006.

KANTARJIAN, H. et al. Acute myeloid leukemia: current progress and future directions. **Blood Cancer Journal**, v. 11, n. 2, p. 41, 2021.

KHALDOYANIDI, S. K. et al. Leukemic stem cells as a target for eliminating acute myeloid leukemia: Gaps in translational research. **Critical Reviews in Oncology/Hematology**, p. 103710, 2022.

KHAN, A. Q. et al. Reactive oxygen species (ROS) in cancer pathogenesis and therapy: An update on the role of ROS in anticancer action of benzophenanthridine alkaloids. **Biomedicine & Pharmacotherapy**, v. 143, p. 112142, 2021.

KHOURY, J. D. et al. The 5th edition of the World Health Organization Classification of Haematolymphoid Tumours: Myeloid and Histiocytic/Dendritic Neoplasms. **Leukemia**, v. 36, n. 7, p. 1703-1719, 2022.

KIKUSHIGE, Yoshikane et al. TIM-3 is a promising target to selectively kill acute myeloid leukemia stem cells. **Cell stem cell**, v. 7, n. 6, p. 708-717, 2010.

KIKUSHIGE, Yoshikane; MIYAMOTO, Toshihiro. TIM-3 as a novel therapeutic target for eradicating acute myelogenous leukemia stem cells. **International journal of hematology**, v. 98, n. 6, p. 627-633, 2013.

KIZAKI, Masahiro. Molecular pathogenesis of leukemia and leukemic stem cells (LSCs). **International journal of hematology**, v. 109, n. 1, p. 3-4, 2019.

KRISHNA, M.; NARANG, H. The complexity of mitogen-activated protein kinases (MAPKs) made simple. **Cellular and Molecular Life Sciences**, v. 65, n. 22, p. 3525-3544, 2008.

LAPIDOT, Tsvee et al. A cell initiating human acute myeloid leukaemia after transplantation into SCID mice. **Nature**, v. 367, n. 6464, p. 645-648, 1994.

LEE, Shannon; RAUCH, Jens; KOLCH, Walter. Targeting MAPK signaling in cancer: mechanisms of drug resistance and sensitivity. **International journal of molecular sciences**, v. 21, n. 3, p. 1102, 2020.

LI, Jia-jun et al. Anti-cancer effects of pristimerin and the mechanisms: a critical review. **Frontiers in pharmacology**, v. 10, p. 746, 2019.

LI, Jing et al. Sensitizing leukemia stem cells to NF- κ B inhibitor treatment in vivo by inactivation of both TNF and IL-1 signaling. **Oncotarget**, v. 8, n. 5, p. 8420, 2017.

KONG, E. H. et al. Piplartine induces caspase-mediated apoptosis in PC-3 human prostate cancer cells. **Oncology Reports**, v. 20, n. 4, p. 785–792, out. 2008.

KUO, H. P. et al. Epigenetic Roles of MLL Oncoproteins Are Dependent on NF- κ B. **Cancer Cell**, v. 24, n. 4, p. 423–437, 14 out. 2013.

LEE, S.; RAUCH, J.; KOLCH, W. Targeting MAPK signaling in cancer: Mechanisms of drug resistance and sensitivity. **International journal of molecular sciences**, v. 21, n. 3, p. 1102, 2020.

LI, W. et al. JNK signaling pathway is involved in piperlongumine-mediated apoptosis in human colorectal cancer HCT116 cells. **Oncology Letters**, v. 10, n. 2, p. 709–715, 2015.

LI, Z. et al. Inhibiting the NF- κ B pathway enhances the antitumor effect of cabazitaxel by downregulating Bcl-2 in pancreatic cancer. **International Journal of Oncology**, v. 57, n. 1, p. 161–170, 2020.

LIU, D. et al. Piperlongumine suppresses bladder cancer invasion via inhibiting epithelial mesenchymal transition and F-actin reorganization. **Biochemical and Biophysical Research Communications**, v. 494, n. 1–2, p. 165–172, 2017.

LIU, Y. et al. Biodegradable nanoassemblies of piperlongumine display enhanced anti-angiogenesis and anti-tumor activities. **Nanoscale**, v. 6, n. 8, p. 4325–4337, 2014.

MARCHAND, T.; PINHO, S. Leukemic Stem Cells: From Leukemic Niche Biology to Treatment Opportunities. **Frontiers in Immunology**, v. 12, p. 775128, 2021.

MASHIMO, M. et al. The 89-kDa PARP1 cleavage fragment serves as a cytoplasmic PAR carrier to induce AIF-mediated apoptosis. **Journal of Biological Chemistry**, v. 296, 2021.

MARTÍNEZ-LIMÓN, Adrián et al. The p38 pathway: from biology to cancer therapy. **International journal of molecular sciences**, v. 21, n. 6, p. 1913, 2020.

MESBAHI, Y. et al. Exploring the Metabolic Landscape of AML: From Haematopoietic Stem Cells to Myeloblasts and Leukaemic Stem Cells. **Frontiers in Oncology**, v. 12, p. 281, 2022.

MITCHELL, K.; STEIDL, U. Targeting immunophenotypic markers on leukemic stem cells: How lessons from current approaches and advances in the Leukemia stem cell (LSC) model can inform better strategies for treating acute myeloid leukemia (AML). **Cold Spring Harbor Perspectives in Medicine**, v. 10, n. 1, 2020.

MOKHTARI, R. B. et al. Combination therapy in combating cancer. **Oncotarget**, v. 8, n. 23, p. 38022, 2017.

MORITA, H. et al. Antimitotic quinoid triterpenes from *Maytenus chuchuhuasca*. **Bioorganic and Medicinal Chemistry Letters**, v. 18, n. 3, p. 1050–1052, 2008.

NAEEM, A. et al. Natural Products as Anticancer Agents: Current Status and Future Perspectives. **Molecules**, v. 27, n. 23, p. 8367, 2022.

NAIR, R.; SALINAS-ILLARENA, A.; BALDAUF, H. M. New strategies to treat AML: novel insights into AML survival pathways and combination therapies. **Leukemia**, v. 35, n. 2, p. 299-311, 2021.

NEWELL, L. F.; COOK, R. J. Advances in acute myeloid leukemia. **BMJ**, v. 375, 2021.

O'REILLY, Eimear et al. Recreating the bone marrow microenvironment to model leukemic stem cell quiescence. **Frontiers in cell and developmental biology**, p. 2319, 2021.

PARAMA, D. et al. The promising potential of piperlongumine as an emerging therapeutics for cancer. **Exploration of Targeted Anti-tumor Therapy**, v. 2, n. 4, p. 323, 2021.

PELCOVITS, A.; NIROULA, R. Acute Myeloid Leukemia: A Review. **Rhode Island medical journal**, v. 103, n. 3, p. 38-40, 2020.

PEI, Shanshan et al. Targeting aberrant glutathione metabolism to eradicate human acute myelogenous leukemia cells. **Journal of Biological Chemistry**, v. 288, n. 47, p. 33542-33558, 2013.

PELUSO, Ilaria et al. MAPK signalling pathway in cancers: Olive products as cancer preventive and therapeutic agents. In: **Seminars in cancer biology**. Academic Press, 2019. p. 185-195.

PIRES, Bruno RB et al. NF-kappaB: two sides of the same coin. **Genes**, v. 9, n. 1, p. 24, 2018.

PISKA, K. et al. Piperlongumine (piplartine) as a lead compound for anticancer agents – Synthesis and properties of analogues: A mini-review. **European journal of medicinal chemistry**, v. 156, p. 13-20, 2018.

POLLYEA, Daniel A.; JORDAN, Craig T. Therapeutic targeting of acute myeloid leukemia stem cells. **Blood**, v. 129, n. 12, p. 1627-1635, 2017.

RAWAT, L. et al. Piperlongumine induces ROS mediated cell death and synergizes paclitaxel in human intestinal cancer cells. **Biomedicine and Pharmacotherapy**, v. 128, 1 ago. 2020.

RODRIGUES, A. C. B. DA C. et al. Cell signaling pathways as molecular targets to eliminate AML stem cells. **Critical Reviews in Oncology/Hematology**, v. 160, p. 103277, 2021.

ROLOFF, G. W. et al. Contemporary Approach to Acute Myeloid Leukemia Therapy in 2022. **American Society of Clinical Oncology Educational Book**, n. 42, p. 568–583, 2022.

ROUX, Philippe P.; BLENIS, John. ERK and p38 MAPK-activated protein kinases: a family of protein kinases with diverse biological functions. **Microbiol. Mol. Biol. Rev.**, v. 68, n. 2, p. 320-344, 2004.

SAITO, Yoriko et al. Induction of cell cycle entry eliminates human leukemia stem cells in a mouse model of AML. **Nature biotechnology**, v. 28, n. 3, p. 275-280, 2010.

SALMINEN, A. et al. Terpenoids: natural inhibitors of NF- κ B signaling with anti-inflammatory and anticancer potential. **Cellular and Molecular Life Sciences**, v. 65, n. 19, p. 2979-2999, 2008.

SANTARPIA, Libero; LIPPMAN, Scott M.; EL-NAGGAR, Adel K. Targeting the MAPK–RAS–RAF signaling pathway in cancer therapy. **Expert opinion on therapeutic targets**, v. 16, n. 1, p. 103-119, 2012.

SARRY, Jean-Emmanuel et al. Human acute myelogenous leukemia stem cells are rare and heterogeneous when assayed in NOD/SCID/IL2R γ c-deficient mice. **The Journal of clinical investigation**, v. 121, n. 1, p. 384-395, 2011.

SEOK, J. S. et al. Piperlongumine decreases cell proliferation and the expression of cell cycle-associated proteins by inhibiting Akt pathway in human lung cancer cells. **Food and Chemical Toxicology**, v. 111, p. 9–18, 1 jan. 2018.

SETZERL, W. N. et al. The cytotoxic activity of a salacia liana species from monteverde, costa rica, is due to a high concentration of tingenone. **Planta medica**, v. 64, n. 06, p. 583-583, 1998.

SHALLIS, R. M. et al. Epidemiology of acute myeloid leukemia: Recent progress and enduring challenges. **Blood reviews**, v. 36, p. 70-87, 2019.

SHIMONY, S.; STAHL, M.; STONE, R. M. Acute myeloid leukemia: 2023 update on diagnosis, risk-stratification, and management. **American Journal of Hematology**, 2023.

SHIROTA, Osamu et al. Cytotoxic aromatic triterpenes from *Maytenus ilicifolia* and *Maytenus chuchuhuasca*. **Journal of natural products**, v. 57, n. 12, p. 1675-1681, 1994.

STAHL, M.; TALLMAN, M. S. Acute promyelocytic leukemia (APL): remaining challenges towards a cure for all. **Leukemia & lymphoma**, v. 60, n. 13, p. 3107-3115, 2019.

STANCHINA, M. et al. Advances in acute myeloid leukemia: Recently approved therapies and drugs in development. **Cancers**, v. 12, n. 11, p. 3225, 2020.

STUBBINS, R. J. et al. Management of Acute Myeloid Leukemia: A Review for General Practitioners in Oncology. **Current Oncology**, v. 29, n. 9, p. 6245-6259, 2022.

SUMBLY, V. et al. Leukemic stem cells and advances in hematopoietic stem cell transplantation for acute myeloid leukemia: a narrative review of clinical trials. **Stem Cell Investigation**, v. 9, p. 10–10, 2022.

SUN, Shao-Cong. The noncanonical NF- κ B pathway. **Immunological reviews**, v. 246, n. 1, p. 125-140, 2012.

SUNG, H. et al.. Global Cancer Statistics 2020: GLOBOCAN Estimates of Incidence and Mortality Worldwide for 36 Cancers in 185 Countries. **CA: a cancer journal for clinicians**, v. 71, n. 3, p. 209-249, 2021.

TAGDE, Ashujit et al. MUC1-C induces DNA methyltransferase 1 and represses tumor suppressor genes in acute myeloid leukemia. **Oncotarget**, v. 7, n. 26, p. 38974, 2016.

TAN, Yuxin; WU, Qiuji; ZHOU, Fuling. Targeting acute myeloid leukemia stem cells: Current therapies in development and potential strategies with new dimensions. **Critical Reviews in Oncology/Hematology**, p. 102993, 2020.

TAUSSIG, David C. et al. Leukemia-initiating cells from some acute myeloid leukemia patients with mutated nucleophosmin reside in the CD34⁻ fraction. **Blood, The Journal of the American Society of Hematology**, v. 115, n. 10, p. 1976-1984, 2010.

TEBBI, C. K. Etiology of acute leukemia: A review. **Cancers**, v. 13, n. 9, p. 2256, 2021.

TERGAONKAR, V.; PANDO, M.; VAFA, O.; WAHL, G.; VERMA, I. p53 stabilization is decreased upon NF κ B activation: a role for NF κ B in acquisition of resistance to chemotherapy. **Cancer Cell**, 2002, 1, 493–503.

THOL, F.; GANSER, A. Treatment of Relapsed Acute Myeloid Leukemia. **Current Treatment Options in Oncology**, v. 21, p. 1-11, 2020.

THOMAS, Daniel; MAJETI, Ravindra. Biology and relevance of human acute myeloid leukemia stem cells. **Blood, The Journal of the American Society of Hematology**, v. 129, n. 12, p. 1577-1585, 2017.

TOURNIER, Cathy. The 2 faces of JNK signaling in cancer. **Genes & cancer**, v. 4, n. 9-10, p. 397-400, 2013.

TUBI, L. Quotti et al. Protein kinase CK2 regulates AKT, NF- κ B and STAT3 activation, stem cell viability and proliferation in acute myeloid leukemia. **Leukemia**, v. 31, n. 2, p. 292-300, 2017.

TYNER, J. W. et al. Functional genomic landscape of acute myeloid leukaemia. **Nature**, v. 562, n. 7728, p. 526–531, 2018.

VAN GILS, N.; DENKERS, F.; SMIT, L. Escape From Treatment; the Different Faces of Leukemic Stem Cells and Therapy Resistance in Acute Myeloid Leukemia. **Frontiers in oncology**, v. 11, p. 659253, 2021.

VAN LOENHOUT, J. et al. Oxidative stress-inducing anticancer therapies: Taking a closer look at their immunomodulating effects. **Antioxidants**, v. 9, n. 12, p. 1188, 2020.

VAN RHENEN, Anna et al. The novel AML stem cell-associated antigen CLL-1 aids in discrimination between normal and leukemic stem cells. **Blood, The Journal of the American Society of Hematology**, v. 110, n. 7, p. 2659-2666, 2007.

VETRIE, David; HELGASON, G. Vignir; COPLAND, Mhairi. The leukaemia stem cell: similarities, differences and clinical prospects in CML and AML. **Nature Reviews Cancer**, v. 20, n. 3, p. 158-173, 2020.

WANG, C.; YOULE, R. J. The role of mitochondria in apoptosis. **Annual review of genetics**, v. 43, p. 95-118, 2009.

WANG, Xuefei; HUANG, Shile; CHEN, Ji-Long. Understanding of leukemic stem cells and their clinical implications. **Molecular cancer**, v. 16, n. 1, p. 1-10, 2017.

WEBSTER, J. A.; LUZNIK, L.; GOJO, I. Treatment of AML Relapse After Allo-HCT. **Frontiers in oncology**, v. 11, p. 812207, 2021.

WU, Qinghua et al. JNK signaling in cancer cell survival. **Medicinal research reviews**, v. 39, n. 6, p. 2082-2104, 2019.

XIONG, X. X. et al. Piperlongumine induces apoptotic and autophagic death of the primary myeloid leukemia cells from patients via activation of ROS-p38/JNK pathways. **Acta Pharmacologica Sinica**, v. 36, n. 3, p. 362–374, 2015.

XIU, Yan et al. Stabilization of NF- κ B-inducing kinase suppresses MLL-AF9-induced acute myeloid leukemia. **Cell reports**, v. 22, n. 2, p. 350-358, 2018.

XU, Bing et al. Disulfiram/copper selectively eradicates AML leukemia stem cells in vitro and in vivo by simultaneous induction of ROS-JNK and inhibition of NF- κ B and Nrf2. **Cell death & disease**, v. 8, n. 5, p. e2797-e2797, 2017.

YAO, Y. et al. Piperlongumine induces apoptosis and reduces bortezomib resistance by inhibiting STAT3 in multiple myeloma cells. **Oncotarget**, v. 7, n. 45, p. 73497, 2016.

YANG, Xiaoxiao et al. Advances in acute myeloid leukemia stem cells. In: **Advances in Hematologic Malignancies**. IntechOpen, 2019. p. 11.

YELANI, T.; HUSSEIN, A. A.; MEYER, J. J. M. Isolation and identification of poisonous triterpenoids from *Elaeodendron croceum*. **Natural Product Research**, v. 24, n. 15, p. 1418–1425, 2010.

YI, M. et al. The global burden and attributable risk factor analysis of acute myeloid leukemia in 195 countries and territories from 1990 to 2017: Estimates based on the global burden of disease study 2017. **Journal of Hematology and Oncology**, v. 13, n. 1, 2020.

YILMAZ, M.; KANTARJIAN, H.; RAVANDI, F. Acute promyelocytic leukemia current treatment algorithms. **Blood cancer journal**, v. 11, n. 6, p. 123, 2021.

YIN, Mei-Chin. Anti-glycative potential of triterpenes: a mini-review. **BioMedicine**, v. 2, n. 1, p. 2-9, 2012.

YINGXIANG et al. Pristimerin Induces Autophagy-Mediated Cell Death in K562 Cells through the ROS/JNK Signaling Pathway. **Chemistry & biodiversity**, v. 16, n. 8, p. e1900325, 2019.

ZHANG, Q. et al. Piperlongumine, a novel TrxR1 inhibitor, induces apoptosis in hepatocellular carcinoma cells by ROS-mediated ER stress. **Frontiers in Pharmacology**, v. 10, p. 1180, 2019.

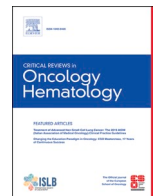
ZHANG, Y. et al. Hematopoietic Hierarchy – An Updated Roadmap. **Trends in cell biology**, v. 28, n. 12, p. 976-986, 2018.

ZHOU, Jianbiao; CHING, Ying Qing; CHNG, Wee-Joo. Aberrant nuclear factor-kappa B activity in acute myeloid leukemia: from molecular pathogenesis to therapeutic target. **Oncotarget**, v. 6, n. 8, p. 5490, 2015.

ZHU, Y. et al. New opportunities and challenges of natural products research: When target identification meets single-cell multiomics. **Acta Pharmaceutica Sinica B**, 2022.

Anexo A

RODRIGUES, A. C. B. C., COSTA, R. G. A., SILVA, S. L. R., DIAS, I. R. S. B., DIAS, R. B., BEZERRA, D. P. Cell signaling pathways as molecular targets to eliminate AML stem cells. **Critical Reviews in Oncology/Hematology**, v. 160, p. 103277, 2021.



Cell signaling pathways as molecular targets to eliminate AML stem cells

Ana Carolina B. da C. Rodrigues, Rafaela G.A. Costa, Suellen L.R. Silva, Ingrid R.S.B. Dias, Rosane B. Dias, Daniel P. Bezerra *

Gonçalo Moriz Institute, Oswaldo Cruz Foundation (IGM-FIOCRUZ/BA), Salvador, Bahia, 40296-710, Brazil

ARTICLE INFO

Keywords:

Acute myeloid leukemia
Cell signaling
Leukemic stem cells
Target therapy

ABSTRACT

Acute myeloid leukemia (AML) remains the most lethal of leukemias and a small population of cells called leukemic stem cells (LSCs) has been associated with disease relapses. Some cell signaling pathways play an important role in AML survival, proliferation and self-renewal properties and are abnormally activated or suppressed in LSCs. This includes the NF- κ B, Wnt/ β -catenin, Hedgehog, Notch, EGFR, JAK/STAT, PI3K/AKT/mTOR, TGF/SMAD and PPAR pathways. This review aimed to discuss these pathways as molecular targets for eliminating AML LSCs. Herein, inhibitors/activators of these pathways were summarized as a potential new anti-AML therapy capable of eliminating LSCs to guide future researches. The clinical use of cell signaling pathways data can be useful to enhance the anti-AML therapy.

1. Introduction

In 2018, the GLOBOCAN database estimated 437,033 new cases of leukemia and 309,006 deaths worldwide (Bray et al., 2018). According to the American Cancer Society, acute myeloid leukemia (AML) remains

the most lethal of leukemias, with a rate of relative 5-year survival (2008–2014) of 25 % in adults (20 years and over) and 67 % in patients aged 0–19 years (American Cancer Society, 2020).

AML affects undifferentiated cells, called blasts, with myeloid characteristics, and can be subclassified into eight subtypes, according to

Abbreviations: [PtdIns (3,4,5)P₃] (PIP3), phosphorylated to phosphatidylinositol 3,4,5 trisphosphate; [PtdIns (4,5)P₂] (PIP2), phosphatidylinositol 4,5 bisphosphate; AMH, anti-mullerianhormone; AML, acute myeloid leukemia; A-PACs, A-type proanthocyanidins; AP-1, activator protein 1; APC, adenomatosis polyposis coli; Ara-C, cytarabine; ATM, ataxia telangiectasia mutated; BAFFR, B-cell-activating factor belonging to TNF family receptor; BCR, B cell receptor; BM, bone marrow; BMP, bone morphogenetic proteins; CEBPa, CCAAT/enhancer-binding protein alpha; CK1 α , casein kinase 1 α ; Co-SMAD, common SMAD mediator; DMAPT, dimethylaminoparthenolide; DNMT1, DNA methyltransferase 1; DNMT3A, DNA methyltransferase 3 alpha; DVL, disheveled; ERK, extracellular signal regulated kinase; ETO, eight twenty one; FDA, Food and Drug Administration; FLT3, FMS-like tyrosine kinase 3; Frz, frizzled; GDFs, growth and differentiation factors; GMP, granulocyte-macrophages; GPCRs, G-protein coupled receptors; GSK3, glycogen synthase kinase 3; HSCs, hematopoietic stem cells; HSP, heat shock proteins; IFNs, interferons; IGF-1, insulin-like growth factor-1; IGFR-1, insulin-like growth factor-1 receptor; IKK, I κ B kinase; IL, interleukin; IL-1R, interleukin-1 receptor; IRS1, insulin receptor substrate 1; I-SMADs, SMAD inhibitor; ITD, internal tandem duplication; JAK, Janus kinase; JNK, c-Jun N-terminal kinase; LEF, lymphocyte-enhancer-binding factor; LICs, leukemia initiator cells; LPA, lysophosphatidic acid; LSCs, leukemic stem cells; LTC-IC, long-term culture initiator cells; LT β R, lymphotoxin β -receptor; MDS, myelodysplastic syndromes; miRNA, microRNA; MLL, mixed lineage leukemia; mTOR, mammalian target of rapamycin; MUC1-C, MUC1 transmembrane C-terminal; NF- κ B, nuclear factor kappa B; NIK, NF- κ B-inducing kinase; NOD, non-obese diabetic; PCP, planar cell polarity; PDGFR, platelet-derived growth factor receptor; PDK-1, phosphoinositide-dependent kinase-1; PDX, patient-derived xenograft; PH, pleckstrin homology; PI-103, propidium iodide; PI3K, phosphatidylinositol-3-kinases; PLZF, promyelocytic leukemia zinc finger; PML, promyelocytic leukemia; PPAR, peroxisome proliferator-activated receptor; PPRE, peroxisome-proliferator responsive element; PTEN, phosphatase and tensin homolog; PYGO, pygopus homolog; RANK, receptor activator for nuclear factor κ B; Raptor, regulatory protein associated with mTOR; RARA, retinoic acid receptor alpha; RHEB, Ras homolog enriched in brain; ROS, reactive oxygen species; R-SMAD, receptor-regulated SMAD; RUNX1, runt-related transcription factor 1; RXR, retinoid X receptor; SCID, severe combined immunodeficiency; siRNA, small interfering RNA; STAT, signal transducers and activators of transcription; TBL1, β -Like 1 transducing; TCF, T-cell factor; TCR, T cell receptor; TGFs, transforming growth factors; TKIs, tyrosine kinase inhibitors; TLR, toll-like receptor; TNF, tumor necrosis factor; TNFR, tumor necrosis factor receptor; TNFSF13, tumor necrosis factor ligand superfamily member 13; TSC, tuberous sclerosis complex; TSGs, tumor suppressor genes; TYK2, tyrosine kinase 2; VEGF, vascular endothelial growth factor; VEGFR, vascular endothelial growth factor receptor; VPS34, vacuolar protein sorting 34; Wnt, Wingless-Int; XIAP, X-linked inhibitor of apoptosis protein; β -TRCP, β -transducing repeat-containing protein.

* Corresponding author.

E-mail address: daniel.bezerra@fiocruz.br (D.P. Bezerra).

<https://doi.org/10.1016/j.critrevonc.2021.103277>

Received 30 September 2020; Received in revised form 25 January 2021; Accepted 27 February 2021

Available online 11 March 2021

1040-8428/© 2021 Elsevier B.V. All rights reserved.

Anexo B

COSTA, R. G. A., SILVA, S. L. R., DIAS, I. R. S. B., OLIVEIRA, M. S., **RODRIGUES, A. C. B. C.**, DIAS, R. B., BEZERRA, D. P. Emerging drugs targeting cellular redox homeostasis to eliminate acute myeloid leukemia stem cells. **Redox Biology**, p. 102692, 2023.



Emerging drugs targeting cellular redox homeostasis to eliminate acute myeloid leukemia stem cells

Rafaela G.A. Costa^a, Suellen L.R. Silva^a, Ingrid R.S.B. Dias^a, Maiara de S. Oliveira^a, Ana Carolina B. da C. Rodrigues^a, Rosane B. Dias^{a,b}, Daniel P. Bezerra^{a,*}

^a Gonçalo Moniz Institute, Oswaldo Cruz Foundation (IGM-FIOCRUZ/BA), Salvador, Bahia, 40296-710, Brazil

^b Department of Propedeutics, School of Dentistry of the Federal University of Bahia, Salvador, Bahia, 40110-909, Brazil

ARTICLE INFO

Keywords:

Acute myeloid leukemia
Leukemia stem cells
Oxidative stress

ABSTRACT

Acute myeloid leukemia (AML) is a very heterogeneous group of disorders with large differences in the percentage of immature blasts that presently are classified according to the specific mutations that trigger malignant proliferation among thousands of mutations reported thus far. It is an aggressive disease for which few targeted therapies are available and still has a high recurrence rate and low overall survival. The main reason for AML relapse is believed to be due to leukemic stem cells (LSCs) that have unlimited self-renewal capacity and long residence in a quiescent state, which promote greater resistance to traditional therapies for this cancer. AML LSCs have low oxidative stress levels, which appear to be caused by a combination of low mitochondrial activity and high activity of ROS-removing pathways. In this sense, oxidative stress has been thought to be an important new potential target for the treatment of AML patients, targeting the eradication of AML LSCs. The aim of this review is to discuss some drugs that induce oxidative stress to direct new goals for future research focusing on redox imbalance as an effective strategy to eliminate AML LSCs.

1. Introduction

Acute myeloid leukemia (AML) is a very heterogeneous group of disorders with large differences in the percentage of immature blasts that presently are classified according to the specific mutations that trigger malignant proliferation among thousands of mutations reported thus far [1–5]. The American Cancer Society estimated 20,380 new cases of AML and 11,310 deaths in the United States for 2023 [6].

According to the French-American-British (FAB) classification, AML can be subclassified into undifferentiated acute myeloblastic leukemia, acute myeloblastic leukemia with minimal maturation, acute myeloblastic leukemia with maturation, acute promyelocytic leukemia, acute myelomonocytic leukemia, acute myelomonocytic leukemia with eosinophilia, acute monocytic leukemia, acute erythroid leukemia and acute megakaryoblastic leukemia [7–10].

In the most recent update of the World Health Organization (WHO) AML classification, there is a separation of AML with defining genetic abnormalities from AML defined by differentiation. AML with defining genetic abnormalities includes acute promyelocytic leukemia with *PML::RARA* fusion; AML with *RUNX1::RUNX1T1* fusion; AML with

CBFB::MYH11 fusion; AML with *DEK::NUP214* fusion; AML with *RBM15::MRTFA* fusion; AML with *BCR::ABL1* fusion; AML with *KMT2A* rearrangement; AML with *MECOM* rearrangement; AML with *NUP98* rearrangement; AML with *NPM1* mutation; AML with *CEBPA* mutation; AML myelodysplasia-related; and AML with other defined genetic alterations. AML defined by differentiation includes AML with minimal differentiation, AML without maturation, AML with maturation, acute basophilic leukemia, acute myelomonocytic leukemia, acute monocytic leukemia, acute erythroid leukemia, and acute megakaryoblastic leukemia [11].

AML can affect individuals of any age; although it is the most common malignancy in children aged 15 years or younger, it becomes more common with aging. Generally, adults correspond to the group of individuals who are most affected by this type of neoplasm, which reduces the success of therapeutic alternatives due to age. Thus, the disease has a poor prognosis when compared to younger individuals affected by AML [4,12–14].

AML is an aggressive disease for which few targeted therapies are available. The standard protocol for treatment has remained almost unchanged for more than four decades and basically consists of the

* Corresponding author.

E-mail address: daniel.bezerra@fiocruz.br (D.P. Bezerra).